HISTIOCYTIC SARCOMA: GENERATION AND UTILIZATION OF PATIENT DERIVED CELL LINES AND XENOGRAFT MODELS TO UNDERSTAND TUMORIGENESIS AND IDENTIFY NOVEL TREATMENT APPROACHES

By

Marilia Takada

A DISSERTATION

Submitted to
Michigan State University
in partial fulfillment of the requirements
for the degree of

Comparative Medicine and Integrative Biology – Doctor of Philosophy

2018

ABSTRACT

HISTIOCYTIC SARCOMA: GENERATION AND UTILIZATION OF PATIENT DERIVED CELL LINES AND XENOGRAFT MODELS TO UNDERSTAND TUMORIGENESIS AND IDENTIFY NOVEL TREATMENT APPROACHES

By

Marilia Takada

Canine histiocytic sarcoma (HS) is a proliferative malignancy of dendritic and macrophage lineages with rapid progression, and limited response to available treatment protocols. As the disease pathogenesis has been unclear, oncologists rely on a small repertoire of nonspecific strategies for therapeutic interventions. To fill this gap of knowledge, we established clinically relevant tools and model systems of histiocytic sarcoma, and utilized these to ask fundamental questions aimed at identifying novel targets for more effective treatment approaches.

We successfully established and fully characterized three HS cell lines derived from neoplasms of dogs from predisposed breeds. These cell lines were utilized for drug screening, including a high throughput screening platform, where potential drug candidates were selected from a pool of about 2,000 compounds. Among the selected drugs, we identified two small molecule inhibitors to be highly effective *in vitro* at nanomolar concentrations: dasatinib, a multi-tyrosine kinase inhibitor, including members of SRC family kinase, and trametinib, an inhibitor of MEK, from the MAPK signaling pathway. To evaluate the drug efficacy *in vivo*, we developed an orthotopic xenograft mouse model harboring intrasplenic HS neoplasms. Immunodeficient mice transplanted with canine HS cells into their spleen showed a consistent tumor growth, and presence of metastasis to multiple organs (i.e. liver, pancreas and omentum), recapitulating an aggressive metastatic form of HS, the one in most need for better treatment options.

Studies with orthotopic intrasplenic HS xenograft mice treated with either dasatinib or trametinib were conducted with promising results. Both drugs effectively inhibited tumor growth, and most importantly, significantly increased survival time of treated mice.

Additionally, oncogenic gain-of-function mutations in *PTPN11* gene were identified in the HS cell lines. *PTPN11* gene encodes SHP-2, a protein tyrosine phosphatase, engaged in enhancement of signaling downstream of growth factor, cytokine and extracellular receptors, including MAPK and PI3K/AKT pathways. One HS cell line, the BD cell line, carries the $PTPN11^{E76K}$ mutation; while three cell lines (OD, PJ and DH82) carry the $PTPN11^{G503V}$ mutation. Moreover, a $KRAS^{Q61H}$ gain-of-function mutation was also found in OD cell line.

We found that somatic *PTPN11* mutations are common in canine HS, particularly in Bernese mountain dogs, the breed with highest incidence of HS. In a study on a large sample of dogs, *PTPN11* mutations were present in 43% of HS from BMDs, and were not identified in any of the lymphoma samples, the second most common neoplasm in this breed.

We have established important model systems of canine HS through which we were able to identify promising drug candidates for treatment and key signaling pathways that are involved in oncogenesis. Our HS cell lines carry oncogenic drivers that are commonly present in canine HS, and in some human cases of human HS. Our xenograft model has proved to be a good surrogate system for drug efficacy, and led to the confirmation of two small molecules, dasatinib and trametinib, as warranting further evaluation in clinical trials in dogs with HS, which can also serve as key proof of concept trials for human HS.

This dissertation is dedicated to my family:
Shuko, Kinichi, Emy and Leo.

ACKNOWLEDGEMENTS

I would like to thank everybody who believed in my potential, and gave me an opportunity to work and grow as a scientist and as a person.

Thank you Vilma Yuzbasiyan-Gurkan. Your mentorship guided me throughout the years to develop a research mindset. You also taught me things that go beyond the lab bench. You showed me kindness, love, and the importance of being mindful to the community around us. Be patient and altruist, and to treat everybody equally. And most importantly, you always supported me to pursue happiness. I will be forever grateful and will never forget all the wonderful years in VYG lab.

Thank you to my family, for all the support and love and care. No matter the distance, I always have you here with me, in my mind and inside my heart.

Gracias Lito, for being here with me through this journey, and many more to come.

"The most important is to be committed and persevere.
Live intensively, love, cry, laugh, give your best.
Be with those who really care about you, fulfill your needs.
Look for answers, find means, make noise.
Be silence, be everything, be you.
Take objective measurements to achieve your goals.
Those are the foundations for your future.
Believe that everything is possible."

Kinichi Takada

TABLE OF CONTENTS

LIST OF TABLES

LIST OF FIGURES

KEY TO ABBREVIATIONS

AML	Acute Myeloid Leukemia
BMD	Bernese Mountain Dog
BLI	Non-invasive Bioluminescence Imaging
CCNU	*N*-(2-chloroethyl)-*N*'-cyclohexyl-N-nitrosourea
CD	Cluster of Differentiation
cHS	Canine Histiocytic Sarcoma
DAB	3,3'-diaminobenzidine
DC	Dendritic Cell
ECD	Erdheim-Chester Disease
FDA	US Food and Drug Administration
H&E	Hematoxylin and Eosin
HTS	High Throughput Drug Screening
HS	Histiocytic Sarcoma
hHS	Human Histiocytic Sarcoma
HHS	Hemophagocytic Histiocytic Sarcoma
IACUC	Institutional Animal Care and Use Committee
IFNγ	Interferon-γ
IHC	Immunohistochemistry
IP	Intraperitoneal
IVIS	In Vivo Imaging System
JMML	Juvenile Myelomonocytic Leukemia
LCH	Langerhans Cell Histiocytosis
MHC	Major Histocompatibility Complex

MSU Michigan State University

MST Median Survival Time

NOEL No-observed-adverse-effect

ORR Overall Response Rate

OS Overall Survival

PAHS Peri-articular Histiocytic Sarcoma

PBMC Peripheral Blood Mononuclear Cells

PFS Progression Free Survival

SEER Surveillance, Epidemiology, and End Results

TD Tolerated Dose

CHAPTER 1

INTRODUCTION AND LITERATURE REVIEW

1.1 Canine histiocytic sarcoma (cHS)

1.1.1 Epidemiology of cHS

Histiocytic sarcoma in dogs is a rare malignancy that represents <1% of all cancers [1]. However, it is seen in an appreciable frequency in certain breeds of dogs, particularly in Bernese mountain dog (BMD) with an incidence of at least 25% [2, 3]. Flat-coated retrievers are also predisposed to cHS, which accounts for about 36% of all their tumors [4, 5]. Other overrepresented breeds include golden retriever and Rottweiler [6-8], and more recently reported in Japan, miniature schnauzer [9] and Pembroke Welsh corgi [10].

Males and females were equally affected, and dogs are often diagnosed in adult age (8-10 years), although dogs younger than two years old have been reported [3, 4, 7, 11-13]. To date, there is no evidence of either environmental nor dietary risk factors related to the development of cHS [14].

The prevalence of cHS in specific breeds suggests the existence of heritable risk factors influencing the development of the disease. Abadie et al. conducted a pedigree analysis of 327 BMDs from Europe tracking an average of 20 generations of dogs [2]. A familial component was confirmed, with 70% of affected dogs having relatives with confirmed cHS, but the disease distribution could not be explained by a fully recessive model, instead, an oligogenic transmission mode was proposed by the authors [2].

1.1.2 Etiology of cHS

Chromosomal structural changes in cHS samples were reported by Hedan et al. While dog karyotype comprises 38 pairs of acrocentric autosome chromosomes and 2 metacentric sex chromosomes (2n=78), in cHS, the chromosome numbers were highly variable, ranging from 42 to 58, with morphological aberrations such as bi-armed chromosomes [15].

Several studies have indicated potential tumor suppressor genes involved in cHS. An analysis of genome-wide array comparative genomic hybridization revealed DNA copy number aberrations shared within a

population of BMDs (n=71) and flat-coated retrievers (n=33) [15]. The most recurrent events were deletions at regions containing important tumor suppressor genes: CFA 11q16 that contains *CDKN2A/B*, CFA 16, CFA 22q11 that includes *RB1*, and CFA 26q25, a locus of *PTEN*. However, these findings contradicted those from Ostrander et al. using a genome-wide association study conducted in a large pool of cHS in BMDs from North America and Europe, where a common single haplotype in the same region of chr11 containing genes *MTAP* and *CDKN2A*, was present in 96% of affected dogs [16]. The most concerning disagreement was the fact that while the first study reported a deletion in the region of *MTAP/CDKN2*, Ostrander et al. demonstrated that cases positive for the reported haplotype had 8.7-16.8 and 2.9-3.9-fold increase expression of *CDKN2A* and *CDKN2B*, respectively, by RT-qPCR studies. Further sequencing studies are needed to support the findings of these research groups.

Mutations in the tumor suppressor gene *TP53* were present in 12 of 26 (46%) dogs with cHS, with 10 dogs harboring the same variant, a 2-base (AT) insertion in exon 5 resulting in a stop codon (c.446_447insAT, p.Tyr150SerfsX8) [17].

Recently, a gain of function mutation in oncogene *PTPN11* (E76K) was reported by our group in a survey of HS cases from various breeds [18]. Interestingly, in cHS in BMDs, the frequency of this mutation was 36.6% in tumors from BMDs, while it as 8.69% in tumors from other breeds [18]. *PTPN11* encodes the SHP2 protein, which is required for the MAPK pathway. Moreover, the *PTPN11*^{E76K} was found to be a gain-of-function mutation promoting the activation of AKT and ERK pathways. Activating mutations in *PTPN11* gene, including E76K, have been also reported in human cases of HS [19-22].

Boerkamp et al. showed a difference in gene expression of cHS in flat-coated retrievers when compared to normal splenic tissue, and validated an altered expression of a set of 9 genes (down-regulated *PPBP, SpiC, VCAM1, ENPEP, ITGAD*; and up-regulated *GTSF1, Col3a1, CD90, LUM*) [23]. However, the reported data was not sufficient to suggest specific pathways implicated to the disease.

Tagawa et al. described the occurrence of an immunosuppressed state in dogs with HS, based on an overexpression of costimulatory molecules CTLA-4 and PDI in circulating lymphocytes, which may result in a negative regulation towards CD8+ T lymphocytes [24]. Similarly, Marcinowska et al. reported the presence of an infiltrating population of lymphocytes in cHS of flat-coated retrievers, mostly composed of FOXP3+ Treg cells [25].

1.1.3 Pathology of cHS

Histiocytic sarcoma is a malignancy of proliferative histiocytes, a class of cells arising from macrophage and dendritic cell (DC) lineage. Both myeloid dendritic antigen presenting cells and macrophages, derive from a common hematopoietic $CD34^+$ stem cell precursor in the bone marrow. Under the influence of various growth factors and cytokines, the progenitor cells develop into either interstitial DC or macrophages. The development of DC can be influenced by FLT3 ligand, granulocyte-macrophage colony-stimulating factor (GM-CSF), TNF- α, IL-4, and tumor growth factor-β (TGF-β). While the differentiation into macrophages is induced by GM-CSF and macrophage colony-stimulating factor (M-CSF) [26, 27]. In dogs, HS is classified as either localized HS, disseminated HS or hemophagocytic HS. Localized and disseminated forms are morphologically and phenotypically identical, arising from myeloid dendritic antigen presenting cells, characterized by a consistent expression of CD1, CD11c, MHC class II, and ICAM-1 [6]. They are then distinguished by their clinical presentation.

The definition of localized cHS is applied to neoplasms found in a single site. This form is most frequently present in the skin/subcutis of the dog extremities, and peri-articular tissues of appendicular joints, and less commonly in the spleen, lymph nodes, lung, and bone marrow [6, 28]. It is associated with a high metastatic rate of 70-91%, spreading to satellite lymph nodes and other organs [5, 7, 28, 29].

A subtype of localized cHS, peri-articular HS (PAHS), is the most common synovial neoplasm in dogs. It presents mostly in one joint, either in the stifle (37-61%), in the elbow (26-28%) or in the shoulder (21%)

[7, 28]. Although there is no clear breed predilection, Rottweilers were overrepresented in a group of 18 dogs with PAHS (61%) [7]. Flat coated retrievers seem to be more predisposed to localized HS than the disseminated form, especially in the skin and subcutis areas of the limbs [11, 15, 23]. Despite its potential to spread to other organs (68-91%), PAHS carries a better prognosis in comparison to other forms of cHS, especially if treated early in the disease [7, 28]. Median survival time for PAHS has been reported as 391 days (48-980), compared to 128 days (14-470) for non-PAHS, based on a retrospective study, although variable treatment protocols were utilized [28]. An association between previous inflammatory joint disease and the development of PAHS has been suggested based on the rationale of inflammation promoting tumorigenesis [7, 30].

The disseminated form of cHS is a multisystem disease, and although it can affect essentially any organ in the body, is primarily localized in the spleen, lungs, bone marrow, liver and lymph nodes [6, 28]. BMDs seem to be more susceptible to disseminated HS than flat-coated retrievers [5, 15].

It is often difficult to distinguish between localized and disseminated HS, due to the fact that the localized form is highly metastatic, therefore a situation of multi-organ involvement could indicate either metastasis and progression of the localized form, or could indicate disseminated disease. Localized and disseminated forms are morphologically and phenotypically identical, and to date, no genetic distinction has been made. Some authors describe these two forms as different entities, however this concept should be used with caution, considering that they could simply represent different stages of the same disease.

As a rule of thumb, treatment of cancer at early stages, when metastases are nonexistent or minimal, reflects in better outcomes. Likewise, surgical resection of cHS for curative intent, when metastasis is not evident, regardless of tumor location, resulted in improved median survival times, 243-500 days [28, 31]. Therefore, one could hypothesize that the better outcome in localized HS could be simply a result of disease stage.

Hemophagocytic HS (HHS) originates from the splenic red pulp and bone marrow macrophages, instead of interstitial DC, as most of the other types of cHS. It is distinguished from the other forms by the presence of marked erythrophagocytosis by the neoplastic cells, and by positive expression of CD11d, a leukocyte αD integrin, mainly expressed on cells of myelomonocytic lineage [32].

Moore et al. reported 17 cases of HHS where the most commonly involved organs were spleen (17/17), liver (15/17), bone marrow (10/11), and lungs (9/9). Additionally, HHS was associated with a more aggressive course and worse prognosis than other forms of cHS, with a reported mean survival time of less than 2 months [33].

1.1.4 Diagnosis of cHS

The initial clinical presentation of dogs with HS may differ according to the location of the primary tumor and also the extent of the disease, but in most cases dogs present with nonspecific clinical signs such as lethargy, anorexia, weakness, weight loss, visible mass, lameness, cough, vomiting, and lymphadenomegaly [3, 6, 29, 31]. Canine HS develops most commonly in the skin/subcutaneous tissue, bone/joint, spleen, lymph nodes, lungs and liver [3]. Clinical signs of dogs with PAHS at initial evaluation consist of lameness (79%) or soft tissue swelling (68%) [28].

The commonly reported clinicopathological abnormalities at presentation include anemia, thrombocytopenia, neutrophilia with or without left shift, hypoalbuminemia, hypercalcemia, and increases in liver enzyme activity [2, 29, 34]. Clinically, patients with HHS commonly presented with responsive anemia, marked thrombocytopenia and hypoalbuminemia [33]. In some cases, the diagnosis of HHS can be misinterpreted as immune-mediated hemolytic anemia because of the similarities in the signalment between the two diseases [33].

Morphologically, cHS are generally poorly demarcated, locally invasive tumors of heterogeneous population of histiocytic-spindle-pleomorphic cells, multinucleated histiocytic giant cells,

erythrophagocytes, and lymphocytes. Marked anysokaryosis and anysocytosis may be displayed, and mitotic figures are often present. Their nuclei are round, oval, or reniform with prominent nucleoli, and their cytoplasm is moderate to abundant, lightly basophilic, and vacuolated [2, 6, 11].

Canine HS presents a high degree of pleomorphism and lacks specific features that can distinguish it from other round cell neoplasms such as some forms of carcinoma, melanoma, or lymphoma [35]. Therefore, besides the histopathologic examination, immunohistochemistry profiling is crucial for a definitive diagnosis of cHS.

Although several cell markers have been studied to characterize cHS neoplasms, only a few of them are applicable in paraffin formalin fixed embedded tissues. For this reason, a standard pattern of CD18+, CD3-, and CD79a- for formalin-fixed tissues has been used for the diagnosis of cHS, and reported by several studies [2, 6, 28, 30]. Recently, CD204, a class A macrophage scavenger receptor, was shown as an antibody with elevated specificity to cHS [36, 37], and it is now included in the profiling of cHS by many institutions.

As mentioned previously, the cells of origin of HHS are macrophages rather than DCs, consequently, this type of cHS can be distinguished by positive diffuse (perimembrane) expression of CD11d, a specific marker for macrophages, resulting in a pattern of CD18+, CD11d+, CD11c−, MHCII+, and minimal expression of CD1 [33, 38].

Other canine histiocytic diseases are also differentiated by immunohistochemistry profiling. Specific cell markers for each histiocytic disease entity are included in **Table 1.1**.

1.1.5 Treatment and prognosis of cHS

Treatment for cHS may vary according to tumor location and presence of distant metastasis. Modalities of treatment consist of surgical excision of the tumor, local radiation therapy, and/or systemic chemotherapy protocols. Although there is no evidence that a single treatment is more beneficial than

other, systemic therapy is recommended in most cases due to the high metastatic potential [29]. Based on current understanding, all forms of cHS are approached similarly in terms of treatment options. Lomustine or 1-(2-Chloroethyl)-3-Cyclohexyl-1-Nitrosourea) (CCNU) has been the most used chemotherapy agent to treat cHS. Lomustine is an alkylating drug, that has shown to provide an overall response rate (ORR) of 29% for a median of 96 days (55-137) as a first line treatment, in a prospective study with 12 dogs [39]. Median survival time (MST) was reported as 124 days (7-482), although second line treatments were variable. In a multi-institutional retrospective study, lomustine resulted in an ORR of 46% for a median of 85 days (29-805). MST was 106 days, based on multi-modality treatments [8]. A preliminary study showed a similar response rate of 46% for a median of 93 days when dogs were treated with the anthracycline antibiotic drug doxorubicin [40]. Doxorubicin has been used as single or alternating agent with lomustine for cHS, although the benefit of this approach has not been confirmed [41].

There is evidence suggesting that dogs with localized cHS treated with a curative intent survived longer, with a MST of 18.9 months, than those with disseminated disease [5, 31]. Similarly, Dervisis et al. showed a difference in survival time between localized cHS (406 days) and disseminated disease (85 days) [3].

Although PAHS has a similar metastatic potential, it seems to carry a more favorable outcome when patients are submitted to multimodality treatment. Dogs with PAHS had a significant longer MST of 391 days when compared 128 days from dogs with non-PAHS [28]. The MST decreased to 61 days for those that didn't receive any form of treatment [30].

HHS tend to behave more aggressively, and regardless of therapy, affected dogs live for only 1 to 2 months [31, 33].

Alternative approaches using liposomal clodronate aiming to induce apoptosis in phagocytic cells showed encouraging responses *in vitro*, however, the response was not re-capitulated *in vivo* [42].

Clinical reports in the literature demonstrated potential therapeutic value of paclitaxel, and immunotherapy using human cytotoxic T-cell line (TALL-104) [43-45].

1.2 Histiocytic sarcoma in humans (hHS)

Histiocytic and dendritic cell neoplasms represent a group of rare hematological diseases in humans described by the current 2016 WHO classification [46, 47]. This class of diseases present highly diverse clinical presentations, which can vary from benign localized lesions to disseminated life-threatening forms [48]. Among this heterogeneous group, the most aggressive entities are: histiocytic sarcoma, Langerhans cell histiocytosis and Erdheim-Chester disease [46].

HS is an extremely rare malignancy in humans, representing <1% of all hematopoietic neoplasms [49, 50]. It affects all ages from 6 months to 89 years (median age: 46 years), with an higher frequency between 50-69 years, and a male predominance [51-53].

1.2.1 Etiology of hHS

The etiology of hHS remains unclear, however there is increasing evidence suggesting the role of an oncogenic MAPK pathway. Activating *BRAF*^{V600E} mutation has been reported in several patients with hHS [54-58], and in one case, treatment with the BRAF inhibitor vemurafenib resulted in favorable response [55]. Other mutations in *BRAF* were observed, including G464V, G466R, F595L, and NS581S [20, 59]. Mutations in other key genes within MAPK pathway have also been described in hHS: *MAP2K1* [56, 60], *KRAS* Q61H [20], and *HRAS* Q61R [59].

Additionally, MAPK signaling seems to be activated in hHS through mutations in *PTPN11* gene, which encodes SHP2. Activating mutations in *PTPN11* were reported in a few cases of hHS [19, 20, 22]. One patient had a copy number gain of *GNA11* in addition to *PTPN11*^{E76K}, supporting the treatment with trametinib, a MEK inhibitor, which resulted in a significant partial response [22].

A single nucleotide polymorphism in *KDR* (Q472H) was identified in 3/5 samples of hHS. *KDR* gene encodes for vascular endothelial growth factor receptor 2 [20].

Hung et al. reported alterations in *KMT2D/MLL2* on chromosome 12q13.2 in three of six hHS patients, a gene involved in chromatin regulation by encoding the *MLL/SET1* class of histone lysine methyltransferases [60].

There is increasing evidence of a process of transdifferentiation of lymphoid malignancies to a subset of HS with immunoglobulin heavy chain (IGH) gene and T-cell receptor gene rearrangements. A number of patients with HS presenting concomitant follicular lymphoma, CLL, B- or T-lymphoblastic neoplasms, or PTCL have been reported in several studies. The mechanism of transdifferentiation remains unclear.

1.2.2 Pathology of hHS

Clinically, hHS often presents at an advanced stage, where the rapid disease progression and limited response to available therapies results in a high mortality rate, and most patients die within 2 years of diagnosis [52, 61]. Due to the rarity of the disease, prognostic factors have not be identified, although some cases presenting a localized form of hHS seemed to carry a favorable outcome.

Existing data suggest that hHS presents mostly within lymph nodes, but often develops at extranodal sites such as gastrointestinal tract, spleen, lungs, head and neck, where it pursues a clinically aggressive course [51, 52]. Data collected from the Surveillance, Epidemiology, and End Results (SEER) Program by Kommalapati et al. showed that among 159 cases of hHS, the disease was observed in: skin/connective tissue (35.8%), lymph nodes (17%), respiratory tract (8.2%), CNS (6.9%), GI tract including hepatobiliary and pancreas (7.5%), bone marrow (4.4%), spleen and reticuloendothelial system (5%) [62].

It is challenging to predict metastatic rate based on the available small cohort of cases, however those suggest that disseminated disease is fairly frequent, and may be associated with a worse outcome. For instance, Hornick et al. reported 5 out of 10 cases of extranodal hHS presenting distant metastasis [52].

Data from a retrospective study showed 9 out of 15 hHS patients with metastatic disease [53]. Due to the challenges in surgically resecting the tumor, patients with CNS hHS carry a poor prognosis when compared to other locations [63].

1.2.3 Diagnosis of hHS

Cytologically, hHS has been characterized as "epithelioid cells and occasional spindle cells characterized by abundant vacuolated cytoplasm, reniform/donut-shaped and occasionally pleomorphic/bizarre nuclei, and conspicuous nucleoli in a lymphoplasmacytic or neutrophilic background" and "voluminous cytoplasm with a giant nucleus (more than 20 times larger than the size of a red blood cell), a monster-like nucleus (multilobulated giant nucleus), and Pac-Man-like nuclei" [60]. Furthermore, lymphoglandular bodies and cytophagocytosis may be important diagnostic clues to hHS on cytology. Histologically, HS presents as a diffuse proliferation of large and round to oval pleomorphic cells. Cytoplasm is usually abundant and eosinophilic, often foamy, vacuolated or clear. Hemophagocytosis and/or cytophagocytosis may be present [64]. Oval to irregular nuclei with vesicular chromatin and large eosinophilic nucleoli. Multilobulated, binucleated or giant multinucleated cells may be seen. Mitotic figures ranged from 1 to 64 per 10 HPF [52]. Necrosis can be present and infiltrate of inflammatory cells, composed of neutrophils, lymphocytes, eosinophils or plasma cells are often observed [64].

The diagnosis of hHS relies on immunoreactivity to markers to confirm the histiocytic origin of cells and to exclude other poorly differentiated large cell neoplasms (large cell lymphoma, carcinomas, melanomas, and certain sarcomas). Histiocytic markers such as CD163, CD68, lysozyme and PU.1 have been used, although CD163 has been reported as having higher specificity [64-66].

Dalia et al. used the positive expression of histiocytic markers CD163, CD68 and lysozyme, and negative expression of CD1a, CD21, and CD35, to confirm the diagnosis of HS [48]. In a study of 6 cases, cytoplasmic immunoreactivity to CD68 and CD163 was observed in 86% and 100% of the cases,

respectively [60]. All cases were negative for cytokeratins, melanocytic markers (MART-1 and HMB45), lymphoma markers (CD3, CD20, PAX5 and ALK-1), markers of common sarcomas (CD34, desmin, ERG, MDM2 and CDK4), dendritic cell markers (CD21), and Langerhans cell markers (CD1a and langerin) [60]. Expression of cell markers used to distinguish the various histiocytic and dendritic cells neoplasms in humans are listed in **Table 1.2**.

1.2.4 Treatment and prognosis of hHS

Given the limited occurrence, there is no consensus on current standard-of-care treatment for hHS. Surgical resection is frequently attempted for accessible tumors, based on tumor location and extent of disease. Adjuvant radiation therapy is often chosen to reduce chances of local recurrence. Disseminated forms of hHS are aggressive and for those, systemic chemotherapy is essential. To date, the optimal protocol is still unclear, therefore, regimens of drugs for lymphoma (cyclophosphamide, doxorubicin, vincristine, prednisone, CHOP, etoposide) or other cytotoxic drugs (gemcitabine, cladribine, ifosfamide) are used for treatment [52, 53, 64]. In some cases of brain hHS, methotrexate is used similarly to primary CNS lymphomas [48]. Case reports have shown therapies with small molecules including sirolimus, sunitinib and imatinib [53], vemurafenib [55], and MEK inhibitors [22, 56].

The information available of autologous or allogeneic stem cell transplantation in patients with hHS has shown favorable outcome, however data is limited to a few case reports [61, 67, 68].

Treatment with humanized monoclonal antibody anti-CD52, alemtuzumab, has been reported in patients with hHS in advanced stage with encouraging outcomes [22, 69]. Alemtuzumab, a drug approved for patients with CLL, target CD52 expressing cells, including monocytes, lymphocytes and eosinophils, with potential to benefit other hematopoietic neoplasms.

Survival time data for hHS is limited, and the available knowledge is based on case reports or small cohorts of patients. Kommalapati et al. evaluated a large database collected from SEER containing 159

cases of hHS, and reported an overall survival time of 6 months [62]. Those patients who had surgical intervention as part of the treatment had a better outcome (bone marrow, spleen and RES involvement was censored), although there was limited information on the specific therapies received by each patient. From 159 hHS patients, 42 (26.4%) had a concomitant neoplastic disease, mostly non-Hodgkin's lymphoma (n=28) and AML (n=6), which was associated with a shorter OS.

1.3 Langerhans cell histiocytosis (LCH) in humans

First recognized in the early 1900s, LCH is the most common histiocytic neoplasm consisting of a clonal population of Langerhans cells within a lesion enriched by a population of inflammatory cells [70]. Langerhans cells are resident antigen presenting cells located in many organs, including the epidermis and dermis of the skin [71]. Children are most commonly affected in a frequency of 5 in 900,000, while in patients older than 15 years the frequency is 1 in one million, with an apparent male predilection [70, 72, 73].

A constitutive MAPK pathway plays a central role in LCH pathogenesis, where the mutation *BRAF*^{V600E} is present in 36-64% of the cases [74-78]. A *BRAF*^{V600E} conditional allele expressed under the CD11c promoter successfully mimicked the phenotype of an aggressive LCH-like disease in mice [77], demonstrating a certain degree of specificity to this mutation.

In a whole exome sequencing study of 41 cases of LCH, another key gene of MAPK pathway was found mutated, *MAP2K1*, in 17/21 (33%), mostly in-frame deletions on exons 1 and 2, in those with wild-type *BRAF* [78]. Mutations observed in *MAP2K1* resulted in upregulation of MAPK in HEK293 cells, and in increased sensitivity to MEK inhibitor drug. Similarly, mutations in *MAP2K1* were reported in other case studies of LCH with a frequency of 10-21% [79, 80]. Reported mutations in other MAPK-associated genes, included *ERBB3, MAP3K1* and *ARAF* [78, 80, 81].

Clinically, LCH has a wide spectrum of manifestations, varying from single self-resolving lesions, to highly aggressive and metastatic disease requiring intense systemic chemotherapy. LCH presents most commonly as skin eruptions or painful bone lesions [82]. In neonates, LCH manifests as vesicles and pustules; while in infants, inflamed and papular lesions are common. Lytic bone lesions are painful and involve the skull, extremities or other flat bones. Additional systemic sites are bone marrow, liver, spleen and CNS. A pulmonary form has been strongly linked with smoking [83].

Patients with LCH involving bone marrow, liver and spleen are classified as "high risk LCH", for which reported mortality rates are over 20%. In contrast, cases of "low risk LCH", limited to non-risk organs, survive nearly 100% of the time [84]. Clinical risk status was not correlated to *BRAF*^{V600E} genotype in a large pool of cases, however, the detection of *BRAF*^{V600E} in circulating cells (0.02-2.2% of PBMC) correlated with higher incidence of recurrence and multi-organ involvement, regardless of the group risk [77].

Histologically, there is no distinction across levels of severity of the disease, which led to the concept of "histiocytosis X" [85]. Langerhans cells are defined morphologically as cells with pale cytoplasm and grooved reniform nucleus, and LCH cells are characterize with a "benign" morphology where mitoses are rarely seen. In comparison to other DCs, Langerhans cells have a lower expression of MHC II, intermediate levels of CD11c, and high levels of langerin [86]. The immunohistochemical markers mostly specific for LCH are CD1a [71], and CD207/langerin [77, 87]. Although LCH can also be positive for S100, CD45, CD101 and CD68. The presence of cytoplasmic Birbeck granules, a feature of epidermal Langerhans cells, can be observed in neoplastic DCs in LCH by electron microscopy [87].

When confined to a single site, LCH is mostly treated surgically with possible adjuvant radiation therapy. In the case of multisystemic disease of with certain presentations (CNS, liver, spleen), systemic therapy is recommended. LC Histiocyte Society guidelines recommend prednisone and vinblastine for 12 months for multisystemic disease for LCH, plus mercaptopurine for high risk patients [84, 88]. However,

resistance or disease recurrence is seen in over half of the cases, which is a poor prognostic factor associated with 57% of survival [88]. Rescue protocols using agents such as cladribine showed promising results, but lacked long term response [89].

As the role of oncogenic MAPK pathway is established in LCH, patients can take advantage of targeted therapies. Treatment of *BRAF*^{V600E} mutated LCH cases with vemurafenib, a BRAF inhibitor, has shown promising results, resulting in a phase 2 clinical trial of LCH or EDC patients [76, 90, 91].

1.4 Erdheim-Chester disease (ECD) in humans

ECD is characterized by xanthogranulomatous multi-system infiltration of typically foamy or lipid-laden histiocytes with surrounding inflammation and fibrosis. Mean age at presentation ranges from 55 to 60 years, with a male predilection [92].

Similar to LCH, mutations in MAPK genes are frequently present in ECD. The most important mutation is *BRAF*^{V600E}, reported with a frequency of 54-57.5% of the cases [93, 94]. Mutations in other key genes have been reported including *NRAS*, *KRAS* and *ARAF* [93, 95, 96]. In the same cohort of cases, *PI3KCA* mutation was present in 10.9% [93]. When put together, mutations activating MAPK summed more than 80% of all ECD cases [97].

The most involved organs include bone (95%) with bilateral symmetric osteoesclerosis [98], cardiovascular system (50%) [99], CNS (51%) [92], and retroperitoneal fibrosis (33%). Diabetes insipidus and/or exophthalmos is seen in 20-30% of the cases [92]. Extracutaneous location and disseminated form of disease, as well as the presence of gain-of-function mutations in oncogenic MAPK genes are features that can be utilized to differentiate ECD from JXG [47].

Immunohistochemical characterization of ECD is based on positive factor XIIIa, CD68 and CD163, and negative CD1a and S100 [47]. The differentiation to LCH is based on negativity to CD1a (langerin) and S100 [100]. ECD has been considered a malignancy associated with an important inflammatory

component, with the detection of high levels of circulating cytokines (IFNα, IL12, MCP1, IL4 and IL7) [101], that may be involved in the local activation and recruitment of histiocytes.

Therapy with interferon-alpha is a commonly used approach for ECD, for which 1-year and 5-year survival rates were reported as 96% and 68%, respectively, based on a multi-institutional study of 58 cases [92].

A clinical trial of vemurafenib for ECD carrying *BRAF*^{V600E} mutation showed promising results [102]. The overall response rate was 54.5%, and although PFS and OS was not reached, a 2-year PFS was 86%, and 2-year OS was 96%. Based on these results, vemurafenib was approved by the FDA for *BRAF*-mutant ECD patients.

1.5 Discussion

In both dogs and humans, histiocytic and dendritic cell neoplasms are rare diseases with variable clinical presentation and behavior, ranging from benign and self-resolving, to highly aggressive and metastatic malignancies. These entities are not related by their cell of origin per se, but rather by the cellular functional properties of phagocytosis and/or antigen processing and presentation. Morphological characteristics are insufficient to differentiate each proliferative process; thus immunohistochemical characterization is an essential tool for an accurate diagnosis. Differential diagnosis includes B and T cell lymphomas, melanoma, metastatic sarcoma, and metastatic carcinoma [48].

Human histiocytic and dendritic cell neoplasms are described by the current 2016 WHO classification as a group that incorporates histiocytic sarcoma (HS), Langerhans cell histiocytosis (LCH), Langerhans cell sarcoma (LCS), indeterminate dendritic cell tumor (IDCT), interdigitating dendritic cell sarcoma (IDCS), follicular dendritic cell sarcoma (FDCS), fibroblastic reticular cell tumor (FRCT), disseminated juvenile xanthogranuloma (JXG), and Erdheim-Chester disease (ECD) [46]. The classification of this

heterogeneous group has been modified for the past 30 years as new findings on cellular characterization, clinical behavior and molecular drivers were discovered [47].

In dogs, histiocytic diseases include cutaneous histiocytoma, Langerhans cell histiocytosis, cutaneous or systemic reactive histiocytosis, HS, and HHS. They can originate either from Langerhans cells (cutaneous histiocytoma and Langerhans cell histiocytosis), interstitial dendritic cells (cutaneous/systemic reactive histiocytosis and HS), or macrophages (HHS) [103]. Among them, HS particularly presents the most aggressive behavior and poor outcome in dogs, and has been one of the main subjects of study in our laboratory.

As the classification of histiocytic diseases within each specie is still been consolidated, it is natural that matching a type of histiocytic disease in dogs with a counterpart in humans would be challenging. That is the case with HS, where we can find many similarities between humans and dogs, as well as differences. HS in both species is diagnosed mostly in adults, and it can present either locally or disseminated to multiple organs, including lymph nodes, skin/subcutis, spleen, liver, CNS and lungs, although it can develop anywhere in the body. In dogs and humans, metastasis is frequently seen and due to a rapid progression and lack of effective treatment, patients invariably carry a poor prognosis.

Histologically, canine and human HS are comparable, and usually described as large, pleomorphic cells with abundant amounts of eosinophilic or vacuolated cytoplasm. Multinucleated giant cells and atypical mitosis are common. Cytophagocytosis or hemophagocytosis may be present, as well as an infiltration of inflammatory cells.

Characterization of cells using IHC markers revealed that cHS are primarily neoplasms of interstitial dendritic cells, whereas hHS cells are likely of macrophage lineage. However, in both species, tumors are positive for macrophage specific markers (CD68 and CD163 for humans, CD204 for dogs). Interestingly, most of cHS positive for CD204, were also positive for CD163, a marker used in the diagnosis of hHS [104], which may represent a shared cell marker. Furthermore, DCs such as interdigitating cells of

lymphoid tissues and Langerhans cells, as well as Langerhans cells related histiocytic neoplasms are negative for CD204 [36, 105], a feature observed with CD163 [106]. Additional studies comparing IHC markers between dogs and humans would be helpful to better understand common phenotypes, however, several antibodies used in human tissues either lack specificity for dogs, or many times may target different populations of cells.

The pathogenesis of either cHS or hHS remains unclear. However, in both species, there are evidences suggesting the role of an oncogenic MAPK pathway, in some cases, driven by the same mutation. Activating mutations in MAPK key genes have been reported in hHS, including *BRAF* (V600E [54, 55, 94], G464V, G466R, NS581S [20]), *KRAS* [20], *HRAS* [59], and *MAP2K1* [75, 78, 94, 107, 108]. Mutations in *PTPN11* that encodes SHP2, upstream of MAPK and PI3K, were reported in four cases of hHS [19-22], two of them of E76K variant [20, 22] and one of G503V variant [20]. The same mutation *PTPN11*^{E76K} was found to be associated with cHS in Bernese mountain dog (36.7% in BMD vs. 8.7% in other breeds), the breed with highest incidence of HS (~25%) [18]. In addition, preliminary data from our laboratory have shown that *KRAS*^{H61Q}, reported in one case of hHS, was found to be present in about 3% of canine HS in a cohort of 96 cases. Additional comparative characteristics of HS in humans and dogs can be found in **Table 1.3**.

Among human histiocytic and dendritic cell neoplasms, LCH and ECD are also entities that can behave aggressively, and share characteristics with HS. LCH neoplasms originate from Langerhans cells that are epithelial dendritic cells; while ECD originates from histiocytes. Similar to HS, LCH and ECD can present as a disseminated disease with multi-organ involvement, although in general, patients carry a better outcome when compared to HS.

Most of LCH and ECD neoplasms were found to be driven by an oncogenic MAPK pathway, and as they carry a significant higher incidence of *BRAF*^{V600E} mutation when compared to other histiocytic disorders [94], these two entities were grouped together based on a recent revised classification of histiocytic

diseases [47], while HS was placed in a separate group. **Table 1.4** contains additional clinicopathological characteristics of LCH and ECD.

Although it is not possible to draw a straight line correlating diseases seen in different species, similar diseases certainly share nodes that can contribute to further understand their pathogenesis. HS was also observed in mouse as a spontaneous developing malignancy. In about 12.6% of C57BL/6J female mice, HS spontaneously developed at older ages (more than 2 years), and was commonly seen in the liver and spleen, although other organs were also involved (uterus, lungs and lymph nodes) [109, 110]. Histologically, murine HS is characterized by large clusters of atypical histiocytes with abundant eosinophilic cytoplasm and by the presence of multinucleated giant cells. Immunohistochemically, murine HS cells are positive for F4/80 and CD204, and weakly/moderately positive for CD68, while negative for cell markers for lymphocytes (CD45R, CD5), smooth muscle cells (alfa-SMA, desmin) and endothelial cells (factor VIIIa). In an experimental mouse model, a combination of loss of tumor suppressors *PTEN* and *INK4/ARF* lead to the development of HS in multiple tissues, including spleen and liver, suggesting the role of *PTEN* in the development of HS [111].

In conclusion, despite the efforts to unravel the causative events in HS in dogs and humans, a full understanding of the factors underlying tumorigenesis has not been yet achieved. Additional studies to better understand the causative events and genetic signature are warranted. For a rare malignancy in humans, utilizing dogs spontaneously developing HS with a significantly higher incidence of the disease provides an opportunity to gain more knowledge towards better treatment approaches for both the canine and human patients.

Given this background, a number of studies were planned to gain further insight into the biology of canine HS, focusing on BMDs, to identify key drivers of tumorigenesis that could be targeted by drugs. In the following chapters, I present the establishment of HS cell lines from BMD HS patients, drug

screening studies, the establishment of the first reported orthotopic xenograft model of HS, and the investigation of somatic mutations present in canine HS.

APPENDIX

Table 1.1. Immunohistochemical expression patterns for canine histiocytic diseases.

		Langerhans cells, DCs	Helper T cells, activated DCs	DCs, NK1 cells	Macrophages	Leukocytes	Macrophage scavenger receptor	Antigen presenting cells	Interstitial DCs	Epidermal Langerhans cells	Mesenchymal cells
	Cell Type	CD1a	CD4	CD11c	CD11d	CD18	CD204	MHCII	Thy-1 (CD90)	E-cad	Vimentin
Cutaneous histiocytoma	Langerhans cells	+	-	+	-	+	-	+	-	+	
Cutaneous Langerhans cell histiocytosis	Langerhans cells	+	-	+	-	+	-	+	-	+	
Reactive histiocytosis	Activated dermal interstitial DCs	+	+	+	-	+	+	+	+	-	
Histiocytic sarcoma	Interstitial DCs	+	-	+	-	+	+	+	-*	-	+
Hemophagocytic HS	Macrophages	+/-	-	-	+	+	+		-	-	+

Antibodies optimized for only frozen tissue samples are in red. *Cutaneous HS are positive for CD90

Table 1.2. Immunohistochemical expression patterns for human dendritic cells and histiocytic diseases

		Langerhans cells, DCs	Langerin	DCs, NK1 cells	Monocytes, macrophages	Monocytes, macrophages	Activated macrophages	Antigen presenting cells	DCs	Leukocytes	Dendritic cells	Follicular DCs	Follicular DCs	Fibrous-associated cells	Mesenchymal cells
	Cell Type	**CD1a**	**CD207**	**CD11c**	**CD68**	**CD163**	**Lysozyme**	**MHCII**	**S100**	**CD45**	**CD21**	**CD23**	**CD35**	**FXIIIa**	**Desmin, VIM, SMA**
Langerhans cell histiocytosis	Langerhans cells	+	+	+	-	+		Low	+	+/-				-	
Langerhans cell sarcoma	Langerhans cells	+	+		+/-			+	+	+	-				
Indeterminate DC tumor	Dendritic accessory cells	+	-		+	-			+		-	-	-		
Interdigitating DC sarcoma	Interdigitating DCs	-			+		+		+	+/-	-	-	-	-	+
Histiocytic sarcoma	Macrophages	-	-		+	+	+		-	-	-		-		-
Follicular DC sarcoma	Follicular DCs	-			+/-		-		+/-		+	+	+		+
Fibroblastic reticular cell tumor	Fibroblastic reticular cells	-									-		-	+	+
Disseminated juvenile xanthogranuloma	Histiocytes	-			+	+	+							+	+
Erdheim-Chester disease	Histiocytes	-			+	+			-						

Table 1.3. Comparison of clinicopathological characteristics between human and canine HS

	Human HS	Canine HS
Incidence	<1% of all hematopoietic neoplasms [1, 2]	<1% of all cancers [3] >25% Bernese mountain dogs [4, 5] Flat-coated retrievers (36% of all their neoplasms) [6, 7] Golden retriever and Rottweiler [8-10]
Age	6 months to 89 years, median age: 46 years Bimodal distribution with small peak at 0-29 years, and a larger peak at 50-69 years [11-13]	Mostly adult age 8-10 years, rare in younger dogs [5, 6, 9, 14-16].
Gender	Male predominance (male:female = 82:56) [11, 17]	No gender predilection
Genetic mutations	PTPN11, including E76K variant [18-21] KRAS [19], HRAS [22], MAP2K1 [23-27] KDR [19] BRAF V600E [25, 28, 29], G464V, G466R, NS581S [19]	$PTPN11^{E76K}$ in BMD (36.67%) and other breeds (8.69%) [30] $KRAS^{H61Q}$ in BMD (5%) PTEN [31]
Location	Localized or disseminated. Lymph nodes, but often in extranodal sites such as gastrointestinal tract, spleen, lungs, head and neck, salivary gland, mediastinum, breast, liver, pancreas, kidney, uterus, CNS, bone, BM [11, 12]	Localized, disseminated or hemophagocytic HS. Skin/subcutis, peri-articular tissues, spleen, liver, lymph nodes, lung, bone marrow [8, 32]
On cytology	Large epithelioid tumor cells with pronounced nuclear pleomorphism, multinucleation, voluminous/vacuolated cytoplasm, and reniform or Pac-Man-like nuclei in an inflammatory background with lymphoglandular bodies and cytophagocytosis [33]	Pleomorphic neoplastic round cells with marked anisocytosis and anisokaryosis with numerous binucleated and multinucleated cells. [34]
On histology	Large epithelioid cells with abundant eosinophilic cytoplasm. Cells with well-defined cell borders and nuclei with vesicular chromatin and prominent nucleoli. Multinucleated giant cells and pleomorphism may be present, and focal spindle cell sarcomatoid morphology is occasionally seen. Inflammatory infiltrate of neutrophils, small lymphocytes or eosinophils. [12]	Dense pleomorphic cell proliferation with multiple areas of necrosis. Individualized large round cells with abundant amphophilic cytoplasm, occasionally vacuolized. Dense proliferations of plump spindle cells with long cytoplasmic processes. Multinucleated giant cells are common. Marked anisokaryosis. Large vesicular nuclei of round or oval or indented and twisted with one or several nucleoli. [8] Infiltration of lymphocytes, mostly FOXP3 Treg cells [35].
IHC markers	CD68 (Histiocyte marker) CD163 (hemoglobin scavenger receptor, histiocyte marker) Lysozyme (Histiocyte marker) PU.1 (macrophage and B-cell TF) CD31 (vascular marker related to macrophages) Negative for: CD1a, CD207 (langerin), S100, CD21, CD35	CD18 (β2 adhesion leukocyte integrin) CD204 (class A macrophage scavenger receptor) CD11d (hemophagocytic HS) CD1, CD11c, MHC class II, and ICAM-1 Negative: CD3, CD79a
Differential diagnosis	Other large cell malignancies, including non-Hodgkin lymphomas (DLBCL and ALCL), metastatic melanoma and metastatic undifferentiated carcinoma	Other round cell neoplasms including poorly differentiated melanoma, carcinoma, and lymphoma
Metastasis	5 of 10 cases of extranodal HS [12] 9 of 15 cases [13]	70-91% metastasis [7, 9, 32, 36]

Table 1.3. (cont'd)

Treatment	Surgical resection, RT, chemotherapy with lymphoma-based protocols	Surgical resection, RT, chemotherapy with lomustine and/or doxorubicin
Survival time	OS: < 2 years [12, 17, 37]	MST peri-articular HS: 391 days MST non-periarticular HS: 128 days [32] MST HHS: < 60 days [38]
Prognostic factors	Possibly tumor size and stage of the disease	Stage of the disease

Table 1.4. Comparison of clinicopathological characteristics between human Langerhans cell histiocytosis and Erdheim-Chester disease

	LCH	**ECD**
Incidence	<15ys: 5-9 cases/million/year >15ys: 1 case/million/year [39-41]	Rare, 600-700 reported cases
Age	Median 30 months (primarily young age, adult cases may occur)	Mean 55-60ys (pediatric cases are rare) [42]
Gender	Male predominance	Male predominance
Genetic mutations	BRAF V600E (36-64%) [24, 27, 43-45] MAP2K1 (10-33%) [27] ERBB3, MAP3K1, ARAF [27, 46, 47]	BRAF V600E (54-57.5%) PI3KCA (10.9%) [48] NRAS, KRAS, ARAF [48-50]
Location	Skin, bone, bone marrow, spleen, liver and CNS [45]	Multi-organ involvement: bone (96%) with symmetric diaphyseal and metaphyseal osteosclerosis, cardiovascular (77%), CNS (51%), pulmonary (43-53%), orbital (27%) [42]
On histology	Histiocytes are mononucleated with kidney shaped nuclei. Eosinophils and multinucleated giant cells may be present. Birbeck granules on electron microscopy.	Foamy mononuclear histiocytes, with presence of fibrosis, reactive lymphocytes, neutrophils and plasma cells. Touton giant cells.
IHC markers	CD1a+, langerin (CD207)+, S100+, CD68+, CD163+, factor XIIIa-	CD68+, CD163+, CD1a-, S100-
Treatment	Vinblastine and prednisone for 12 months for multisystemic disease, plus mercaptopurine for high risk [51, 52] Vemurafenib and dabrafenib (clinical trials) [44, 53, 54]	Interferon alfa [42] Vemurafenib [55]
Survival time		1-y ST: 96%, 5-y ST: 68% [42]
Prognostic factors	Location (high vs. low risk organs), and resistance to therapy [51]	

BIBLIOGRAPHY

BIBLIOGRAPHY

1. Bruner SR, *Updates in therapeutics for veterinary dermatology.* The Veterinary clinics of North America. Small animal practice, 2006. 36(1): p. 39.

2. Abadie J, Hedan B, et al., *Epidemiology, pathology, and genetics of histiocytic sarcoma in the Bernese mountain dog breed.* J Hered, 2009. 100 Suppl 1: p. S19.

3. Dervisis NG, Kiupel M, et al., *Clinical prognostic factors in canine histiocytic sarcoma.* Vet Comp Oncol, 2016.

4. Dobson J, Hoather T, et al., *Mortality in a cohort of flat-coated retrievers in the UK.* Vet Comp Oncol, 2009. 7(2): p. 115.

5. Fidel J, Schiller I, et al., *Histiocytic sarcomas in flat-coated retrievers: a summary of 37 cases (November 1998-March 2005).* Vet Comp Oncol, 2006. 4(2): p. 63.

6. Affolter VK and Moore PF, *Localized and disseminated histiocytic sarcoma of dendritic cell origin in dogs.* Vet Pathol, 2002. 39(1): p. 74.

7. Craig LE, Julian ME, et al., *The diagnosis and prognosis of synovial tumors in dogs: 35 cases.* Vet Pathol, 2002. 39(1): p. 66.

8. Skorupski KA, Clifford CA, et al., *CCNU for the treatment of dogs with histiocytic sarcoma.* J Vet Intern Med, 2007. 21(1): p. 121.

9. Lenz JA, Furrow E, et al., *Histiocytic sarcoma in 14 miniature schnauzers - a new breed predisposition?* J Small Anim Pract, 2017. 58(8): p. 461.

10. Takahashi M, Tomiyasu H, et al., *Clinical characteristics and prognostic factors in dogs with histiocytic sarcomas in Japan.* J Vet Med Sci, 2014. 76(5): p. 661.

11. Constantino-Casas F, Mayhew D, et al., *The clinical presentation and histopathologic-immunohistochemical classification of histiocytic sarcomas in the Flat Coated Retriever.* Vet Pathol, 2011. 48(3): p. 764.

12. Dobson JM, *Breed-predispositions to cancer in pedigree dogs.* ISRN Vet Sci, 2013. 2013: p. 941275.

13. Morris JS, Bostock DE, et al., *Histopathological survey of neoplasms in flat-coated retrievers, 1990 to 1998.* The Veterinary record, 2000. 147(11): p. 291.

14. Ruple A and Morley PS, *Risk Factors Associated with Development of Histiocytic Sarcoma in Bernese Mountain Dogs.* J Vet Intern Med, 2016. 30(4): p. 1197.

15. Hedan B, Thomas R, et al., *Molecular cytogenetic characterization of canine histiocytic sarcoma: A spontaneous model for human histiocytic cancer identifies deletion of tumor suppressor genes*

and highlights influence of genetic background on tumor behavior. BMC Cancer, 2011. 11: p. 201.

16. Shearin AL, Hedan B, et al., *The MTAP-CDKN2A locus confers susceptibility to a naturally occurring canine cancer.* Cancer Epidemiol, 2012. 21(7): p. 1019.

17. Asada H, Tsuboi M, et al., *A 2-base insertion in exon 5 is a common mutation of the TP53 gene in dogs with histiocytic sarcoma.* J Vet Med Sci, 2017. 79(10): p. 1721.

18. Thaiwong T, Sirivisoot S, et al., *Gain-of-function mutation in PTPN11 in histiocytic sarcomas of Bernese Mountain Dogs.* Vet Comp Oncol, 2017.

19. Zhang Q, Shibani A, et al., *an aggressive multifocal primary CNS histiocytosis with PTPN11 (Shp2) mutation.* Neuropathol Appl Neurobiol, 2017.

20. Liu Q, Tomaszewicz K, et al., *Somatic mutations in histiocytic sarcoma identified by next generation sequencing.* Virchows Arch, 2016. 469(2): p. 233.

21. Batra S, Martin SC, et al., *Histiocytic Sarcoma Associated with Coombs Negative Acute Hemolytic Anemia: A Rare Presentation.* Case Rep Oncol Med, 2016. 2016: p. 3179147.

22. Voruz S, Cairoli A, et al., *Response to MEK inhibition with trametinib and tyrosine kinase inhibition with imatinib in multifocal histiocytic sarcoma.* Haematologica, 2018. 103(1): p. e39.

23. Boerkamp KM, van der Kooij M, et al., *Gene expression profiling of histiocytic sarcomas in a canine model: the predisposed flatcoated retriever dog.* PLoS One, 2013. 8(8): p. e71094.

24. Tagawa M, Maekawa N, et al., *Evaluation of Costimulatory Molecules in Peripheral Blood Lymphocytes of Canine Patients with Histiocytic Sarcoma.* PLoS One, 2016. 11(2): p. e0150030.

25. Marcinowska A, Constantino-Casas F, et al., *T Lymphocytes in Histiocytic Sarcomas of Flat-Coated Retriever Dogs.* Vet Pathol, 2017. 54(4): p. 605.

26. Larregina AT, Morelli AE, et al., *Dermal-resident CD14+ cells differentiate into Langerhans cells.* Nat Immunol, 2001. 2(12): p. 1151.

27. Shortman K and Liu YJ, *Mouse and human dendritic cell subtypes.* Nature reviews. Immunology, 2002. 2(3): p. 151.

28. Klahn SL, Kitchell BE, et al., *Evaluation and comparison of outcomes in dogs with periarticular and nonperiarticular histiocytic sarcoma.* J Am Vet Med Assoc, 2011. 239(1): p. 90.

29. Skorupski KA, Clifford CA, et al., *CCNU for the treatment of dogs with histiocytic sarcoma.* Journal of veterinary internal medicine / American College of Veterinary Internal Medicine, 2007. 21(1): p. 121.

30. van Kuijk L, van Ginkel K, et al., *Peri-articular histiocytic sarcoma and previous joint disease in Bernese Mountain Dogs.* Journal of veterinary internal medicine / American College of Veterinary Internal Medicine, 2013. 27(2): p. 293.

31. Skorupski KA, Rodriguez CO, et al., *Long-term survival in dogs with localized histiocytic sarcoma treated with CCNU as an adjuvant to local therapy.* Vet Comp Oncol, 2009. 7(2): p. 139.

32. Noti JD, *Expression of the myeloid-specific leukocyte integrin gene CD11d during macrophage foam cell differentiation and exposure to lipoproteins.* Int J Mol Med, 2002. 10(6): p. 721.

33. Moore PF, Affolter VK, et al., *Canine hemophagocytic histiocytic sarcoma: a proliferative disorder of CD11d+ macrophages.* Vet Pathol, 2006. 43(5): p. 632.

34. Rassnick KM, Moore AS, et al., *Phase II, open-label trial of single-agent CCNU in dogs with previously untreated histiocytic sarcoma.* Journal of veterinary internal medicine / American College of Veterinary Internal Medicine, 2010. 24(6): p. 1528.

35. Withrow SJ, Vail DM, et al., *Withrow and MacEwen's small animal clinical oncology*. 5th ed. 2013, St. Louis, Mo.: Elsevier/Saunders. xvi.

36. Kato Y, Murakami M, et al., *The class A macrophage scavenger receptor CD204 is a useful immunohistochemical marker of canine histiocytic sarcoma.* J Comp Pathol, 2013. 148(2-3): p. 188.

37. Kato Y, Funato R, et al., *Immunocytochemical detection of the class A macrophage scavenger receptor CD204 using air-dried cytologic smears of canine histiocytic sarcoma.* Vet Clin Pathol, 2014. 43(4): p. 589.

38. Moore P. *The histiocyte disease complex*. in *American College of Veterinary Internal Medicine Annual Meeting*. 2004. Minneapolis, MN.

39. Rassnick KM, Moore AS, et al., *Phase II, open-label trial of single-agent CCNU in dogs with previously untreated histiocytic sarcoma.* J Vet Intern Med, 2010. 24(6): p. 1528.

40. Higuchi T, Dervisis N, et al. *Efficacy of doxorubicin for histiocytic sarcoma in dogs*. in *30th Annual Veterinary Cancer Society Meeting Conference*. 2010. San Diego.

41. Cannon C, Borgatti A, et al., *Evaluation of a combination chemotherapy protocol including lomustine and doxorubicin in canine histiocytic sarcoma.* J Small Anim Pract, 2015. 56(7): p. 425.

42. Hafeman SD, Varland D, et al., *Bisphosphonates significantly increase the activity of doxorubicin or vincristine against canine malignant histiocytosis cells.* Vet Comp Oncol, 2012. 10(1): p. 44.

43. Vail DM, Kravis LD, et al., *Preclinical trial of doxorubicin entrapped in sterically stabilized liposomes in dogs with spontaneously arising malignant tumors.* Cancer Chemother Pharmacol, 1997. 39(5): p. 410.

44. Poirier VJ, Hershey AE, et al., *Efficacy and toxicity of paclitaxel (Taxol) for the treatment of canine malignant tumors.* J Vet Intern Med, 2004. 18(2): p. 219.

45. Visonneau S, Cesano A, et al., *Successful treatment of canine malignant histiocytosis with the human major histocompatibility complex nonrestricted cytotoxic T-cell line TALL-104.* Clin Cancer Res, 1997. 3(10): p. 1789.

46. Swerdlow SH, Campo E, et al., *The 2016 revision of the World Health Organization classification of lymphoid neoplasms.* Blood, 2016. 127(20): p. 2375.

47. Emile JF, Abla O, et al., *Revised classification of histiocytoses and neoplasms of the macrophage-dendritic cell lineages.* Blood, 2016. 127(22): p. 2672.

48. Dalia S, Jaglal M, et al., *Clinicopathologic characteristics and outcomes of histiocytic and dendritic cell neoplasms: the moffitt cancer center experience over the last twenty five years.* Cancers (Basel), 2014. 6(4): p. 2275.

49. Jaffe ES and World Health Organization., *Pathology and genetics of tumours of haematopoietic and lymphoid tissues*. World Health Organization classification of tumors. 2001, Lyon: IARC Press. 351 p.

50. Jaffe ES, *Histiocytoses of lymph nodes: biology and differential diagnosis.* Semin Diagn Pathol, 1988. 5(4): p. 376.

51. Takahashi E and Nakamura S, *Histiocytic sarcoma : an updated literature review based on the 2008 WHO classification.* Journal of clinical and experimental hematopathology : JCEH, 2013. 53(1): p. 1.

52. Hornick JL, Jaffe ES, et al., *Extranodal histiocytic sarcoma: clinicopathologic analysis of 14 cases of a rare epithelioid malignancy.* Am J Surg Pathol, 2004. 28(9): p. 1133.

53. Gounder M, Desai V, et al., *Impact of surgery, radiation and systemic therapy on the outcomes of patients with dendritic cell and histiocytic sarcomas.* Eur J Cancer, 2015. 51(16): p. 2413.

54. Michonneau D, Kaltenbach S, et al., *BRAFV600E Mutation in a Histiocytic Sarcoma Arising From Hairy Cell Leukemia.* J Clin Oncol, 2014. 32(35): p. e117.

55. Idbaih A, Mokhtari K, et al., *Dramatic response of a BRAF V600E-mutated primary CNS histiocytic sarcoma to vemurafenib.* Neurology, 2014. 83(16): p. 1478.

56. Facchetti F, Pileri SA, et al., *Histiocytic and dendritic cell neoplasms: what have we learnt by studying 67 cases.* Virchows Arch, 2017. 471(4): p. 467.

57. Go H, Jeon YK, et al., *Frequent detection of BRAF(V600E) mutations in histiocytic and dendritic cell neoplasms.* Histopathology, 2014. 65(2): p. 261.

58. Shimono J, Miyoshi H, et al., *Prognostic factors for histiocytic and dendritic cell neoplasms.* Oncotarget, 2017. 8(58): p. 98723.

59. Kordes M, Roring M, et al., *Cooperation of BRAF(F595L) and mutant HRAS in histiocytic sarcoma provides new insights into oncogenic BRAF signaling.* Leukemia, 2016. 30(4): p. 937.

60. Hung YP, Lovitch SB, et al., *Histiocytic sarcoma: New insights into FNA cytomorphology and molecular characteristics.* Cancer Cytopathol, 2017. 125(8): p. 604.

61. Pileri SA, Grogan TM, et al., *Tumours of histiocytes and accessory dendritic cells: an immunohistochemical approach to classification from the International Lymphoma Study Group based on 61 cases.* Histopathology, 2002. 41(1): p. 1.

62. Kommalapati A, Tella SH, et al., *Histiocytic sarcoma: a population-based analysis of incidence, demographic disparities, and long-term outcomes.* Blood, 2018. 131(2): p. 265.

63. Clifton W, Akinduro OO, et al., *Infection or Glioma? The False Dilemma of Primary Central Nervous System Histiocytic Sarcoma.* World Neurosurg, 2017. 106: p. 1053 e1.

64. Vos JA, Abbondanzo SL, et al., *Histiocytic sarcoma: a study of five cases including the histiocyte marker CD163.* Mod Pathol, 2005. 18(5): p. 693.

65. Lau SK, Chu PG, et al., *CD163: a specific marker of macrophages in paraffin-embedded tissue samples.* Am J Clin Pathol, 2004. 122(5): p. 794.

66. Nguyen TT, Schwartz EJ, et al., *Expression of CD163 (hemoglobin scavenger receptor) in normal tissues, lymphomas, carcinomas, and sarcomas is largely restricted to the monocyte/macrophage lineage.* Am J Surg Pathol, 2005. 29(5): p. 617.

67. Tsujimura H, Miyaki T, et al., *Successful treatment of histiocytic sarcoma with induction chemotherapy consisting of dose-escalated CHOP plus etoposide and upfront consolidation auto-transplantation.* Int J Hematol, 2014. 100(5): p. 507.

68. Zeidan A, Bolanos-Meade J, et al., *Human leukocyte antigen-haploidentical hematopoietic stem cell transplant for a patient with histiocytic sarcoma.* Leuk Lymphoma, 2013. 54(3): p. 655.

69. Shukla N, Kobos R, et al., *Successful treatment of refractory metastatic histiocytic sarcoma with alemtuzumab.* Cancer, 2012. 118(15): p. 3719.

70. Berres ML, Merad M, et al., *Progress in understanding the pathogenesis of Langerhans cell histiocytosis: back to Histiocytosis X?* Br J Haematol, 2015. 169(1): p. 3.

71. Newman B, Hu W, et al., *Aggressive histiocytic disorders that can involve the skin.* J Am Acad Dermatol, 2007. 56(2): p. 302.

72. Guyot-Goubin A, Donadieu J, et al., *Descriptive epidemiology of childhood Langerhans cell histiocytosis in France, 2000-2004.* Pediatr Blood Cancer, 2008. 51(1): p. 71.

73. Stalemark H, Laurencikas E, et al., *Incidence of Langerhans cell histiocytosis in children: a population-based study.* Pediatr Blood Cancer, 2008. 51(1): p. 76.

74. Gatalica Z, Bilalovic N, et al., *Disseminated histiocytoses biomarkers beyond BRAFV600E: frequent expression of PD-L1.* Oncotarget, 2015. 6(23): p. 19819.

75. Badalian-Very G, Vergilio JA, et al., *Recurrent BRAF mutations in Langerhans cell histiocytosis.* Blood, 2010. 116(11): p. 1919.

76. Bubolz AM, Weissinger SE, et al., *Potential clinical implications of BRAF mutations in histiocytic proliferations.* Oncotarget, 2014. 5(12): p. 4060.

77. Berres ML, Lim KP, et al., *BRAF-V600E expression in precursor versus differentiated dendritic cells defines clinically distinct LCH risk groups.* J Exp Med, 2014. 211(4): p. 669.

78. Chakraborty R, Hampton OA, et al., *Mutually exclusive recurrent somatic mutations in MAP2K1 and BRAF support a central role for ERK activation in LCH pathogenesis.* Blood, 2014. 124(19): p. 3007.

79. Xerri L, Adelaide J, et al., *CDKN2A/B Deletion and Double-hit Mutations of the MAPK Pathway Underlie the Aggressive Behavior of Langerhans Cell Tumors.* Am J Surg Pathol, 2018. 42(2): p. 150.

80. Nelson DS, van Halteren A, et al., *MAP2K1 and MAP3K1 mutations in Langerhans cell histiocytosis.* Genes Chromosomes Cancer, 2015. 54(6): p. 361.

81. Nelson DS, Quispel W, et al., *Somatic activating ARAF mutations in Langerhans cell histiocytosis.* Blood, 2014. 123(20): p. 3152.

82. Tran G, Huynh TN, et al., *Langerhans cell histiocytosis: A neoplastic disorder driven by Ras-ERK pathway mutations.* J Am Acad Dermatol, 2018. 78(3): p. 579.

83. Vassallo R and Limper AH, *Pulmonary Langerhans' cell histiocytosis.* Semin Respir Crit Care Med, 2002. 23(2): p. 93.

84. Gadner H, Grois N, et al., *Improved outcome in multisystem Langerhans cell histiocytosis is associated with therapy intensification.* Blood, 2008. 111(5): p. 2556.

85. Lichtenstein L, *Histiocytosis X; integration of eosinophilic granuloma of bone, Letterer-Siwe disease, and Schuller-Christian disease as related manifestations of a single nosologic entity.* AMA Arch Pathol, 1953. 56(1): p. 84.

86. Merad M, Romani N, et al., *Langerhans cells at the interface of medicine, science, and industry.* J Invest Dermatol, 2008. 128(2): p. 251.

87. Chikwava K and Jaffe R, *Langerin (CD207) staining in normal pediatric tissues, reactive lymph nodes, and childhood histiocytic disorders.* Pediatr Dev Pathol, 2004. 7(6): p. 607.

88. Gadner H, Minkov M, et al., *Therapy prolongation improves outcome in multisystem Langerhans cell histiocytosis.* Blood, 2013. 121(25): p. 5006.

89. Weitzman S, Braier J, et al., *2'-Chlorodeoxyadenosine (2-CdA) as salvage therapy for Langerhans cell histiocytosis (LCH). results of the LCH-S-98 protocol of the Histiocyte Society.* Pediatr Blood Cancer, 2009. 53(7): p. 1271.

90. Haroche J, Cohen-Aubart F, et al., *Dramatic efficacy of vemurafenib in both multisystemic and refractory Erdheim-Chester disease and Langerhans cell histiocytosis harboring the BRAF V600E mutation.* Blood, 2013. 121(9): p. 1495.

91. Haroche J, Cohen-Aubart F, et al., *Vemurafenib as first line therapy in BRAF-mutated Langerhans cell histiocytosis.* J Am Acad Dermatol, 2015. 73(1): p. e29.

92. Arnaud L, Hervier B, et al., *CNS involvement and treatment with interferon-alpha are independent prognostic factors in Erdheim-Chester disease: a multicenter survival analysis of 53 patients.* Blood, 2011. 117(10): p. 2778.

93. Emile JF, Diamond EL, et al., *Recurrent RAS and PIK3CA mutations in Erdheim-Chester disease.* Blood, 2014. 124(19): p. 3016.

94. Haroche J, Charlotte F, et al., *High prevalence of BRAF V600E mutations in Erdheim-Chester disease but not in other non-Langerhans cell histiocytoses.* Blood, 2012. 120(13): p. 2700.

95. Diamond EL, Abdel-Wahab O, et al., *Detection of an NRAS mutation in Erdheim-Chester disease.* Blood, 2013. 122(6): p. 1089.

96. Diamond EL, Durham BH, et al., *Diverse and Targetable Kinase Alterations Drive Histiocytic Neoplasms.* Cancer Discov, 2016. 6(2): p. 154.

97. Haroun F, Millado K, et al., *Erdheim-Chester Disease: Comprehensive Review of Molecular Profiling and Therapeutic Advances.* Anticancer Res, 2017. 37(6): p. 2777.

98. Haroche J, Amoura Z, et al., *Cardiovascular involvement, an overlooked feature of Erdheim-Chester disease: report of 6 new cases and a literature review.* Medicine (Baltimore), 2004. 83(6): p. 371.

99. Haroche J, Cluzel P, et al., *Images in cardiovascular medicine. Cardiac involvement in Erdheim-Chester disease: magnetic resonance and computed tomographic scan imaging in a monocentric series of 37 patients.* Circulation, 2009. 119(25): p. e597.

100. Diamond EL, Dagna L, et al., *Consensus guidelines for the diagnosis and clinical management of Erdheim-Chester disease.* Blood, 2014. 124(4): p. 483.

101. Arnaud L, Gorochov G, et al., *Systemic perturbation of cytokine and chemokine networks in Erdheim-Chester disease: a single-center series of 37 patients.* Blood, 2011. 117(10): p. 2783.

102. Diamond EL, Subbiah V, et al., *Vemurafenib for BRAF V600-Mutant Erdheim-Chester Disease and Langerhans Cell Histiocytosis: Analysis of Data From the Histology-Independent, Phase 2, Open-label VE-BASKET Study.* JAMA Oncol, 2017.

103. Maxie G, *Jubb, Kennedy & Palmer's Pathology of Domestic Animals*. 2015: Elsevier Health Sciences.

104. Thongtharb A, Uchida K, et al., *Histological and immunohistochemical studies on primary intracranial canine histiocytic sarcomas.* J Vet Med Sci, 2016. 78(4): p. 593.

105. Tomokiyo R, Jinnouchi K, et al., *Production, characterization, and interspecies reactivities of monoclonal antibodies against human class A macrophage scavenger receptors.* Atherosclerosis, 2002. 161(1): p. 123.

106. Ohnishi K, Komohara Y, et al., *Macrophages in Langerhans cell histiocytosis are differentiated toward M2 phenotype: their possible involvement in pathological processes.* Pathol Int, 2010. 60(1): p. 27.

107. Lee LH, Gasilina A, et al., *Real-time genomic profiling of histiocytoses identifies early-kinase domain BRAF alterations while improving treatment outcomes.* JCI Insight, 2017. 2(3): p. e89473.

108. Brown NA, Furtado LV, et al., *High prevalence of somatic MAP2K1 mutations in BRAF V600E-negative Langerhans cell histiocytosis.* Blood, 2014. 124(10): p. 1655.

109. Ohnishi K, Tanaka S, et al., *Immunohistochemical detection of possible cellular origin of hepatic histiocytic sarcoma in mice.* J Clin Exp Hematop, 2012. 52(3): p. 171.

110. Lacroix-Triki M, Lacoste-Collin L, et al., *Histiocytic sarcoma in C57BL/6J female mice is associated with liver hematopoiesis: review of 41 cases.* Toxicol Pathol, 2003. 31(3): p. 304.

111. Carrasco DR, Fenton T, et al., *The PTEN and INK4A/ARF tumor suppressors maintain myelolymphoid homeostasis and cooperate to constrain histiocytic sarcoma development in humans.* Cancer Cell, 2006. 9(5): p. 379.

112. Takada M, Parys M, et al., *A novel canine histiocytic sarcoma cell line: initial characterization and utilization for drug screening studies.* BMC Cancer, 2018. 18(1): p. 237.

CHAPTER 2

A NOVEL CANINE HISTIOCYTIC SARCOMA CELL LINE: INITIAL CHARACTERIZATION AND UTILIZATION FOR DRUG SCREENING STUDIES

This study was previously published under Creative Commons Attribution-Non Commercial License: Takada M, Parys M, Gregory-Bryson E, Vilar Saavedra P, Kiupel M, Yuzbasiyan-Gurkan V. A novel canine histiocytic sarcoma cell line: initial characterization and utilization for drug screening studies. BMC Cancer, Volume 18, pages 237 – 249, February 2018

2.1 Introduction

Histiocytic sarcoma (HS) is a highly aggressive hematopoietic neoplasm in humans and animals. In humans, HS accounts for less than 1% of all hematopoietic neoplasms [1, 2], affects all ages, but predominately adults, and involves lymph nodes and/or a variety of extranodal organs including skin, bone marrow, spleen, the gastrointestinal tract and the central nervous system [56, 57]. This malignancy is often approached with a combination of various modalities of treatment, including multi-drug chemotherapeutic protocols, radiation therapy, surgery, and bone marrow transplantation [58-60]. However, patients with HS in general respond poorly to any form of treatment, therefore this neoplasm carries a poor prognosis and has a high mortality rate. The low number of clinical cases is a limitation for an extended understanding of the pathogenesis of this disease in people, and restricts the investigation for novel and more efficacious forms of treatment.

In dogs, a similar disorder is commonly found in certain breeds, especially the Bernese mountain dog (BMD), in which the prevalence ranges from 15 to 25% of the population [4, 6, 38, 61, 62]. The genetic susceptibility to HS in dogs has been the focus of several investigations. Current published data of a population of BMD from US and Europe, suggests deregulation of the tumor suppressor genes *MTAP/CDKN2A*/*B* located within the region homologous to human chromosome 9p21 [63, 64]. Studying HS in dogs is of high importance as, similarly to people, it is a fatal disease characterized by rapid progression and high metastatic rate [7-9, 65]. Thus dogs, with spontaneously occurring HS, are a crucial model for development of new approaches to treat this orphan disease in people. Affected canine patients also respond poorly to treatment. The currently most effective drug is *N*-(2-chloroethyl)-*N*'-cyclohexyl-N-nitrosourea (CCNU) that provides a reported response rate ranging from 29 to 46% for a median survival time of 85-96 days [10, 65]. A preliminary study using another cytotoxic drug, doxorubicin, showed a similar response rate of 46% for a median survival time of 93 days [66]. Additional alternatives of treatment have been investigated on small cohorts of dogs, including delivery

of the human MHC non-restricted T-cell line TALL-104, frameless stereotactic radiosurgery, and chemotherapy using either paclitaxel or pegylated-liposomal doxorubicin; however, none has shown promising results [66-70].

Research groups have demonstrated the therapeutic potential of drugs as small molecule inhibitors against HS, based on *in vitro* studies [71-73]. Screening a large library of small molecules, Ito et al. successfully identified eight compounds of high potency (>60% inhibition) at concentration of 100nM [71]. Interestingly, only two drugs shared the same main target, showing the diversity of factors driving tumorigenesis in HS, and the potential benefit of drug combination hitting multiple targets. In humans, there is only a single report of four patients with HS treated with small molecule inhibitors, associated with the overexpression of targets for those drugs within the neoplasm, however efficacy could not be evaluated due to the small cohort of patients [74]. No published studies exist reporting the clinical use of small molecule inhibitors in dogs with HS.

We present here details of a novel HS cell line from a BMD, named the BD cell line, we have successfully established and demonstrated its utility in identification of potential novel therapeutic options [75]. Considering that to date, there is no human HS cell line available for research purposes, we believe that this cell line will provide an essential scientific tool for the study of this disease.

2.2 Materials and Methods

2.2.1 Origin of primary tumor

Fresh post-mortem tissue samples from both an abdominal and a pulmonary neoplasm were aseptically obtained from an 8-year-old spayed female BMD presented to the Michigan State University Veterinary Teaching Hospital. The diagnosis of HS was based on histopathology findings of the tumor and positive staining for CD18 by immunohistochemistry **(Figure 2.1)** [4, 8, 32, 76].

Treatment with various chemotherapeutic agents was attempted over a year, including CCNU, doxorubicin and prednisone. The dog responded with only short periods of tumor remission until the owners opted for humane euthanasia due to the poor physical condition of the animal. Samples were collected immediately following euthanasia under informed owner consent.

2.2.2 Preparation and maintenance of cell culture

The tissue samples were minced in small fragments with a surgical blade and placed in a solution of Hank's Balanced Salt Solution with 1% collagenase (Sigma) for cell disaggregation. After 40 minutes, the solution was transferred to a 70µm cell strainer, and the filtered portion was plated in Roswell Park Memorial Institute 1640 medium (Life Technologies) supplemented with 10% heat-inactivated fetal bovine serum (FBS) (Life Technologies), 1% antibiotic-antimycotic 100X (Life Technologies), and 0.1% gentamycin (Life Technologies). The cell culture was then incubated at 37^{o}C in a humidified atmosphere of 5% CO_2. For culture maintenance, the medium was thoroughly changed every 2-3 days. The cells were confirmed to be of canine origin and no mammalian interspecies contamination was detected based on results from CellCheck Plus test (IDEXX BioResearch). A genetic profile using a panel of microsatellite markers for genotyping is available and can be used in future monitoring, the detailed genotype is presented in **Table 2.3**.

2.2.3 Cytology and immunohistochemistry

Concentrated cytospin slide of cell suspension was prepared, and stained with Diff-Quik for morphologic characterization by a board certified veterinary clinical pathologist. For immunohistochemistry analysis of the cell line, the cell pellet was fixed in 10% formalin for up to 24 hours and transferred to 70% ethanol until embedding in paraffin. Sections from the paraffin block containing the cell pellet were

deparaffinized in xylene and rehydrated in ethanol at different concentrations. Hydrogen peroxide 3% was used to neutralize endogenous peroxidases.

Antigen retrieval of formalin-fixed, paraffin embedded tissues was performed on the PT Link (Dako North America), using the EnVision FLEX Target Retrieval Solution, Low pH (Dako North America) for 20 minutes. For immunolabeling with the primary antibodies (CD3, CD18, CD79a and CD204), sections were processed with the Autostainer Link 48 (Dako North America) using the EnVision Flex+ detection system (Dako North America), and the immunoreaction was visualized with 3,3'-diaminobenzidine substrate (DAB) (Dako North America) and sections were counterstained with haematoxylin. For immunolabeling with antibody vimentin, the Discovery Ultra Automated Staining system (Ventana Medical Systems) was used with UltraMap alkaline phosphatase red detection system (Ventana Medical Systems) with a red chromogen. Antigen retrieval was achieved using the Ventana medical System antigen retrieval solution CC1 (Ventana Medical Systems) for 60 mins. Details of the antibodies are available in **Table 2.4**.

2.2.4 Flow cytometry

BD cells harvested from cell culture were labeled with the following monoclonal antibodies: anti-canine CD3 (CA17.2A12, Serotec), anti-canine CD11c (CA11.6A1, UC Davis/NIH NeuroMab Facility), anti-bovine CD14 (MM61A, WSU MAC), anti-canine CD21 (CA2.1D6, Serotec), anti-canine CD45 (YKIX716.13, Serotec), anti-canine CD79a (HM57, LS Bio), anti-bovine CD172a (DH59B, WSU MAC), anti-canine MHC II (YKIX334.2, eBioscience), and anti-bovine MHC I (MHC CL I, WSU MAC). Isotype matched control antibodies were used to exclude non specific binding. The flow cytometers BD LSR II and BD Accuri C6 (BD Bioscience, Bedford, MA) were used for analysis. For the stimulation studies, BD cells were treated with either LPS 50 ng/ml (Sigma Aldrich, St. Louis, MO) or IFNγ 50 ng/ml (Peprotech), for 24 and 48 hours. Details of antibodies are listed in **Table 2.4**.

2.2.5 Phagocytosis assay

The phagocytic and endocytic properties of the established cell line were evaluated using 2% pHrodo™ E. coli Bioparticles® (Life Technologies). Using a 24-well plate, 100,000 cells were plated per well and left overnight. Culture medium was removed and replaced by 2% pHrodo™ E. coli Bioparticles® diluted in Live Cell Imaging Solution (Life Technologies) for 1.5-2 hours before imaging. Confocal images were obtained using Leica TCS SPE confocal system (Leica Microsystems) on excitation wavelength of 460 nm. Commercially available murine macrophage cell line J774.A (ATCC® TIB-67™), a canine HS cell line DH82, derived from a macrophage derived sarcoma, hemophagocytic HS (ATCC® CRL-10389™), and canine fibroblasts isolated from the tunica albuginea were used for functional comparison purposes.

2.2.6 Neoplastic cell growth and characterization in a xenograft mouse

In order to evaluate the ability of the cells to form tumor *in vivo*, $1x10^6$ neoplastic cells were injected into one ten-week old female mouse of NOD scid gamma strain (NOD.Cg-Prkdc^{scid} Il2rg^{tm1Wjl}/SzJ, The Jackson Laboratory). One million cells were suspended in 100µl of Dulbecco's Modified Eagle Medium (Life Technologies) with 10% FBS, and mixed with BD Matrigel™ Matrix HC in 1:1 ratio (BD Biosciences). The cell suspension was then inoculated subcutaneously into the left flank of the mouse under anesthesia.

Tumor growth in the inoculated mouse was monitored daily using calipers, until the tumor measured close to 10mm in diameter as this was one of our humane endpoints. The mouse was sacrificed using carbon dioxide gas, and a full necropsy evaluated the presence of metastases into other organs. Tissues that had macroscopic changes were fixed in 10% formalin, routinely processed, and embedded in paraffin wax. Paraffin sections were stained with H&E for microscopic examination. For further characterization of the neoplasm, immunohistochemistry for CD18 was performed on paraffin sections.

2.2.7 Drug-screening assays

For the drug-screening assays, we used both the BD cell line, and the DH82 cell line, established from a golden retriever with HHS. In total, 13 drugs **(Table 2.1)** were tested from stock solutions prepared with the appropriate solvent as indicated, stored at -20°C, and protected from light. Serial dilutions of each drug were made from the stock solutions in culture medium immediately before adding to the cells in such a way that the solvent concentration was always <1%. Each compound was tested at different concentrations in order to bracket the corresponding IC_{50} (concentration of drug necessary to inhibit the cell growth by 50%).

2.2.8 Viability assay and data analysis

For viability assay, DH82 and BD cell lines were seeded on 96-well plates with 7,500 cells/well and 12,000 cells/well, respectively. After a 24-hour incubation time, the cell culture medium was replaced with 100µl of complete medium with drug, and cells were then incubated for 72hours. Subsequently, the viability of the cells was analyzed using a CellTiter 96® AQueous Non-Radioactive Cell Proliferation Assay (MTS) (Promega). The formazan product was measured using EnVision® Multimode Plate Reader (PerkinElmer) at a wavelength of 490 nm. Each experiment was run in triplicate.

The background absorbance was subtracted from the absorbance values generated by the cells exposed to drugs. The effect on cell viability caused by each drug was calculated as follows: viability (%) = [1-(A-B)/(C-B)] x 100, where A is the response with drug, B is the background response with no drug, and C is the response with vehicle. The absorbance generated by the "cells alone" control was denoted as $AbsIC_{100}$ (100%) and the absorbance generated by water control was denoted as $AbsIC_0$ (0%). The calculated percentage at each (log10) drug concentration was then plotted using GraphPad Prism 5 software nonlinear regression curve fitting (PRISM 5, GraphPad Software). The IC_{50} was determined as the drug concentration corresponding to the value of the mean between 0 and 100% viability. "Cells

alone" control was treated with the vehicle DMSO 1%, the same concentration used to the cells exposed to the drugs.

2.2.9 Drug combination assays

Both HS cell lines were counted and seeded in 96-well plates as described in *Viability assay and data analysis* section. Each cell line was incubated with 5 different concentrations of dasatinib with or without doxorubicin. The concentrations of dasatinib were defined to bracket the IC_{50} for each cell line, and the concentration of doxorubicin was fixed with the concentration necessary to inhibit cell viability by 70%. Cell viability was measured by MTS proliferation assay after 72hours of incubation. Each experiment was run in triplicate.

2.2.10 Western Blotting

BD cells treated with either vehicle (0.1%) or dasatinib for 4 hours. Cells were lysed using CellLytic M (Sigma-Aldrich) supplemented with 1% protease inhibitor and phosphatase cocktail inhibitor (P8340/P5726 – Sigma-Aldrich). A total of 40μg of protein per lane were separated by Novex NuPAGE SDS-PAGE (4-12%), and transferred to polyvinylidene difluoride membrane. Membranes were blocked with 5% BSA in TBS buffer, and probed overnight with monoclonal rabbit anti-human antibodies against phospho-SRC (44-660G, Thermo Fisher) or SRC (2109, Cell Signaling), and monoclonal mouse anti-human β-actin (8H10D10, Cell Signaling). Secondary antibodies include IRDye 800CW goat anti-mouse and 680RD goat anti-rabbit (LI-COR). Infrared fluorescence was detected using Odyssey Imaging System (LI-COR), and analyzed using Image Studio Lite software (LI-COR).

2.2.11 Statistical analysis

Comparison of means of the cell viability rate among groups of different drug concentrations was done by one-way ANOVA, followed by Tukey's multiple means comparison test. In order to determine whether the addition of dasatinib to doxorubicin increased the anti-proliferative effect, two-way ANOVA was utilized. Statistical analyses were performed using GraphPad Prism 5 software (PRISM 5, GraphPad Software). Differences were considered statistically significant when $p<0.05$.

2.3 Results

2.3.1 Characteristics of BD cell line

Neoplastic cells in culture grew satisfactorily in 10% FBS without the addition of specific growth factors with the vast majority of the population growing as adherent and non-clustering cells. BD cell line was maintained in tissue culture for a minimum of 50 passages over 12 months, with a doubling time of approximately 36hours. Cytospins stained with Diff-Quik from cells harvested from cell culture showed the presence of significant cellular pleomorphism, marked anisocytosis and anisokaryosis. Giant cells and multinucleation were frequently observed **(Figure 2.2).**

The established cell line showed lack of expression of both CD3 and CD79a, and positive expression of CD18, CD204 and vimentin on immunohistochemistry, consistent with features observed initially in the primary neoplasm **(Figure 2.3)**. The positive expression of myeloid marker CD45 and the lack of expression of lymphoid markers CD3, CD21 and CD79a were confirmed by flow cytometry. BD cell line expressed CD11c, CD14, CD172a and MHC I at a high level, and MHC II at a lower level **(Figure 2.4)**. MHC II expression was not affected by the stimulation with IFNγ, however it was significantly increased under the stimulation with LPS over time

.

2.3.2 Phagocytic properties of BD cell line

For the phagocytosis assays, the majority of cells from BD cell line were capable of phagocytizing the bioparticles, demonstrated by fluorescent intracellular signal on most of the cells **(Figure 2.5a)**. Both the murine macrophage cell line J774A.1 and the canine HS cell line DH82 demonstrated a high capability of phagocytosis, as expected **(Figure 2.5b and 2.5c)**. In contrast, we observed the presence of the bioparticles inside only a few canine fibroblasts **(Figure 2.5d)**.

2.3.3 Experiment with xenograft mouse

The xenograft mouse developed a palpable soft tissue mass of 5mm of diameter detected at the injection site 29 days after injection. The tumor increased rapidly in size over 6 days until it reached 10mm of diameter, when the mouse was humanely euthanized. A full necropsy revealed a large lobulated subcutaneous mass at the injection site measuring 25 x 15 x 10 mm, showed in more detail in **Figure 2.9**. The neoplasm had locally invaded the musculature of the abdominal wall dorsally to the tumor. No other significant macroscopic changes were observed in other organs.

2.3.4 Evaluation of inhibitory effects of drugs on the growth of canine HS cells

The inhibition of cell growth by the drugs was variable between the two HS cell lines, BD and DH82. Dose-response curves were generated based on the cell viability at various concentrations of drug, from which IC_{50} values were determined. The results of IC_{50} **(Table 2.2)** values indicated that across 13 drugs tested, only dasatinib and doxorubicin were capable of inhibiting the growth of HS cells, within a pharmacologically relevant concentration. Both drugs exhibited statistically significant inhibitory effects on cell growth in a dose dependent manner using one-way ANOVA analysis ($p<0.0001$). The IC_{50}s of dasatinib were 10 and 9 nM, and of doxorubicin were 90 and 412 nM for BD and DH82 cell lines, respectively **(Figure 2.6).** These concentrations were within the known tolerable plasma concentration

values **(Table 2.2)**. The maximum achievable plasma concentrations of the drugs were based on the plasma concentration values of the no-observed-adverse-effect level (NOAEL), or on the level of the therapeutic dosage described in the veterinary and human medicine literature. When available, the plasma concentration values encountered for dogs were used over those for humans.

2.3.5 Exploring synergistic combinations of drugs

We next assessed the resulting cytostatic effect caused by increasing concentrations of dasatinib combined to doxorubicin at a fixed concentration close to the correspondent cell line's IC_{50}. When BD cell line was treated with the drug combination for 72hours, there was no significant increase in the antiproliferative activity in comparison to the cells treated with dasatinib alone. On the other hand, dasatinib and doxorubicin combination significantly increased the inhibitory effect on the growth of DH82 cells (p=0.0003) **(Figure 2.7).**

2.3.6 Effect of dasatinib on SRC activity

The expression of total SRC and phopho-SRC was evaluated on cells treated with escalating concentrations of dasatinib. We observed a decrease in phospho-SRC but not in total SRC in both cell lines, BD and DH82, after 4hours of treatment. Expression of phosphor-SRC was minimal at the concentration of 100nM of dasatinib **(Figure 2.8)**.

2.4 Discussion

The use of the naturally occurring histiocytic sarcoma in the dog as a translational model for human HS represents a valuable opportunity to further understand this malignancy, and to find better tools for treatment. In this article we have presented the initial characterization of a novel HS cell line - BD cell line - and investigated potential novel treatment approaches.

Histiocytic sarcomas are frequently associated with a high level of cellular pleomorphism, therefore, the definitive diagnosis is determined by a pattern of expression of markers specific for histiocytes. Although, several markers have been used to characterize human HS including CD163, CD68, CD11c, lysozyme, and CD14 [57, 77, 78], two different markers were validated for HS tumors in dogs: CD18 (integrin beta chain beta 2) and CD204 (class A macrophage scavenger receptor) [4, 8, 32, 76, 79]. The novel BD cell line showed positive expression of CD18 and CD204, consistent with the diagnosis of HS. The negative expression of CD3, CD21 and CD79a excluded lymphoid malignancies, while positive vimentin, a type III intermediate filament protein, confirmed the mesenchymal origin, and positive CD45 confirmed the myeloid origin. Interestingly, the stimulation of BD cells with LPS, a lipopolysaccharide component of Gram-negative bacteria walls, resulted in increased expression of MHC class II. A similar increase in MHC Class II expression was reported when murine dendritic cells were exposed to LPS, including CD14 positive dendritic cells [80, 81]. CD14 expression is mainly present in macrophages and monocytes, however it can also be found in DCs, where it has been proposed to play a role on the immunologic responses in DCs [82]. The same effect was not observed when the cells were stimulated with interferon-γ (IFNγ). Due to the fact that the majority of BD cells expressed MHC I and MHC II, we could confirm an antigen presenting cell profile. Both macrophages and DCs are antigen presenting cells that, despite their differences in biological functions, are only distinguished by a few surface markers. Candidate markers that have an increased specificity for DC and DC subsets have been identified in several studies [83-86]. Two DC-specific markers were tested in the present study, CD11c and CD172a, for which the vast majority of BD cells were positive. Together, these findings indicated a pattern of expression associated with a dendritic cell origin.

Dendritic cells are professional phagocytes that have an important role in processing antigens for adaptive immune recognition [87]. The majority of cells from the newly established cell line were able to phagocytize pHrodo E. coli bioparticles when coincubated for 2hours. In this assay, the bioparticles

would only emit fluorescence once they are inside the phagosomes of the cells, where the pH is low. Therefore, this pH-sensitive fluorescent method permits a clear discrimination of where the particles are located in respect to the cells [88]. As a representation of positive controls for this assay, the two macrophage cell lines, J774.A and DH82, showed a high level of phagocytosis. In contrast, we could appreciate phagocytic activity in only a very small number of canine fibroblasts, which were used as negative control.

When transplanted to an immunodeficient xenograft mouse, BD cell line successfully grew as a palpable soft tissue mass after 29 days, a time-frame comparable to other tumor xenograft studies [89]. We were able to confirm that BD cell line is a tumorigenic cell line, and could potentially be useful for *in vivo* studies as an experimental tool to study histiocytic sarcoma. Further studies with a larger number of animals are warranted to truly establish the transplantability and metastatic potential. A few xenograft mouse models of canine HS have been successfully established and were used for the evaluation of their metastatic potential, and to study the phenomenon of resistance to CCNU-based treatment [90, 91]; however, none of these cell lines had originated from BMDs, the most frequently affected breed. To the best of our knowledge, across the many existent canine HS cell lines, only two others were reported to be originated from tumors of BMDs [92]; and these two were not part of their drug response report.

Results from the *in vitro* drug-screening experiment showed a variable response between the different drugs, and across the cell lines. Across a total of 13 compounds, dasatinib and doxorubicin effectively inhibited the cell growth of both HS cell lines within a clinically tolerable and achievable plasma concentration according to the veterinary and human literature.

Doxorubicin was the only conventional chemotherapeutic drug that elicited a favorable response against the HS cell lines. Several studies have reported the use of doxorubicin for the treatment of histiocytic disorders, including HS [12, 28, 37, 58, 59, 78, 93]. Due to the low number of cases, the effectiveness of doxorubicin could not be determined in those studies, especially as single agent, as the drug was

invariably used in a drug combination protocol. Our results agree with previous *in vitro* studies that considered doxorubicin an effective drug against canine HS [66, 94]. The potential of doxorubicin for the treatment of dogs with HS was suggested by a preliminary clinical study, where the response to doxorubicin was comparable to the response to the drug with the best response reported to date, CCNU. [66].

Our positive results with dasatinib are in accordance with results from a study by Ito et al., where dasatinib was effective against 4 out of 7 canine HS cell lines derived from various breeds. The calculated IC_{50} values from that study varied from 5.4 to 54.5 nM, while the average IC_{50} value in our study was 9.5 nM, clearly within their range [71]. Dasatinib is an multi tyrosine kinase inhibitor with multiple main targets, including the SRC family kinases (SRC, LCK, YES, and FYN), the BCR-ABL, and to a lesser extent, c-KIT, PDGFRβ and EPHA2 [95]. We demonstrated that dasatinib inhibited the activation of SRC, as revealed by decrease of p-SRC (phospho-SRC) in both cell lines, BD and DH82. We hypothesize that the downregulation of p-SRC could be associated with the inhibitory effect of dasatinib on the HS cell lines, however, as a multi-kinase inhibitor, many other molecular targets might also be affected. However, the SRC pathway is a major oncogenic driver involved in HS against which dasatinib and other novel compounds may be used. Although dasatinib has been investigated in many human cancers, its clinical therapeutic value for HS has never been documented. [96-100]. However, the use of other small inhibitors for the treatment of HS has been reported in one study where human patients were treated with imatinib, sorafenib and bevacizumab, based on the pattern of expression of key molecular targets [74]. Another set of studies reported two patients carrying a HS associated with a mutation in $BRAF^{V600E}$ gene, most commonly seen in melanomas in humans [28, 29]. Neoplasms that are driven by this mutation are suitable for vemurafenib-based treatment, a BRAF small molecule inhibitor. In fact, a human patient from one of the studies was treated with vemurafenib and experienced therapeutic response for a couple of months [29]. Although the efficacy of these drugs could not be evaluated due

to the small cohort of patients, the identification of druggable targets in HS shows the value of targeted therapy for this disease.

We demonstrated that the combination of dasatinib and doxorubicin resulted in a favorable additive effect against one of the two HS cell lines, DH82 cell line. The association of small inhibitors with chemotherapeutic drugs has been strategized as a treatment with broader spectrum, which resulted in synergistic anticancer activity for many tumors [72, 101, 102]. Often the increased efficiency is accompanied with a dose reduction of the drugs, and consequently decreased treatment related side effects. The combination of drugs with different mechanisms of action should be considered as a relevant strategy to optimize the therapeutic effect of each inhibitor against HS.

2.5 Conclusions

The present study was able to establish and fully characterize a DC-subtype HS cell line from a tumor in a BMD. This novel HS cell line represents a model available not only for the investigation of potential therapeutic drugs, but also for the studies of gene expression and genetic variability associated with HS. The existence of cancer cell lines has been a critical tool for the understanding of cancer biology and response to therapy. For that matter, panels of human cancer cell lines such as NCI60 and GDSC have become available for researches, so that the collective use of these resources would generate more efficiently information including genomics and drug sensitivity of these cell lines [103, 104]. Nevertheless, it is valuable to mention that cell lines are prone to genetic changes over time, and early passages should be a better model of the tumor of origin. More recently, a panel of canine cancer cell lines has been created covering the most important cancers seen in canine patients [105]. Due to the rarity of HS in humans, studies based on spontaneous HS in dogs can provide important and relevant translational understanding of this malignancy. Moreover, we also propose BD cell line as a useful system for studies where a cell line of dendritic cell origin can be of value.

APPENDIX

Figure 2.1. Histopathology and immunohistochemistry analysis of the primary neoplastic tissue. Sections of lung stained with hematoxylin and eosin (H&E) with a well-demarcated region of neoplastic cells replacing the normal pulmonary parenchyma. Neoplastic cells presented as a highly pleomorphic population of malignant histiocytic cells with marked anisocytosis and anisokaryosis. The cells contained large amounts of basophilic and typically mildly vacuolated cytoplasm. Multinucleation, megalocytosis and megalokaryosis were common features. One to several prominent nucleoli were present in most nuclei. Perimembranous expression of CD18 was strongly detected by immunohistochemistry.

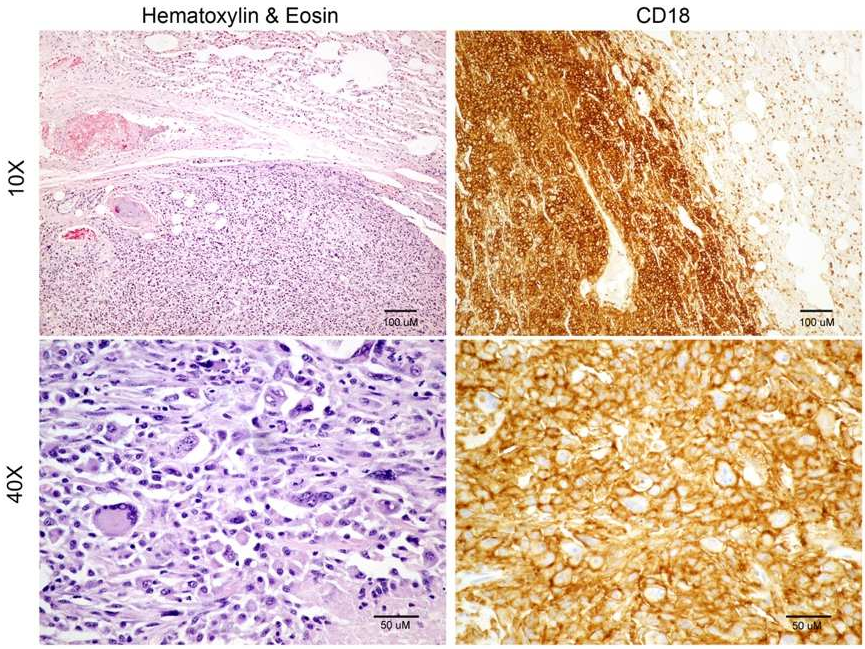

Figure 2.2. Image of BD cell cytospin stained with Diff-Quik showing a population of pleomorphic neoplastic round cells with marked anisocytosis and anisokaryosis with numerous binucleated and multinucleated cells. Calibration bar: 50 µm.

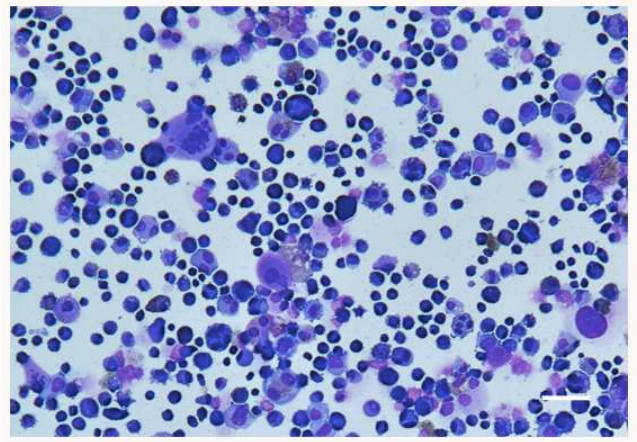

Figure 2.3. Immunohistochemistry of BD cell line with strong expression of CD18, vimentin, and CD204, while neoplastic cells are negative for CD3 and CD79a (left column). Middle and right columns are negative control and positive control sections, respectively. For CD18, CD204, CD3 and CD79a antibodies, DAB chromogen was used; and for vimentin antibody, alkaline phosphatase red chromogen. Calibration bar: 50 µm.

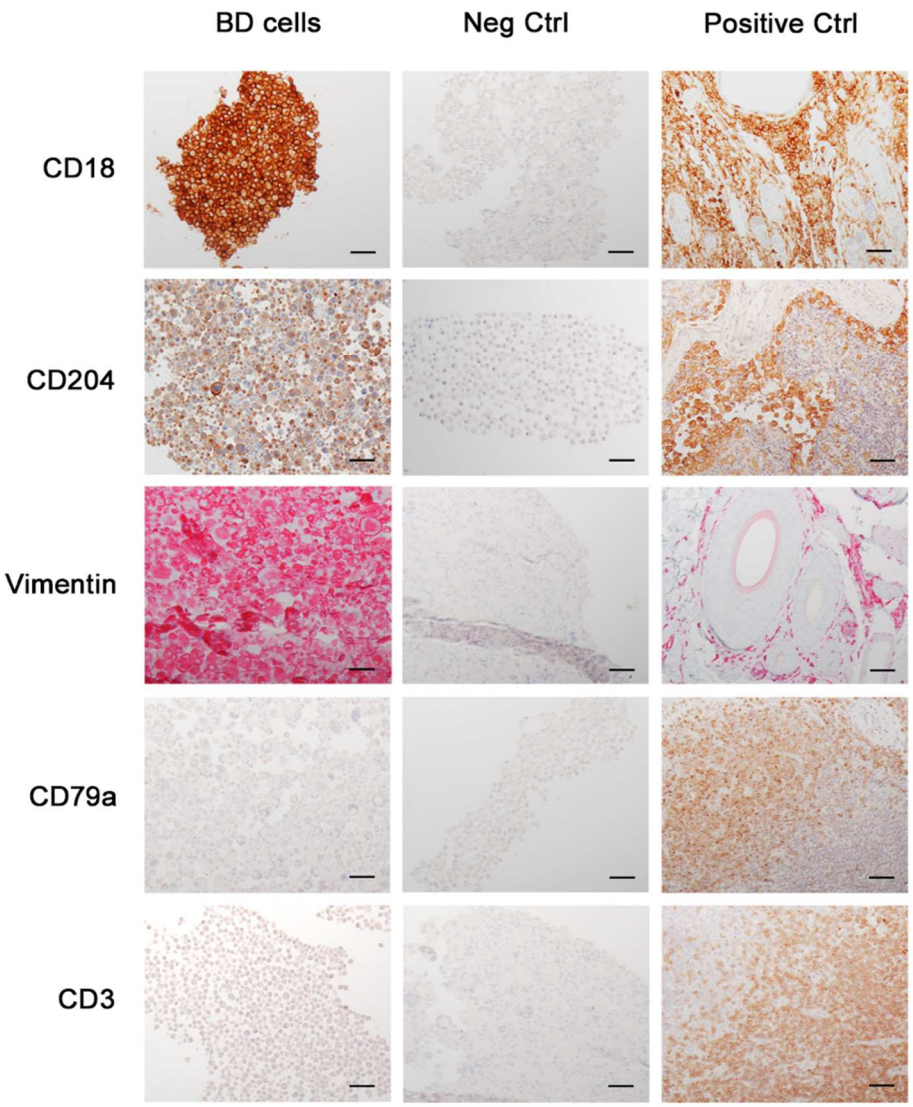

Figure 2.4. Flow cytometry results for expression of CD45, CD3, CD21, CD79a, CD14, CD172a, CD11c, MHC I, and MHC II. Expression of MHC II was also evaluated on cells treated with either LPS or IFNγ for 24 and 48 hours. (BD cell line shown in red, isotype control in blue)

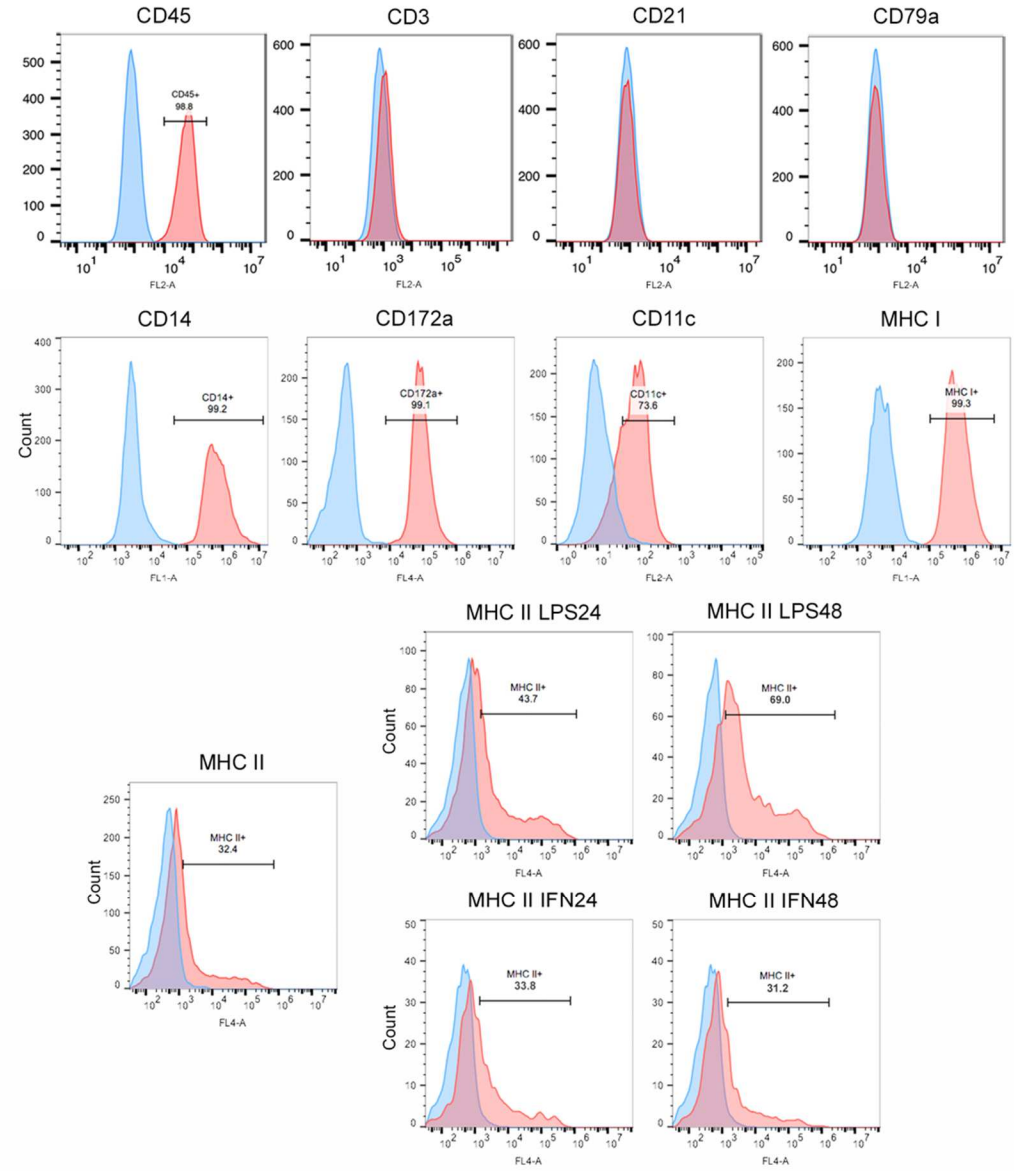

Figure 2.5. PHrodo Phagocytosis assay with strong uptake of red particles by the **(a)** BD cell line, the **(b)** canine HS cell line DH82, the **(c)** murine macrophage cell line J774A.1, and weak uptake by **(d)** canine fibroblasts.

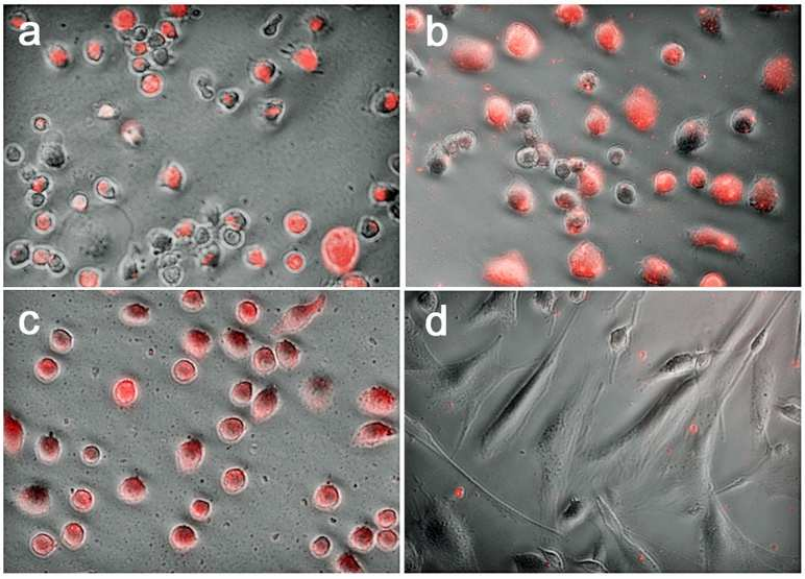

Figure 2.6. Dose-dependent antiproliferative activity of doxorubicin **(A)** and dasatinib **(B)** against BD and DH82 cells after 72 hours of treatment. Cells treated with vehicle DMSO were used as control cells.

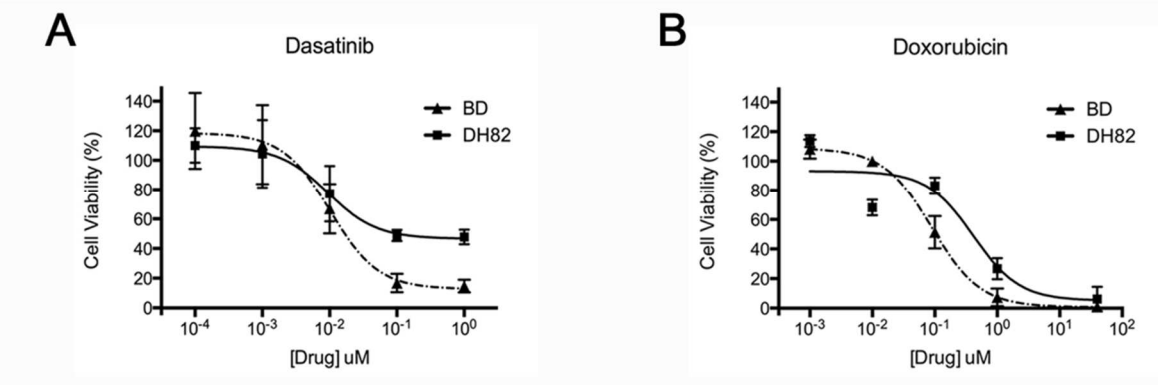

Figure 2.7. The effect of dasatinib on cell viability administered alone and in combination with doxorubicin on BD **(A)** and DH82 **(B)** cell lines.

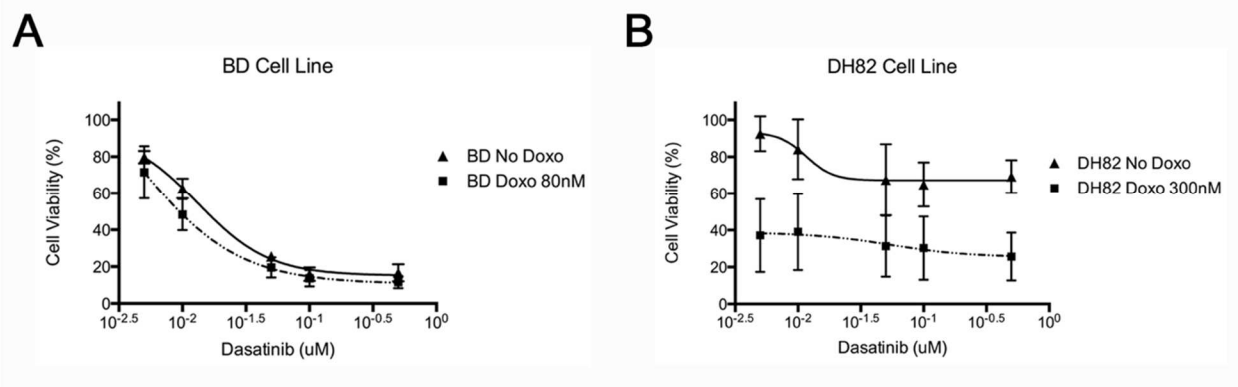

Figure 2.8. The effect of dasatinib on expression of phospho-SRC on BD and DH82 cell lines.

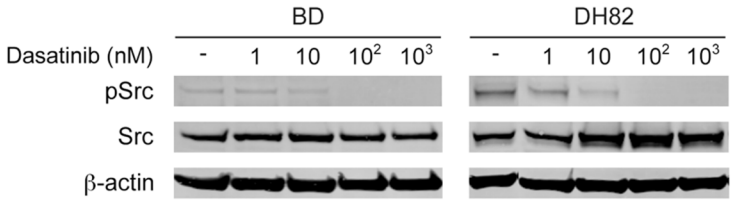

Figure 2.9. Xenograft tumor in a mouse. On necropsy, a large lobulated subcutaneous mass was present at the site of injection of tumor cells 35 days after transplantation (black arrow).

Table 2.1. Compounds from drug-screening assay

Name	Solvent	Main Targets [106-112]
Dasatinib	DMSO	ABL, PDGFR, KIT, SRC
Erlotinib	DMSO	EGFR
Gefitinib	DMSO	EGFR
Imatinib	DMSO	ABL, PDGFR, KIT
Masitinib	DMSO	c-KIT, PDGFRα, -β, Lyn, FGFR3, FAK pathway
Nilotinib	DMSO	ABL, PDGFR, KIT
Toceranib	DMSO	VEGFR2, PDGFRβ, c-KIT
Sorafenib	DMSO	VEGFR2, PDGFR, KIT, FLT3, BRAF
Sunitinib	DMSO	VEGFR, KIT, PDGFR, RET, CSF1R, FLT3
Tozasertib	DMSO	SRC, GSK3, FLT3, JAK2, BCR-ABL
CCNU	Ethanol	Alkylation and cross-linking of DNA
Cladribine	DMSO	Purine analogue
Doxorubicin	Saline	Inhibits DNA topoisomerase II, induces DNA damage and apoptosis

List of the drugs with their respective solvent used in serial dilutions, and main known targets.

Table 2.2. Results from drug screening and referenced achievable plasma concentrations

Drug	IC_{50} (μM)		Achievable concentrations in plasma (based on the literature)				
	BD	DH82	[plasma] (μM)	Species	Dose	Effect	Ref.
Dasatinib	0.01	0.009	0.3	dog	3 mg/kg	NOAEL	[113]
Erlotinib	3.2	4.3	6.9	dog	150 mg	TD	[114]
Gefitinib	30.7	46.4	2.6	dog	100 mg/kg	NOAEL	[115]
Imatinib	34	39.2	0.66	dog	10 mg/kg	NOAEL	[116]
Masitinib	15.7	39.1	1.5	dog	10 mg/kg	TD	[117]
Nilotinib	29.9	26.2	1.4	dog	20 mg/kg	NOAEL	[118]
Toceranib	1.9	1.7	0.1	dog	3.25 mg/kg	TD	[119]
Sorafenib	36.3	13.6	13.3	human	400 mg	TD	[120]
Sunitinib	4.5	17.9	0.12	human	50 mg	TD	[121]
Tozasertib	7.7	1.3	0.27	human	8 mg/m^2	TD	[122]
CCNU	105	139.5	4.2	human	130 mg/m^2	TD	[110]
Cladribine *	64	222	0.028	human	0.09 mg/kg	TD	[123]
Doxorubicin *	0.09	0.41	1.13	dog	30 mg/m^2	TD	[124]

* Compounds administered intravenously
NOAEL: no-observed-adverse-effect level
TD: therapeutic dosage

Results of IC_{50} (nM) values of drugs for each HS cell line, and associated values of achievable plasma concentration described in the veterinary and human medicine literature.

Table 2.3. Genetic profile of a panel of microsatellite markers for genotyping of BD cell line

Marker	Locus	Chromosome	BD cell line profile
Canine 1	FH3210	2	285, 293
Canine 17	PEZ12	3	301
Canine 2	FH3241	8	260, 264
Canine 3	FH2004	11	170, 174
Canine 16	FH2054	12	156, 160
Canine 4	FH2658	14	116
Canine 5	FH4012	15	119, 127
Canine 6	REN214L11	16	150
Canine 13	WILMS-TF	18	279
Canine 7	FH2010	24	155
Canine 14	PEZ6	27	183, 188
Canine 19	VWF.X	27	155
Canine 8	FH2361	33	248
Canine 15	FH2611	36	193, 197
Sex	AR (X), Sry1.1 (Y)	X, Y	X, X

Table 2.4. Description of primary and secondary antibodies

	Antibodies	Catalog#	Clone	Host	Manufacturer
Immuno histochemistry	CD3	A0452	polyclonal	Rabbit	Dako
	CD18	CD18 canine	CA16.3C10	Mouse	UC Davis
	CD79a	LS-C44954	HM57	Mouse	LSBio
	CD204	KT022	SRA-E5	Mouse	Transgenic Inc
	Vimentin	790-2917	V9	Mouse	Ventana
Flow cytometry	CD3	MCA1774GA	CA17.2A12	Mouse	Serotec
	CD11c	MCA1778S	CA11.6A1	Mouse	UC Davis
	CD21	MCA1781R	CA2.1D6	Mouse	Serotec
	CD14	BOV2109	MM61A	Mouse	WSU MAC
	CD45	MCA1042GA	YKIX716.13	Rat	Serotec
	CD79a	LS-C44954	HM57	Mouse	LSBio
	CD172a	BOV2049	DH59B	Mouse	WSU MAC
	MHC II	17-590941	YKIX334.2	Rat	eBioscience
	MHC I	P-BOV2002	PG-PT85A	Mouse	WSU MAC
Western Blot	SRC	2109	36D10	Rabbit	Cell Signaling
	p-SRC (Tyr418)	44-660G		Rabbit	Thermo Fisher
	ß-actin	3700S	8H10D10	Mouse	Cell Signaling
	IRDye 800CW	926-32210		Goat	LI-COR
	IRDye 680RD	926-68071		Goat	LI-COR

BIBLIOGRAPHY

BIBLIOGRAPHY

1. Jaffe ES and World Health Organization., *Pathology and genetics of tumours of haematopoietic and lymphoid tissues*. World Health Organization classification of tumors. 2001, Lyon: IARC Press. 351 p.

2. Jaffe ES, *Histiocytoses of lymph nodes: biology and differential diagnosis.* Semin Diagn Pathol, 1988. 5(4): p. 376.

3. Bruner SR, *Updates in therapeutics for veterinary dermatology.* The Veterinary clinics of North America. Small animal practice, 2006. 36(1): p. 39.

4. Abadie J, Hedan B, et al., *Epidemiology, pathology, and genetics of histiocytic sarcoma in the Bernese mountain dog breed.* J Hered, 2009. 100 Suppl 1: p. S19.

5. Dervisis NG, Kiupel M, et al., *Clinical prognostic factors in canine histiocytic sarcoma.* Vet Comp Oncol, 2016.

6. Dobson J, Hoather T, et al., *Mortality in a cohort of flat-coated retrievers in the UK.* Vet Comp Oncol, 2009. 7(2): p. 115.

7. Fidel J, Schiller I, et al., *Histiocytic sarcomas in flat-coated retrievers: a summary of 37 cases (November 1998-March 2005).* Vet Comp Oncol, 2006. 4(2): p. 63.

8. Affolter VK and Moore PF, *Localized and disseminated histiocytic sarcoma of dendritic cell origin in dogs.* Vet Pathol, 2002. 39(1): p. 74.

9. Craig LE, Julian ME, et al., *The diagnosis and prognosis of synovial tumors in dogs: 35 cases.* Vet Pathol, 2002. 39(1): p. 66.

10. Skorupski KA, Clifford CA, et al., *CCNU for the treatment of dogs with histiocytic sarcoma.* J Vet Intern Med, 2007. 21(1): p. 121.

11. Takahashi E and Nakamura S, *Histiocytic sarcoma : an updated literature review based on the 2008 WHO classification.* Journal of clinical and experimental hematopathology : JCEH, 2013. 53(1): p. 1.

12. Hornick JL, Jaffe ES, et al., *Extranodal histiocytic sarcoma: clinicopathologic analysis of 14 cases of a rare epithelioid malignancy.* Am J Surg Pathol, 2004. 28(9): p. 1133.

13. Gounder M, Desai V, et al., *Impact of surgery, radiation and systemic therapy on the outcomes of patients with dendritic cell and histiocytic sarcomas.* Eur J Cancer, 2015. 51(16): p. 2413.

14. Constantino-Casas F, Mayhew D, et al., *The clinical presentation and histopathologic-immunohistochemical classification of histiocytic sarcomas in the Flat Coated Retriever.* Vet Pathol, 2011. 48(3): p. 764.

15. Dobson JM, *Breed-predispositions to cancer in pedigree dogs.* ISRN Vet Sci, 2013. 2013: p. 941275.

16. Morris JS, Bostock DE, et al., *Histopathological survey of neoplasms in flat-coated retrievers, 1990 to 1998.* The Veterinary record, 2000. 147(11): p. 291.

17. Kommalapati A, Tella SH, et al., *Histiocytic sarcoma: a population-based analysis of incidence, demographic disparities, and long-term outcomes.* Blood, 2018. 131(2): p. 265.

18. Zhang Q, Shibani A, et al., *an aggressive multifocal primary CNS histiocytosis with PTPN11 (Shp2) mutation.* Neuropathol Appl Neurobiol, 2017.

19. Liu Q, Tomaszewicz K, et al., *Somatic mutations in histiocytic sarcoma identified by next generation sequencing.* Virchows Arch, 2016. 469(2): p. 233.

20. Batra S, Martin SC, et al., *Histiocytic Sarcoma Associated with Coombs Negative Acute Hemolytic Anemia: A Rare Presentation.* Case Rep Oncol Med, 2016. 2016: p. 3179147.

21. Voruz S, Cairoli A, et al., *Response to MEK inhibition with trametinib and tyrosine kinase inhibition with imatinib in multifocal histiocytic sarcoma.* Haematologica, 2018. 103(1): p. e39.

22. Kordes M, Roring M, et al., *Cooperation of BRAF(F595L) and mutant HRAS in histiocytic sarcoma provides new insights into oncogenic BRAF signaling.* Leukemia, 2016. 30(4): p. 937.

23. Lee LH, Gasilina A, et al., *Real-time genomic profiling of histiocytoses identifies early-kinase domain BRAF alterations while improving treatment outcomes.* JCI Insight, 2017. 2(3): p. e89473.

24. Badalian-Very G, Vergilio JA, et al., *Recurrent BRAF mutations in Langerhans cell histiocytosis.* Blood, 2010. 116(11): p. 1919.

25. Haroche J, Charlotte F, et al., *High prevalence of BRAF V600E mutations in Erdheim-Chester disease but not in other non-Langerhans cell histiocytoses.* Blood, 2012. 120(13): p. 2700.

26. Brown NA, Furtado LV, et al., *High prevalence of somatic MAP2K1 mutations in BRAF V600E-negative Langerhans cell histiocytosis.* Blood, 2014. 124(10): p. 1655.

27. Chakraborty R, Hampton OA, et al., *Mutually exclusive recurrent somatic mutations in MAP2K1 and BRAF support a central role for ERK activation in LCH pathogenesis.* Blood, 2014. 124(19): p. 3007.

28. Michonneau D, Kaltenbach S, et al., *BRAFV600E Mutation in a Histiocytic Sarcoma Arising From Hairy Cell Leukemia.* J Clin Oncol, 2014. 32(35): p. e117.

29. Idbaih A, Mokhtari K, et al., *Dramatic response of a BRAF V600E-mutated primary CNS histiocytic sarcoma to vemurafenib.* Neurology, 2014. 83(16): p. 1478.

30. Thaiwong T, Sirivisoot S, et al., *Gain-of-function mutation in PTPN11 in histiocytic sarcomas of Bernese Mountain Dogs.* Vet Comp Oncol, 2017.

31. Asada H, Tsuboi M, et al., *A 2-base insertion in exon 5 is a common mutation of the TP53 gene in dogs with histiocytic sarcoma.* J Vet Med Sci, 2017. 79(10): p. 1721.

32. Klahn SL, Kitchell BE, et al., *Evaluation and comparison of outcomes in dogs with periarticular and nonperiarticular histiocytic sarcoma.* J Am Vet Med Assoc, 2011. 239(1): p. 90.

33. Hung YP, Lovitch SB, et al., *Histiocytic sarcoma: New insights into FNA cytomorphology and molecular characteristics.* Cancer Cytopathol, 2017. 125(8): p. 604.

34. Takada M, Parys M, et al., *A novel canine histiocytic sarcoma cell line: initial characterization and utilization for drug screening studies.* BMC Cancer, 2018. 18(1): p. 237.

35. Marcinowska A, Constantino-Casas F, et al., *T Lymphocytes in Histiocytic Sarcomas of Flat-Coated Retriever Dogs.* Vet Pathol, 2017. 54(4): p. 605.

36. Skorupski KA, Clifford CA, et al., *CCNU for the treatment of dogs with histiocytic sarcoma.* Journal of veterinary internal medicine / American College of Veterinary Internal Medicine, 2007. 21(1): p. 121.

37. Pileri SA, Grogan TM, et al., *Tumours of histiocytes and accessory dendritic cells: an immunohistochemical approach to classification from the International Lymphoma Study Group based on 61 cases.* Histopathology, 2002. 41(1): p. 1.

38. Moore PF, Affolter VK, et al., *Canine hemophagocytic histiocytic sarcoma: a proliferative disorder of CD11d+ macrophages.* Vet Pathol, 2006. 43(5): p. 632.

39. Berres ML, Merad M, et al., *Progress in understanding the pathogenesis of Langerhans cell histiocytosis: back to Histiocytosis X?* Br J Haematol, 2015. 169(1): p. 3.

40. Guyot-Goubin A, Donadieu J, et al., *Descriptive epidemiology of childhood Langerhans cell histiocytosis in France, 2000-2004.* Pediatr Blood Cancer, 2008. 51(1): p. 71.

41. Stalemark H, Laurencikas E, et al., *Incidence of Langerhans cell histiocytosis in children: a population-based study.* Pediatr Blood Cancer, 2008. 51(1): p. 76.

42. Arnaud L, Hervier B, et al., *CNS involvement and treatment with interferon-alpha are independent prognostic factors in Erdheim-Chester disease: a multicenter survival analysis of 53 patients.* Blood, 2011. 117(10): p. 2778.

43. Gatalica Z, Bilalovic N, et al., *Disseminated histiocytoses biomarkers beyond BRAFV600E: frequent expression of PD-L1.* Oncotarget, 2015. 6(23): p. 19819.

44. Bubolz AM, Weissinger SE, et al., *Potential clinical implications of BRAF mutations in histiocytic proliferations.* Oncotarget, 2014. 5(12): p. 4060.

45. Berres ML, Lim KP, et al., *BRAF-V600E expression in precursor versus differentiated dendritic cells defines clinically distinct LCH risk groups.* J Exp Med, 2014. 211(4): p. 669.

46. Nelson DS, Quispel W, et al., *Somatic activating ARAF mutations in Langerhans cell histiocytosis.* Blood, 2014. 123(20): p. 3152.

47. Nelson DS, van Halteren A, et al., *MAP2K1 and MAP3K1 mutations in Langerhans cell histiocytosis.* Genes Chromosomes Cancer, 2015. 54(6): p. 361.

48. Emile JF, Diamond EL, et al., *Recurrent RAS and PIK3CA mutations in Erdheim-Chester disease.* Blood, 2014. 124(19): p. 3016.

49. Diamond EL, Abdel-Wahab O, et al., *Detection of an NRAS mutation in Erdheim-Chester disease.* Blood, 2013. 122(6): p. 1089.

50. Diamond EL, Durham BH, et al., *Diverse and Targetable Kinase Alterations Drive Histiocytic Neoplasms.* Cancer Discov, 2016. 6(2): p. 154.

51. Gadner H, Grois N, et al., *Improved outcome in multisystem Langerhans cell histiocytosis is associated with therapy intensification.* Blood, 2008. 111(5): p. 2556.

52. Gadner H, Minkov M, et al., *Therapy prolongation improves outcome in multisystem Langerhans cell histiocytosis.* Blood, 2013. 121(25): p. 5006.

53. Haroche J, Cohen-Aubart F, et al., *Dramatic efficacy of vemurafenib in both multisystemic and refractory Erdheim-Chester disease and Langerhans cell histiocytosis harboring the BRAF V600E mutation.* Blood, 2013. 121(9): p. 1495.

54. Haroche J, Cohen-Aubart F, et al., *Vemurafenib as first line therapy in BRAF-mutated Langerhans cell histiocytosis.* J Am Acad Dermatol, 2015. 73(1): p. e29.

55. Diamond EL, Subbiah V, et al., *Vemurafenib for BRAF V600-Mutant Erdheim-Chester Disease and Langerhans Cell Histiocytosis: Analysis of Data From the Histology-Independent, Phase 2, Open-label VE-BASKET Study.* JAMA Oncol, 2017.

56. Soria C, Orradre JL, et al., *True histiocytic lymphoma (monocytic sarcoma).* Am J Dermatopathol, 1992. 14(6): p. 511.

57. Vos JA, Abbondanzo SL, et al., *Histiocytic sarcoma: a study of five cases including the histiocyte marker CD163.* Mod Pathol, 2005. 18(5): p. 693.

58. Saygin C, Uzunaslan D, et al., *Dendritic cell sarcoma: A pooled analysis including 462 cases with presentation of our case series.* Crit Rev Oncol Hematol, 2013. 88(2): p. 253.

59. Soriano AO, Thompson MA, et al., *Follicular dendritic cell sarcoma: a report of 14 cases and a review of the literature.* Am J Hematol, 2007. 82(8): p. 725.

60. Abidi MH, Tove I, et al., *Thalidomide for the treatment of histiocytic sarcoma after hematopoietic stem cell transplant.* Am J Hematol, 2007. 82(10): p. 932.

61. Erich SA, Rutteman GR, et al., *Causes of death and the impact of histiocytic sarcoma on the life expectancy of the Dutch population of Bernese mountain dogs and Flat-coated retrievers.* Vet J, 2013.

62. Fulmer AK and Mauldin GE, *Canine histiocytic neoplasia: an overview.* Can Vet J, 2007. 48(10): p. 1041.

63. Hedan B, Thomas R, et al., *Molecular cytogenetic characterization of canine histiocytic sarcoma: A spontaneous model for human histiocytic cancer identifies deletion of tumor suppressor genes and highlights influence of genetic background on tumor behavior.* BMC Cancer, 2011. 11: p. 201.

64. Shearin AL, Hedan B, et al., *The MTAP-CDKN2A locus confers susceptibility to a naturally occurring canine cancer.* Cancer Epidemiol, 2012. 21(7): p. 1019.

65. Rassnick KM, Moore AS, et al., *Phase II, open-label trial of single-agent CCNU in dogs with previously untreated histiocytic sarcoma.* J Vet Intern Med, 2010. 24(6): p. 1528.

66. Higuchi T, Dervisis N, et al. *Efficacy of doxorubicin for histiocytic sarcoma in dogs*. in *30th Annual Veterinary Cancer Society Meeting Conference*. 2010. San Diego.

67. Visonneau S, Cesano A, et al., *Successful treatment of canine malignant histiocytosis with the human major histocompatibility complex nonrestricted cytotoxic T-cell line TALL-104.* Clin Cancer Res, 1997. 3(10): p. 1789.

68. Vail DM, Kravis LD, et al., *Preclinical trial of doxorubicin entrapped in sterically stabilized liposomes in dogs with spontaneously arising malignant tumors.* Cancer Chemother Pharmacol, 1997. 39(5): p. 410.

69. Poirier VJ, Hershey AE, et al., *Efficacy and toxicity of paclitaxel (Taxol) for the treatment of canine malignant tumors.* J Vet Intern Med, 2004. 18(2): p. 219.

70. Mariani CL, Schubert TA, et al., *Frameless stereotactic radiosurgery for the treatment of primary intracranial tumours in dogs.* Vet Comp Oncol, 2013.

71. Ito K, Kuroki S, et al., *Identification of dasatinib as an in vitro potent growth inhibitor of canine histiocytic sarcoma cells.* Vet J, 2013.

72. Thamm DH, Rose B, et al., *Masitinib as a chemosensitizer of canine tumor cell lines: a proof of concept study.* Vet J, 2012. 191(1): p. 131.

73. Kisseberth WC, Murahari S, et al., *Evaluation of the effects of histone deacetylase inhibitors on cells from canine cancer cell lines.* Am J Vet Res, 2008. 69(7): p. 938.

74. Schlick K, Aigelsreiter A, et al., *Histiocytic sarcoma - targeted therapy: novel therapeutic options? A series of 4 cases.* Onkologie, 2012. 35(7-8): p. 447.

75. Takada M PM, Gregory-Bryson E, Yuzbasiyan-Gurkan V. *A novel canine histiocytic sarcoma cell line provides a potential path to effective treatments with relevance for translational and*

comparative studies in humans. in *American Association of Cancer Research Annual Meeting*. 2014. San Diego, CA.

76. van Kuijk L, van Ginkel K, et al., *Peri-articular histiocytic sarcoma and previous joint disease in Bernese Mountain Dogs.* J Vet Intern Med, 2013. 27(2): p. 293.

77. Skoog L and Tani E, *Histiocytic and dendritic neoplasms.* Monogr Clin Cytol, 2009. 18: p. 56.

78. Lauritzen AF, Delsol G, et al., *Histiocytic sarcomas and monoblastic leukemias. A clinical, histologic, and immunophenotypical study.* Am J Clin Pathol, 1994. 102(1): p. 45.

79. Kato Y, Murakami M, et al., *The class A macrophage scavenger receptor CD204 is a useful immunohistochemical marker of canine histiocytic sarcoma.* J Comp Pathol, 2013. 148(2-3): p. 188.

80. Casals C, Barrachina M, et al., *Lipopolysaccharide up-regulates MHC class II expression on dendritic cells through an AP-1 enhancer without affecting the levels of CIITA.* J Immunol, 2007. 178(10): p. 6307.

81. Mahnke K, Becher E, et al., *CD14 is expressed by subsets of murine dendritic cells and upregulated by lipopolysaccharide.* Adv Exp Med Biol, 1997. 417: p. 145.

82. Zanoni I, Ostuni R, et al., *CD14 regulates the dendritic cell life cycle after LPS exposure through NFAT activation.* Nature, 2009. 460(7252): p. 264.

83. Bimczok D, Sowa EN, et al., *Site-specific expression of CD11b and SIRPalpha (CD172a) on dendritic cells: implications for their migration patterns in the gut immune system.* Eur J Immunol, 2005. 35(5): p. 1418.

84. Mansouri-Attia N, Oliveira LJ, et al., *Pivotal role for monocytes/macrophages and dendritic cells in maternal immune response to the developing embryo in cattle.* Biol Reprod, 2012. 87(5): p. 123.

85. Kaisho T, *Pathogen sensors and chemokine receptors in dendritic cell subsets.* Vaccine, 2012. 30(52): p. 7652.

86. Schutz F and Hackstein H, *Identification of novel dendritic cell subset markers in human blood.* Biochem Biophys Res Commun, 2014. 443(2): p. 453.

87. Savina A and Amigorena S, *Phagocytosis and antigen presentation in dendritic cells.* Immunol Rev, 2007. 219: p. 143.

88. Beletskii A, Cooper M, et al., *High-throughput phagocytosis assay utilizing a pH-sensitive fluorescent dye.* Biotechniques, 2005. 39(6): p. 894.

89. Morton CL and Houghton PJ, *Establishment of human tumor xenografts in immunodeficient mice.* Nat Protoc, 2007. 2(2): p. 247.

90. Thongtharb A, Uchida K, et al., *Variations in Histiocytic Differentiation of Cell Lines From Canine Cerebral and Articular Histiocytic Sarcomas.* Vet Pathol, 2017: p. 300985817690211.

91. Yamazaki H, Takagi S, et al., *Survivin suppressor (YM155) enhances chemotherapeutic efficacy against canine histiocytic sarcoma in murine transplantation models.* Res Vet Sci, 2015. 99: p. 137.

92. Azakami D, Bonkobara M, et al., *Establishment and biological characterization of canine histiocytic sarcoma cell lines.* J Vet Med Sci, 2006. 68(12): p. 1343.

93. Soslow RA, Davis RE, et al., *True histiocytic lymphoma following therapy for lymphoblastic neoplasms.* Blood, 1996. 87(12): p. 5207.

94. Hafeman SD, Varland D, et al., *Bisphosphonates significantly increase the activity of doxorubicin or vincristine against canine malignant histiocytosis cells.* Vet Comp Oncol, 2012. 10(1): p. 44.

95. Steinberg M, *Dasatinib: a tyrosine kinase inhibitor for the treatment of chronic myelogenous leukemia and philadelphia chromosome-positive acute lymphoblastic leukemia.* Clin Ther, 2007. 29(11): p. 2289.

96. Kantarjian HM, Shah NP, et al., *Dasatinib or imatinib in newly diagnosed chronic-phase chronic myeloid leukemia: 2-year follow-up from a randomized phase 3 trial (DASISION).* Blood, 2012. 119(5): p. 1123.

97. Kantarjian H, Shah NP, et al., *Dasatinib versus imatinib in newly diagnosed chronic-phase chronic myeloid leukemia.* N Engl J Med, 2010. 362(24): p. 2260.

98. Benjamini O, Dumlao TL, et al., *Phase II trial of hyper CVAD and dasatinib in patients with relapsed Philadelphia chromosome positive acute lymphoblastic leukemia or blast phase chronic myeloid leukemia.* Am J Hematol, 2014. 89(3): p. 282.

99. Spreafico A, Chi KN, et al., *A randomized phase II study of cediranib alone versus cediranib in combination with dasatinib in docetaxel resistant, castration resistant prostate cancer patients.* Invest New Drugs, 2014.

100. Safdari Y, Khalili M, et al., *Recent advances in head and neck squamous cell carcinoma - A review.* Clin Biochem, 2014. 47(13-14): p. 1195.

101. Gleixner KV, Rebuzzi L, et al., *Synergistic antiproliferative effects of KIT tyrosine kinase inhibitors on neoplastic canine mast cells.* Exp Hematol, 2007. 35(10): p. 1510.

102. Robat C, London C, et al., *Safety evaluation of combination vinblastine and toceranib phosphate (Palladia(R)) in dogs: a phase I dose-finding study.* Vet Comp Oncol, 2012. 10(3): p. 174.

103. Shoemaker RH, *The NCI60 human tumour cell line anticancer drug screen.* Nat Rev Cancer, 2006. 6(10): p. 813.

104. Barretina J, Caponigro G, et al., *The Cancer Cell Line Encyclopedia enables predictive modelling of anticancer drug sensitivity.* Nature, 2012. 483(7391): p. 603.

105. Fowles JS, Dailey DD, et al., *The Flint Animal Cancer Center (FACC) Canine Tumour Cell Line Panel: a resource for veterinary drug discovery, comparative oncology and translational medicine.* Vet Comp Oncol, 2016.

106. Doriano F, *25 years of small molecular weight kinase inhibitors: potentials and limitations.* Molecular Pharmacology, 2014.

107. Sun L, Tran N, et al., *Identification of substituted 3-[(4,5,6, 7-tetrahydro-1H-indol-2-yl)methylene]-1,3-dihydroindol-2-ones as growth factor receptor inhibitors for VEGF-R2 (Flk-1/KDR), FGF-R1, and PDGF-Rbeta tyrosine kinases.* J Med Chem, 2000. 43(14): p. 2655.

108. Harrington EA, Bebbington D, et al., *VX-680, a potent and selective small-molecule inhibitor of the Aurora kinases, suppresses tumor growth in vivo.* Nat Med, 2004. 10(3): p. 262.

109. Thorn CF, Oshiro C, et al., *Doxorubicin pathways: pharmacodynamics and adverse effects.* Pharmacogenet Genomics, 2011. 21(7): p. 440.

110. Lee FY, Workman P, et al., *Clinical pharmacokinetics of oral CCNU (lomustine).* Cancer Chemother Pharmacol, 1985. 14(2): p. 125.

111. Saven A and Piro L, *Newer purine analogues for the treatment of hairy-cell leukemia.* N Engl J Med, 1994. 330(10): p. 691.

112. Dubreuil P, Letard S, et al., *Masitinib (AB1010), a potent and selective tyrosine kinase inhibitor targeting KIT.* PLoS One, 2009. 4(9): p. e7258.

113. Kamath AV, Wang J, et al., *Preclinical pharmacokinetics and in vitro metabolism of dasatinib (BMS-354825): a potent oral multi-targeted kinase inhibitor against SRC and BCR-ABL.* Cancer Chemother Pharmacol, 2008. 61(3): p. 365.

114. EMEA. *Scientific discussion for the approval of Erlotinib*. 2005 Accessed 28 Feb 2017 [cited 2017 28 Feb 2017]; Available from: http://www.ema.europa.eu/docs/en_GB/document_library/EPAR_-_Scientific_Discussion/human/000618/WC500033991.pdf.

115. EMEA. *Assessment report for Iressa*. 2009 Accessed 28 Feb 2017; Available from: http://www.ema.europa.eu/docs/en_GB/document_library/EPAR_-_Public_assessment_report/human/001016/WC500036361.pdf.

116. EMEA. *Scientific discussion for the approval of Imatinib*. 2004 Accessed 28 Feb 2017; Available from: http://www.ema.europa.eu/docs/en_GB/document_library/EPAR_-_Scientific_Discussion/human/000406/WC500022203.pdf.

117. Hahn KA, Ogilvie G, et al., *Masitinib is safe and effective for the treatment of canine mast cell tumors.* J Vet Intern Med, 2008. 22(6): p. 1301.

118. EMEA. *Scientific discussion for the approval of Nilotinib*. 2007 Accessed 28 Feb 2017; Available from: http://www.ema.europa.eu/docs/en_GB/document_library/EPAR_-_Scientific_Discussion/human/000798/WC500034398.pdf.

119. Zavodovskaya R, Liao AT, et al., *Evaluation of dysregulation of the receptor tyrosine kinases Kit, Flt3, and Met in histiocytic sarcomas of dogs.* Am J Vet Res, 2006. 67(4): p. 633.

120. Blanchet B, Billemont B, et al., *Validation of an HPLC-UV method for sorafenib determination in human plasma and application to cancer patients in routine clinical practice.* J Pharm Biomed Anal, 2009. 49(4): p. 1109.

121. Goodman VL, Rock EP, et al., *Approval summary: sunitinib for the treatment of imatinib refractory or intolerant gastrointestinal stromal tumors and advanced renal cell carcinoma.* Clin Cancer Res, 2007. 13(5): p. 1367.

122. Traynor AM, Hewitt M, et al., *Phase I dose escalation study of MK-0457, a novel Aurora kinase inhibitor, in adult patients with advanced solid tumors.* Cancer Chemother Pharmacol, 2011. 67(2): p. 305.

123. EMEA. *Scientific discussion for the approval of Cladribine*. 2005 Accessed 28 Feb 2017; Available from: http://www.ema.europa.eu/docs/en_GB/document_library/EPAR_-_Scientific_Discussion/human/000504/WC500041660.pdf.

124. Gustafson DL and Thamm DH, *Pharmacokinetic modeling of doxorubicin pharmacokinetics in dogs deficient in ABCB1 drug transporters.* J Vet Intern Med, 2010. 24(3): p. 579.

CHAPTER 3

AN ORTHOTOPIC INTRASPLENIC XENOGRAFT MODEL OF CANINE HISTIOCYTIC SARCOMA FOR THE EVALUATION OF EFFICACY OF TREATMENT WITH DASATINIB

3.1 Introduction

Histiocytic sarcoma (HS) in dogs is a highly aggressive hematopoietic neoplasm of malignant cells of dendritic cell or macrophage lineage. Although rare (<1% of all cancers [1]), certain breeds are highly predisposed to HS, including BMD (>25% of population [2, 3]), flat-coated retriever [4, 5], golden retriever and Rottweiler [6-8]. Canine HS most frequently develops in the spleen, lymph nodes, liver, lung and bone marrow [6, 9], where it progresses rapidly, disseminating to multiple organs in 70-91% of the cases [5, 7, 9, 10]. Due to the lack of effective options for treatment, patients respond poorly to available protocols, resulting in a median survival time that ranges from weeks to 3 months [8, 11, 12]. A similar and equally aggressive malignancy observed in humans, HS is an extremely rare disease, accounting for <1% of all hematopoietic neoplasms [13, 14]. In humans, HS is associated with poor prognosis and a short survival time, of less than one year [15, 16]. It may present as a localized disease treatable with surgical resection or radiation therapy, however it often presents at an advanced stage, where multiple organs are involved including lymph nodes, gastrointestinal tract, spleen, and lungs [17-19]. Patients with the latter scenario carry the worst outcome due to the limited response to available systemic treatments [17, 20]. Studies to identify more effective therapeutic approaches are warranted, but given the low incidence of HS in humans, research progress is slow. Dog is the only species that spontaneously develops a similar form of HS with an appreciable frequency, thus represents an important translational model for this rare disease in humans.

Xenograft mouse models are paramount tools to evaluate the response *in vivo* to novel cancer therapeutic interventions. Although to date, there is no human HS xenograft model reported in the literature, xenograft models of subcutaneous canine HS were successfully established in two studies, however, neither of these models developed metastatic disease [21, 22]. Thongtharb et al. described a xenograft model presenting disseminated disease when canine HS cells were injected intravenously into SCID mice [23]. Although this model mimicked a metastatic behavior, the study included only three

mice, and there was no description of an effective method to track tumor progression over the course of the study, limiting its applicability.

The goal of our study was to establish a clinically relevant animal model of HS by transplanting HS cells derived from a tumor in a BMD into immunodeficient mice, and to test its utility in evaluating treatment efficacy with novel drugs. We first report an interesting phenomenon of spontaneous regression of subcutaneous xenograft tumors in mice, associated with necrosis and an inflammatory process enriched with a neutrophilic population. However, following injection into a more orthotopic site, the spleen, we observed consistent tumor growth, and development of metastasis to the liver and other neighboring organs. Use of HS cells transfected with a luciferase vector further allowed us to carry out studies in smaller number of mice per group, while following in detail the growth and distribution of tumors in this model. In addition, the intrasplenic xenograft model was suitable to assess response to treatment, showing promising response to dasatinib, a multi-kinase inhibitor, previously reported by our group and others, as a potential novel approach for canine HS [24-26].

Our orthotopic intrasplenic xenograft model represents an aggressive, metastatic form of HS, and is a useful tool for predicting efficacy for cancer agents. This model provides valuable preclinical information of novel treatment approaches for canine HS that can translate to similar diseases in humans.

3.2 Materials and Methods

3.2.1 Cell culture establishment

BD cell line originated from an HS neoplasm of a BMD. A comprehensive characterization of this cell line was recently reported by our group [24]. Briefly, for tumor cells isolation, a sample of tumor tissue was minced with a surgical blade and placed in complete medium with 1% collagenase (C9891, Sigma) for disaggregation. After at least one hour, the solution was washed thoroughly with phosphate buffer saline, and cells were plated in RPMI 1640 media (11875-093, ThermoFisher) supplemented with 10%

heat-inactivated fetal bovine serum (10100147, ThermoFisher), 1% antibiotic-antimycotic 100X (10378016, ThermoFisher), and 0.1% gentamycin (15710064, ThermoFisher), and incubated at 37°C in 5% CO_2.

3.2.2 Transfection of cancer cells with a luciferase expression vector

BD cells were transfected with luciferase expression vector to enable cells tracking by non-invasive bioluminescence imaging (BLI). Briefly, cells were incubated with vector pGL4.51 [*luc2*/CMV/Neo] (E1320, Promega) and Lipofectamine 2000 reagent (11668027, ThermoFisher) for up to 48 hours. Transfected cells were selected using Geneticin (G418, ThermoFisher) at 140 µg/ml for 10 days. Transfection efficacy was evaluated *in vitro*, where bioluminescence signal was detected in a population of as low as 12,500 cells. BD cells stably transfected with the luciferase vector are here on referred to as BD-luc cells.

3.2.3 Harvesting HS cells from culture for injection into mice

To maximize their viability, cells were given fresh complete media the day before surgery, and for injection, were harvested during exponential growth (no more than 70-80% confluency). BD-luc cells in complete media were mixed 1:1 with matrix matrigel (CB-40234C, Corning), to a final concentration of $1x10^8$ cells/ml ($1x10^7$/100µl), and $2x10^7$ cells/ml ($1x10^6$/50µl) for subcutaneous, and intrasplenic injection, respectively, and kept on ice until use. The cells were prepared for injection as close to the time of injection as possible.

3.2.4 Subcutaneous xenograft mouse model

One day prior to surgery, hair from the area of the right rear flank of five anesthetized 7-week old female NOD scid gamma mice (NOD.Cg-Prkdc^{scid} Il2rg^{tm1Wjl}/SzJ, The Jackson Laboratory) was removed

using Nair depilatory cream (Church & Dwight Co.). A total of 100µl of cell suspension containing $10x10^6$ BD-luc cells was inoculated subcutaneously into the right rear flank of each anesthetized mouse using a syringe with a 25G needle. Weekly non-invasive BLI and biweekly caliper measurements were performed to monitor tumor growth. All animal studies were performed in accordance with institutional guidelines and approved by the MSU-IACUC.

3.2.5 Intrasplenic orthotopic xenograft mouse model

For the intrasplenic xenograft model, hair from the left thoracic and abdominal area of ten 6-week old immune-deficient female NOD scid gamma anesthetized mice (NOD.Cg-*Prkdc*^{scid} *Il2rg*^{tm1Wjl}/SzJ, The Jackson Laboratory) was removed using Nair depilatory cream (Church & Dwight Co.). The following day, mice were anesthetized and injected in the spleen with BD-luc cells via a laparotomy approach.

3.2.6 Step-by-step description of surgical procedure for intrasplenic injection

1. A class II type A2 biological safety cabinet was used for all procedures. Sterile drapes were placed over the working areas to help maintain a clean environment **(Figure 3.1A)**. Mice were anesthetized using gas anesthesia (isoflurane). Initially animals were placed inside a small anesthesia induction chamber with isoflurane percentage of up to 4% in 0.8L/min oxygen, and for maintenance, they were placed at the nose cone of a non-rebreathing circuit with 1.5-2% isoflurane, in right lateral recumbence over a heating pad **(Figure 3.1C)**. Eye ointment was applied to avoid dryness, and a rectal probe was placed to monitor body temperature during surgery.
2. Surgical site was aseptically prepared with three rounds of alternating sterile solutions (saline, chlorhexidine gluconate 4% and povidone-iodine solution 10%), and covered with a sterile paper drape.

3. The skin was incised (~1 cm) at the level of the spleen with a #15 scalpel blade by lifting up the skin with forceps to avoid damaging underneath structures **(Figure 3.1D)**. At this point, the spleen appeared as a dark colored linear structure through the translucent abdominal wall.
4. The abdominal wall was incised using scissors at the level of the spleen, which was partially exteriorized by gently pulling it out by the underlying fat **(Figures 3.1E/F)**. When necessary, a cotton tipped swab was used to push the stomach cranially to better expose the spleen. Warm sterile saline solution was applied to keep the spleen moist.
5. Tumor cell suspension kept on ice was gently homogenized, and a total volume of 50µl containing $1x10^6$ BD-luc cells mixed 1:1 with matrix matrigel (CB-40234C, Corning) was loaded into an 30G insulin syringe (328411, BD).
6. The syringe needle was inserted into the lower pole of the spleen cranially (about 0.3-0.4 mm) **(Figure 3.1G)**, and the content was slowly discharged as the needle was being pulled out caudally.
7. Once the cell injection was complete, the needle was slowly removed, and a small amount of absorbable hemostat Surgicel Fibrillar (1961, Ethicon) was placed over the injection site and pressed down with a cotton tipped swab to ensure adequate hemostasis **(Figure 3.1H/I)**.
8. The spleen was gently pushed back into the abdominal cavity, and the incision closed in two layers (abdominal wall and skin) using a 5-0 PDS II Plus violet absorbable suture (PDP303, Ethicon) in a simple interrupted pattern.
9. To prevent loss of fluids a total of 300µl of warm saline solution was given subcutaneously in the dorsal region.
10. Mice were placed inside sterile cages over water blankets for recovery i.e. until mobile and breathing regularly **(Figure 3.1B)**.

For analgesia, pre-operative medications consisting of buprenorphine 0.05mg/kg, and meloxicam 1mg/kg were administered subcutaneously about 20 minutes prior to surgery. Post-operative analgesia included buprenorphine 0.05mg/kg twice a day and meloxicam 1mg/kg once a day subcutaneously for 48 hours post-operatively. Mice were monitored daily and their behavior and health assessed as described below.

3.2.7 Treatment protocol and health assessment

Fifteen days post cell injection, mice were randomly divided into two treatment groups of five mice each. Mice were treated daily either with 30mg/kg of dasatinib (11498, Cayman) or vehicle β-cyclodextrin 10% (16169, Cayman) intraperitoneally (IP). As neoplasms were growing internally, tumor progression was monitored based on non-invasive BLI, and health assessment, as changes in hair coat, eyes, and posture indicate internal changes in the animal. Non-invasive BLI was performed bi-weekly. Animals health was assessed using a body condition scoring and health signs scoring **(Table 3.1)**, systems to monitor animals' well-being and to assess the need for euthanasia. Mice were euthanized as soon as they reached any of the following humane endpoints: body condition score <2, weight loss >15%, lack of movement, abnormal posture and haircoat, and/or clinical signs score ≥15. Additionally, Campus Animal Resources (CAR) veterinary staff and animal care staff monitored each animals' health daily. Animals were euthanized when humane end-points were reached or after 65 days post cells injection.

3.2.8 In vivo bioluminescence imaging

Non-invasive bioluminescence imaging with an IVIS Spectrum (Perkin Elmer, Hopkinton, MA) was used to monitor tumor growth, and metastasis. Mice were injected with D-luciferin (LUCK-100, GoldBio) 150mg/kg IP, and anesthetized (2-2.5% isoflurane). Images were acquired 15 minutes post

administration of D-luciferin. Bioluminescent radiance (p/sec/cm^2/sr) from the region of interest of each animal was analyzed using Living Image software (Perkin Elmer).

3.2.9 Histopathology of mice tissues

Tissues from mice were fixed in 10% formalin for 24hours and transferred to 70% ethanol until embedded in paraffin. For each mouse, one representative section of an organ of interest was stained with hematoxylin and eosin. For immunohistochemistry, sections from the paraffin blocks were deparaffinized in xylene and rehydrated in ethanol at different concentrations. Hydrogen peroxide 3% was used to neutralize endogenous peroxidase. Antigen retrieval of formalin-fixed, paraffin embedded tissues was performed on the PT Link (Dako NA), using the EnVision FLEX Target Retrieval Solution, low pH (Dako NA) for 20 minutes. Sections were labeled with monoclonal antibody against CD204 (KT022, clone SRA-E5, Transgenic Inc.), using an Autostainer Link 48 and the EnVision Flex+ detection system (Dako). Immunoreaction was visualized with 3,3'diaminobenzidine substrate (Dako) and sections were counterstained with haematoxylin. Images were acquired using a Nikon H600L Microscope as brightfield images using a 10X dry objective. The images were displayed and analyzed using NIS-Elements AR 3.1 software. Assessment of histopathology was performed by a board certified veterinary pathologist (S.C.).

3.3 Results

3.3.1 Spontaneous regression of subcutaneous xenograft neoplasms

On day 15 after subcutaneous injection of HS cells, there was evidence of tumor growth based on an initial increase in bioluminescence signal and in tumor volume **(Figure 3.2A)**. All five mice developed a palpable subcutaneous tumor in the right flank, that reached 100mm^3 volume between days 27 and 30 after cells injection. However, following a peak of growth, a sudden decline in bioluminescence signal

was observed, as well as a decrease in tumor volume **(Figure 3.2B)**. This phenomenon was associated with the skin overlying or adjacent to the tumors becoming progressively dark brown to red, followed by ulceration and formation of a firm, serocellular crust **(Figure 3.2C)**. By day 42 post-injection, bioluminescence signal was minimal, and tumors had shrunk significantly. Histologically, all tumors had some degree of necrosis and neutrophilic inflammation. The skin lesions were secondary to tumor growth within the superficial dermis. This resulted in necrosis, ulceration, and neutrophilic inflammation of the overlying epidermis **(Figure 3.2D)**. None of the animals presented any evident clinical signs related to tumor formation or regression.

3.3.2 Consistent tumor growth and development of metastasis in the intrasplenic xenograft HS model

In ten out of ten mice injected intrasplenically, a bioluminescence signal was detected from day 3 post injection forward. BLI signals were detected mainly in the hypogastric region of the mice, where the spleen is located. The signal increased consistently over time for at least 27 days, when mice were euthanized as the pre-determined humane endpoints were reached. At necropsy, the majority of splenic parenchyma was replaced by a firm, 1-1.5 cm diameter, tan to white mass. The liver was enlarged with rounded edges and contained numerous pinpoint to 1mm, tan foci on the capsular and cut surface, suggestive of metastatic disease **(Figure 3.3A)**. In accordance to the macroscopic findings, post-mortem BLI images of mice showed signal coming from the liver and lungs **(Figure 3.3A)**. Histologically, neoplastic formation was observed in the spleen and liver, and it was characterized by a diffuse infiltration of highly pleomorphic neoplastic round cells, with marked anisocytosis, anisokaryosis, and numerous multinucleated cells **(Figure 3.3B)**.

3.3.3 Treatment with dasatinib inhibited tumor growth and prolonged survival time of HS xenograft mice

Treatment with either dasatinib or vehicle was initiated 15 days post injection. BLI images taken biweekly showed a lower rate of increase in signal in mice treated with dasatinib when compared to untreated mice, and values of each group were statistically different based on Student t test analysis ($p=0.002$), as shown in **Figure 3.3C**, and graphically represented in **Figure 3.3D**. A marked drop in bioluminescent signal from control/vehicle treated mice towards the endpoint was commonly seen and can be related to the poor vascularization as tumor gets larger in size, limiting the substrate and oxygen that generate the bioluminescent signal [27]. Treatment with either dasatinib or vehicle continued until mice reached the pre-determined endpoints, when they were humanely euthanized. While mice from the control group reached the endpoints on day 27 ($n=4$) and 30 post-injection mice treated with dasatinib were euthanized on days 61, 62 ($n=2$), and 65 ($n=2$), due to their poor health conditions. Survival time between groups, represented in the Kaplan-Meier survival curve in **Figure 3.3E**, was significantly different ($p=0.0016$) using Mantel-Cox statistical test.

Metastatic lesions were present in all animals, however the extension of metastatic disease could not be compared between treatment groups, as animals were euthanized at different time points throughout the study, when humane endpoints were reached and when disease was at an advanced stage.

3.4 Discussion

Xenograft mouse models are an important preclinical tool for the evaluation of novel drug treatment approaches. However, establishing a model with clinical relevance can be challenging in regards to the site of implantation and the effects the surrounding microenvironment have on tumor growth. We observed an interesting phenomenon in the subcutaneous xenograft mice where tumors regressed spontaneously after a peak growth. Those tumors presented some degree of necrosis and neutrophilic

inflammation, and no signs of infection. We hypothesize that there was insufficient neovascularization to support the rapid tumor growth, leading to a process of necrosis, and triggering an innate immune system response. Similar findings were reported by Ho et al. when breast cancer cells were injected subcutaneously in mice, resulting in ulceration and necrosis [28]. The phenomenon was prevented when cells were injected into the mammary fat pad, considered a more orthotopic site. Injection of tumor cells to orthotopic sites has been shown to produce xenograft models more efficiently with a higher take rate than ectopic injections (72-90% vs. 3-58%) [28-32].

Our intrasplenic xenograft mouse model represents a more orthotopic model for HS, providing more consistent tumor growth in ten out of ten animals as reported in this study. Additional studies in our laboratory with a larger number of mice (n=60) injected intrasplenically with HS BD-luc cells demonstrated a high level of reproducibility for this model with a consistent 100% take rate and tumor growth (data not shown). Importantly, splenic tumors had the capability to spread to other organs as the liver and lungs, which indicated that our intrasplenic xenograft model mimics a metastatic/disseminated form of HS, considered the most clinically challenging and refractory to available treatment options. Likewise, Bouvet et al. showed that intrasplenic injection of colon cancer cells resulted in large splenic tumors, and liver micrometastasis in more than 50% of cases [33].

Dasatinib has been shown to be a potent inhibitor *in vitro* by Ito et al. [26], in HS cells derived from Maltese, Shetland sheepdog, flat coated retriever and golden retriever breeds and more recently, by our group [24] in HS cells from a BMD. We successfully recapitulated our *in vitro* findings using the intrasplenic xenograft mouse model. We showed that mice with intrasplenic xenograft HS had a significant suppression of tumor growth ($p=0.002$ – Student t-test) when treated with dasatinib. More importantly, mice treated with dasatinib had a significant increase in survival time (two-fold increase) when compared to mice treated with vehicle only ($p=0.0016$ – Mantel Cox test). Our results confirmed findings reported by Ito et al. that dasatinib effectively inhibits tumor growth in subcutaneous xenograft

mice models of canine HS [25]. Dasatinib is a multi-tyrosine kinase inhibitor that targets the SRC family kinases (SRC, LCK, YES, and FYN), approved for people with Philadelphia chromosome positive chronic myeloid leukemia or acute lymphoblastic leukemia [34]. The efficacy of dasatinib in human HS is unknown. In dogs, reports of dasatinib use are limited to two studies where it was used to treat a total of four patients with osteosarcoma. A dose of 0.75mg/kg/day of dasatinib was administered orally for 6.5-25 months, and considered safe and well tolerated [35, 36].

In conclusion, we established an intrasplenic xenograft model of HS that represents a clinically relevant model of an aggressive form of HS, that permits the study of novel treatment approaches. Furthermore, our findings indicate the potential dasatinib has for treatment of HS in dogs and in similar diseases in humans. Additional studies, including proof of concept clinical trials testing the efficacy of dasatinib in canine HS are warranted. While such clinical trials may be highly costly in dogs, due to the high cost of dasatinib, (daily dose for adults in humans estimated to cost about $450), such studies may be justified as translational and relevant for both dogs and humans.

APPENDIX

Figure 3.1. Surgical procedure for intrasplenic injection of cells performed through a laparotomy approach. An aseptic field of work was prepared for the surgical procedures and post-operative monitoring **(A, B)**. Position the mouse in right lateral recumbence under gas anesthesia (2-4% isoflurane) **(C)**. The Spleen was accessed through an incision in the skin with a surgical blade, followed by an incision into the abdominal musculature with surgical scissors **(D, E, F)**. A total of $1x10^6$ BD-luc cells were injected into the spleen with a 30G insulin syringe **(G)**, and an absorbable material for hemostasis was placed over the site of injection **(H)**. After the delivery of cells suspension, the spleen expands and appears light colored **(I)**.

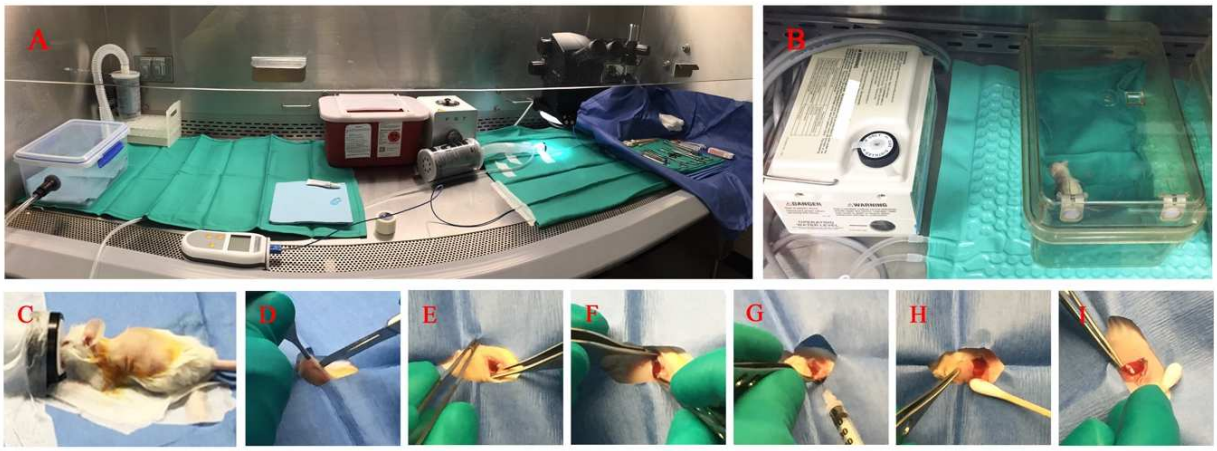

Figure 3.2. Subcutaneous xenograft tumors in mice showed spontaneous regression after 29 days of injection. **(A)** An increase in tumor growth based on average bioluminescent signal (black line) and total volume (orange line) was observed until day 22 and 29 post injection, respectively. After which a spontaneous regression represented as a rapid decline of these two parameters occurred over time. Error bars correspond to standard error of the mean values. **(B)** Representative pictures of the decrease in bioluminescence signal observed at day 36 after a peak of signal on day 22. **(C)** Images on day 30 showing the initial development of a firm scar tissue (left), and an ulceration/black colored scar covering most of the tumor (right). **(D)** Histiocytic sarcoma within the superficial dermis and subcutis. The overlying epidermis is ulcerated, and the surrounding superficial dermis is necrotic (left - H&E stain). Neoplastic cells within the subcutaneous tumors show strong positive cytoplasmic immunoreactivity for CD204 (right). Adjacent neutrophilic inflammation was negative.

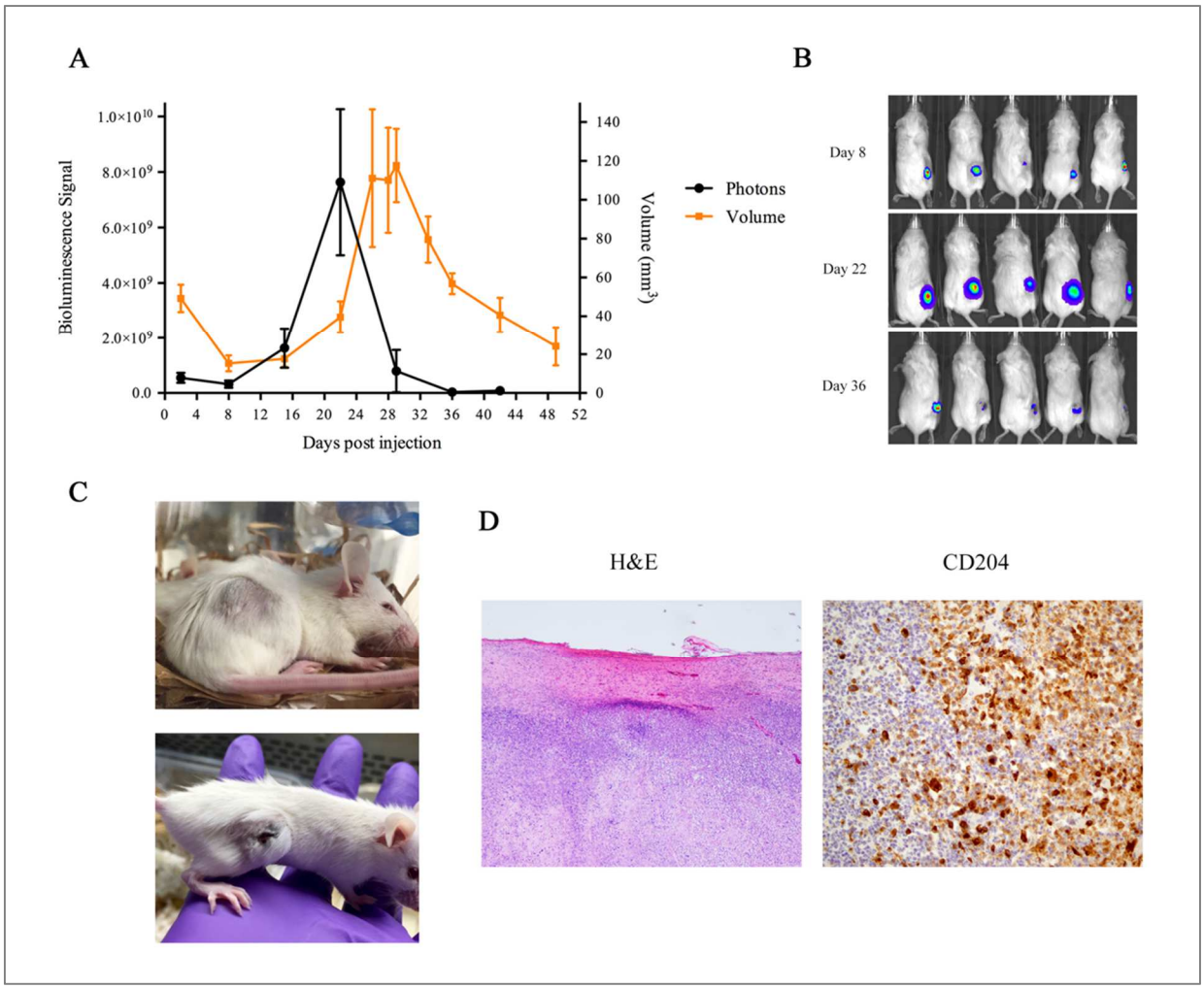

Figure 3.3. Intrasplenic xenograft model showed consistent tumor growth, enabling the evaluation of the efficacy of the treatment with dasatinib. **(A)** Intrasplenic xenograft mice developed a large tumor in the spleen with metastasis to liver and lungs. Tumors were visible upon necropsy and following *ex-vivo* bioluminescence imaging. **(B)** H&E images of tumors in the spleen and liver, and tumor cells positive for CD204. **(C)** Mice treated with dasatinib had a significantly lower rate of tumor growth, when compared to untreated mice, based on Student t-test analysis, where thicker lines represent mean values of each group, graphically represented in **(D)**. Kaplan-Meier survival curves show that mice treated with dasatinib survived twice as long as untreated mice, and the difference in survival is statistically significant based on Mantel-Cox test **(E)**.

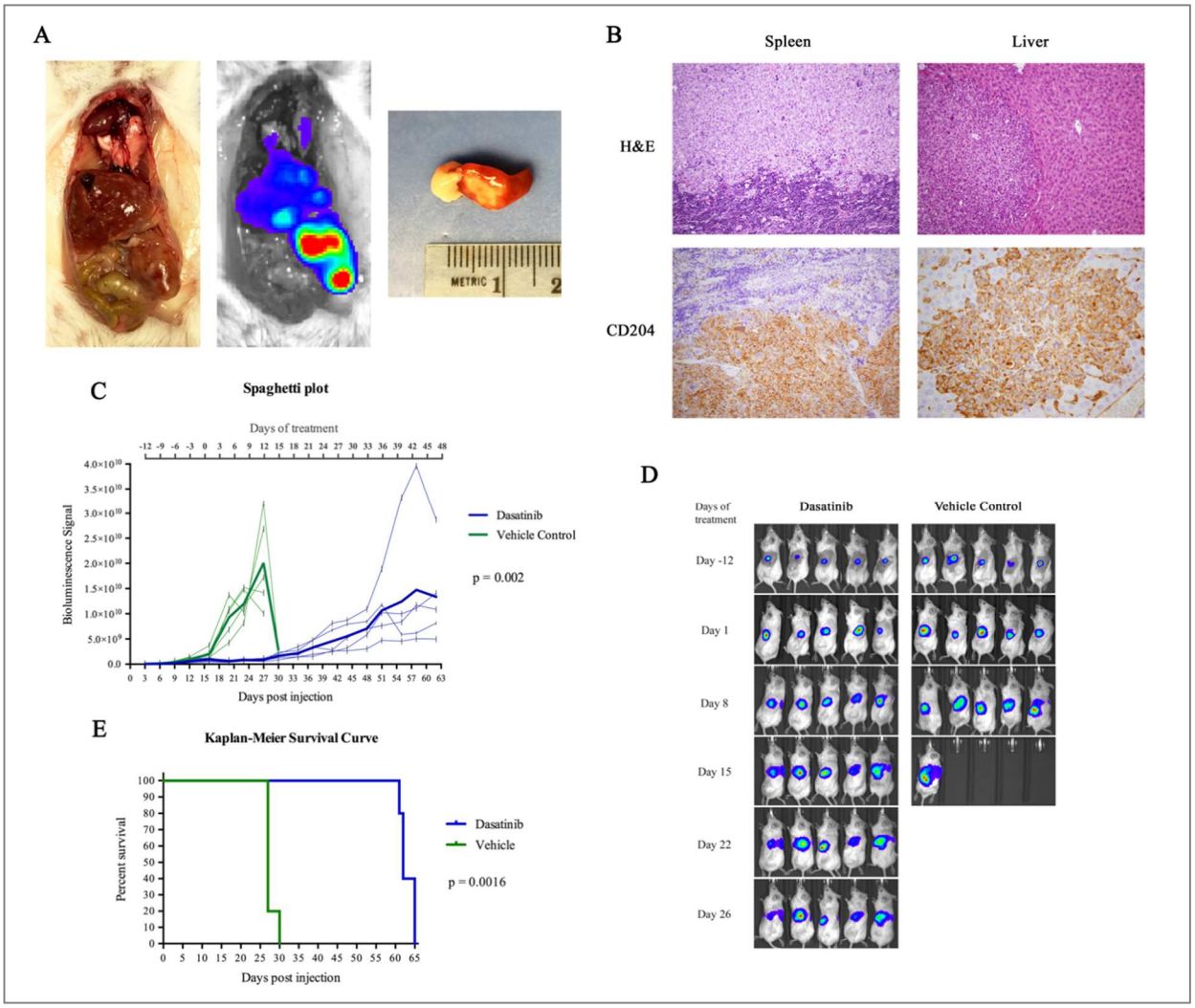

Table 3.1. Clinical signs score sheet for health assessment

Observations in:		Description of		Score
Body Weight Changes		Normal		0
		< 10% weight loss		1
		10-15% weight loss		2
		> 20% weight loss		3
Body Condition Score, BCS		BCS >3 (well-conditioned to over-conditioned)		0
		BCS >2 and <3 (mouse is becoming under-conditioned)		1
		BCS >1 and <2 (mouse is under-conditioned)		2
		BCS of 1 or less (mouse is emaciated)		3
Physical Appearance: Coat		Shiny, well-groomed		0
		Dull, unkempt (lack of grooming)		1
		Very rough coat (piloerection)		3
Physical Appearance: Posture		Normal		0
		Slightly hunched		1
		Moderate to severely hunched (able to rear up or stretch out)		2
		Severely hunched (unable to rear up to access food/water)		3
Physical Appearance: Eyes		Normal, open >75%		0
		Open 50-75%		1
		Open 25-49%		2
		Open <25% (squinting, closed/crusty discharge)		3
Behavior: Natural		Normal (interactive in environment)		0
		Slight decrease in activity, less interactive		1
		Abnormal, decreased activity/alertness, isolated		2
		Self-mutilation, either hyperactive or immobile		3
Behavior: Provoked (response to external stimulus)		Normal i.e. quickly moves away		0
		Slow to move away or exaggerated response		1
		Abnormal, moves away after short period of time		2
		Doesn't move or reacts with excessively exaggerated response		3
Clinical Signs	**Mucous membranes**	Normal		0
		Jaundice		2
		Anemia		2
		Cyanosis		2
	Respiration	Normal		0
		Abnormal (increased)		1
		Labored		2
	Body Temperature	Normal		0
		Cool to the touch		2
	Wound healing	Scratching of Wound	No	0
			Occasionally	1
			Constantly	2
Other Signs		Dehydration		2
		Feces	Normal	0
			Diarrhea (wet tail)	2

Euthanize mice if health assessment score total is ≥ 15

BIBLIOGRAPHY

BIBLIOGRAPHY

1. Bruner SR, *Updates in therapeutics for veterinary dermatology.* The Veterinary clinics of North America. Small animal practice, 2006. 36(1): p. 39.

2. Abadie J, Hedan B, et al., *Epidemiology, pathology, and genetics of histiocytic sarcoma in the Bernese mountain dog breed.* J Hered, 2009. 100 Suppl 1: p. S19.

3. Dervisis NG, Kiupel M, et al., *Clinical prognostic factors in canine histiocytic sarcoma.* Vet Comp Oncol, 2016.

4. Dobson J, Hoather T, et al., *Mortality in a cohort of flat-coated retrievers in the UK.* Vet Comp Oncol, 2009. 7(2): p. 115.

5. Fidel J, Schiller I, et al., *Histiocytic sarcomas in flat-coated retrievers: a summary of 37 cases (November 1998-March 2005).* Vet Comp Oncol, 2006. 4(2): p. 63.

6. Affolter VK and Moore PF, *Localized and disseminated histiocytic sarcoma of dendritic cell origin in dogs.* Vet Pathol, 2002. 39(1): p. 74.

7. Craig LE, Julian ME, et al., *The diagnosis and prognosis of synovial tumors in dogs: 35 cases.* Vet Pathol, 2002. 39(1): p. 66.

8. Skorupski KA, Clifford CA, et al., *CCNU for the treatment of dogs with histiocytic sarcoma.* J Vet Intern Med, 2007. 21(1): p. 121.

9. Klahn SL, Kitchell BE, et al., *Evaluation and comparison of outcomes in dogs with periarticular and nonperiarticular histiocytic sarcoma.* J Am Vet Med Assoc, 2011. 239(1): p. 90.

10. Skorupski KA, Clifford CA, et al., *CCNU for the treatment of dogs with histiocytic sarcoma.* Journal of veterinary internal medicine / American College of Veterinary Internal Medicine, 2007. 21(1): p. 121.

11. Rassnick KM, Moore AS, et al., *Phase II, open-label trial of single-agent CCNU in dogs with previously untreated histiocytic sarcoma.* J Vet Intern Med, 2010. 24(6): p. 1528.

12. Higuchi T, Dervisis N, et al. *Efficacy of doxorubicin for histiocytic sarcoma in dogs*. in *30th Annual Veterinary Cancer Society Meeting Conference*. 2010. San Diego.

13. Jaffe ES and World Health Organization., *Pathology and genetics of tumours of haematopoietic and lymphoid tissues*. World Health Organization classification of tumors. 2001, Lyon: IARC Press. 351 p.

14. Jaffe ES, *Histiocytoses of lymph nodes: biology and differential diagnosis.* Semin Diagn Pathol, 1988. 5(4): p. 376.

15. Vos JA, Abbondanzo SL, et al., *Histiocytic sarcoma: a study of five cases including the histiocyte marker CD163.* Mod Pathol, 2005. 18(5): p. 693.

16. Kommalapati A, Tella SH, et al., *Histiocytic sarcoma: a population-based analysis of incidence, demographic disparities, and long-term outcomes.* Blood, 2018. 131(2): p. 265.

17. Hornick JL, Jaffe ES, et al., *Extranodal histiocytic sarcoma: clinicopathologic analysis of 14 cases of a rare epithelioid malignancy.* Am J Surg Pathol, 2004. 28(9): p. 1133.

18. Takahashi E and Nakamura S, *Histiocytic sarcoma : an updated literature review based on the 2008 WHO classification.* Journal of clinical and experimental hematopathology : JCEH, 2013. 53(1): p. 1.

19. Shimono J, Miyoshi H, et al., *Prognostic factors for histiocytic and dendritic cell neoplasms.* Oncotarget, 2017. 8(58): p. 98723.

20. Gounder M, Desai V, et al., *Impact of surgery, radiation and systemic therapy on the outcomes of patients with dendritic cell and histiocytic sarcomas.* Eur J Cancer, 2015. 51(16): p. 2413.

21. Azakami D, Bonkobara M, et al., *Establishment and biological characterization of canine histiocytic sarcoma cell lines.* J Vet Med Sci, 2006. 68(12): p. 1343.

22. Yamazaki H, Takagi S, et al., *Survivin suppressor (YM155) enhances chemotherapeutic efficacy against canine histiocytic sarcoma in murine transplantation models.* Res Vet Sci, 2015. 99: p. 137.

23. Thongtharb A, Uchida K, et al., *Variations in Histiocytic Differentiation of Cell Lines From Canine Cerebral and Articular Histiocytic Sarcomas.* Vet Pathol, 2017: p. 300985817690211.

24. Takada M, Parys M, et al., *A novel canine histiocytic sarcoma cell line: initial characterization and utilization for drug screening studies.* BMC Cancer, 2018. 18(1): p. 237.

25. Ito K, Miyamoto R, et al., *Effect of dasatinib in a xenograft mouse model of canine histiocytic sarcoma and in vitro expression status of its potential target EPHA2.* J Vet Pharmacol Ther, 2018. 41(1): p. e45.

26. Ito K, Kuroki S, et al., *Identification of dasatinib as an in vitro potent growth inhibitor of canine histiocytic sarcoma cells.* Vet J, 2013.

27. Khalil AA, Jameson MJ, et al., *The Influence of Hypoxia and pH on Bioluminescence Imaging of Luciferase-Transfected Tumor Cells and Xenografts.* Int J Mol Imaging, 2013. 2013: p. 287697.

28. Ho KS, Poon PC, et al., *Blood vessel hyperpermeability and pathophysiology in human tumour xenograft models of breast cancer: a comparison of ectopic and orthotopic tumours.* BMC Cancer, 2012. 12: p. 579.

29. Kellar A, Egan C, et al., *Preclinical Murine Models for Lung Cancer: Clinical Trial Applications.* Biomed Res Int, 2015. 2015: p. 621324.

30. Cunningham D and You Z, *In vitro and in vivo model systems used in prostate cancer research.* J Biol Methods, 2015. 2(1).

31. Stewart E, Shelat A, et al., *Development and characterization of a human orthotopic neuroblastoma xenograft.* Dev Biol, 2015. 407(2): p. 344.

32. McIntyre RE, Buczacki SJ, et al., *Mouse models of colorectal cancer as preclinical models.* Bioessays, 2015. 37(8): p. 909.

33. Bouvet M, Tsuji K, et al., *In vivo color-coded imaging of the interaction of colon cancer cells and splenocytes in the formation of liver metastases.* Cancer Res, 2006. 66(23): p. 11293.

34. Steinberg M, *Dasatinib: a tyrosine kinase inhibitor for the treatment of chronic myelogenous leukemia and philadelphia chromosome-positive acute lymphoblastic leukemia.* Clin Ther, 2007. 29(11): p. 2289.

35. Davis LE, Hofmann NE, et al., *A case study of personalized therapy for osteosarcoma.* Pediatr Blood Cancer, 2013. 60(8): p. 1313.

36. Marley K, Gullaba J, et al., *Dasatinib Modulates Invasive and Migratory Properties of Canine Osteosarcoma and has Therapeutic Potential in Affected Dogs.* Transl Oncol, 2015. 8(4): p. 231.

CHAPTER 4

TARGETING MEK IN A TRANSLATIONAL MODEL OF HISTIOCYTIC SARCOMA

4.1 Introduction

Histiocytic and dendritic cell neoplasms encompass a group of proliferative entities with variable clinical behaviors and prognosis in humans [1]. Among them, histiocytic sarcoma (HS) is by far the most aggressive disorder with the worst prognosis [2]. It is an exceedingly rare hematological malignancy (< 1% of all hematopoietic neoplasms) [3, 4] that affects all ages, but mostly adults, with a male predominance [5]. Existing data show that HS develops within lymph nodes and at extranodal sites including the gastrointestinal tract, spleen, lungs, and head and neck [2, 5, 6]. Given the limited occurrence, there is no consensus on standard-of-care treatment for HS in human patients. While surgical resection and radiation therapy are attempted for local control, metastases frequently occur, and in these cases, systemic chemotherapy with regimens of drugs used for lymphoma is often utilized [6-8]. More options of medical intervention are needed to improve patients' survival time, which does not extend beyond one year [9, 10]. Although the etiology of HS is not yet clear, there is evidence suggesting a central role of the oncogenic RAS-RAF-MEK-ERK signaling pathway [11-15]. A number of HS cases in humans were reported to carry activating mutations in *BRAF* (V600E, F595L) [11-14, 16, 17], *KRAS* (Q61H) [15] and *HRAS* (Q61R) [14], with some cases showing favorable response after targeted therapy with vemurafenib, a BRAF inhibitor, and with MEK inhibitors, including trametinib [12, 16, 18]. Other histiocytic and dendritic cell neoplasms including Langerhans cell histiocytosis (LCH) and Erdheim-Chester disease (ECD) seem to share the MAPK oncogenic pathway based on recurring activating mutations in *BRAF* (V600E, N486_P490del), *MAP2K1*, and *ALK* gene fusion [19-23].

Similar to humans, dogs also present with spontaneously occurring forms of histiocytic disorders, with HS being the most aggressive entity. Clinical presentation and biological behavior are variable across these disorders, ranging from benign and self-resolving (i.e. cutaneous histiocytoma), inflammatory (i.e. reactive histiocytosis), to highly aggressive entities (hemophagocytic HS). HS is a rare disease in dogs (<1% of all cancers) [24], however, it is overrepresented in certain breeds, especially in BMD (incidence

of about ~25% in the population) [25]. Other breeds that also present with HS include the flat-coated retriever, golden retriever and Rottweiler. Males and females are equally affected, and dogs are most often in adult age (8-10 years) [26, 27]. In dogs, HS presents most commonly in the skin, bone/joint, spleen, lymph node, lungs, and liver [27-29]. Due to a high incidence of metastasis, reported as 70-91% [27, 28, 30-32], systemic chemotherapy is the treatment of choice with drugs such as lomustine and/or doxorubicin, resulting in a median survival time of 3-6 months [27, 31, 33, 34]. Although the disease etiology is unclear, the deregulation of the tumor suppressor genes *MTAP/CDKN2A*/*B* located within the region homologous to human chromosome 9p21 [35, 36] has been implicated in genome wide association studies. As in humans, MAPK pathway seems to contribute to HS in dogs, as exemplified through a gain-of-function mutation *PTPN11*^{E76K}, a gene that encodes SHP2, required for MAPK. This mutation was recently reported in canine HS by our group, and found to be significantly prevalent in BMDs than in other breeds (37% vs. 9%) [37].

The immunohistochemical profile is critical to differentiate the histiocytic diseases in both humans and dogs, which often present a high level of pleomorphism. Numerous cell markers are used to characterize cells by their subtype and activated state. In humans, CD68, lysozyme and CD163 are markers used for HS, with the latter considered of highest specificity [38-40]. The diagnosis in dogs are based on different cell markers, CD18 [25, 28, 29, 41], a leukocyte integrin, and CD204, a macrophage scavenger receptor [42, 43]. Thongtharb et al. reported a strong positive expression of CD163 in 17 out of 23 cases of canine HS, suggesting that CD163 might be a common marker between the two species [44].

As the only specie that spontaneously develops HS, dogs represent an excellent translational model for this rare disease in humans. To date, there is no human HS cell line available for study. We have derived and characterized canine HS cell lines, one of which has been described in detail in [45]. We were able to capitalize on this opportunity by using HS cell lines established from dogs as tools for the systematic discovery of novel treatment approaches. A high throughput screening (HTS) of about 2,000 compounds

identified trametinib, a MEK inhibitor, as a highly potent drug against canine HS cells. Trametinib is an FDA-approved drug for patients with advanced melanoma carrying a *BRAF* V600E or V600K mutation [46]. Other activating mutations in *NRAS*, *KRAS* and *HRAS*, upstream of *BRAF*, are also susceptible to MEK inhibition [47, 48]. Here, we report the use of trametinib as an effective inhibitor against three canine HS cell lines, two carrying known activating mutations previously reported in HS human patients (15, 18, 48), one carrying the *PTPN11*^{E76K}, and another *KRAS*^{Q61H}, reported for the first time in dogs in this study. We demonstrate that the inhibition of MEK promotes cell cycle blockage with arrest of sensitive HS cell lines in G1 phase, and that most specifically, MEK inhibition triggers a significant increase in apoptosis. This effect seen *in vitro* with trametinib was then recapitulated in mice harboring HS xenografts, where we demonstrate intratumoral target engagement. Our study indicates that trametinib is a promising targeted therapy for canine HS, and provides a rational for the initiation of clinical trials and further understanding on safety and anti-tumor efficacy in dogs. Importantly, we expect that our findings can be potentially translated to similar human diseases driven by a deregulated MAPK signaling pathway.

4.2 Material and Methods

4.2.1 Cell culture establishment and maintenance

Neoplastic tissues were collected from client owned dogs at post-mortem examination, with owner's written consent, approved as an "exempt" procedure by MSU Institutional Animal Care and Use Committee (IACUC). Detailed characteristics of tissue donors are listed in **Table 4.1**. Minced tissues were disaggregated in 1% collagenase (C9891, Sigma) for one hour, then transferred to medium with 10% heat-inactivated fetal bovine serum, 1% antibiotic-antimycotic 100X, and 0.1% gentamycin (ThermoFisher), and incubated at 37°C in 5% CO_2. For medium, RPMI1640 (ThermoFisher) was used for BD, OD and PJ, whereas DMEM (ThermoFisher) was used for fibroblasts. DH82, a commercially available

cell line derived from a macrophage derived sarcoma, HHS (CRL-10389, ATCC), was kept in EMEM (ATCC).

4.2.2 Fingerprinting of cell lines

Genomic DNA from HS cell lines BD, PJ, and OD was submitted for analysis of genetic profiles (CellCheck Plus, IDEXX). All HS cell lines were confirmed to be of canine origin with no mammalian interspecies contamination. Based on a panel of STR markers, there was no cross contamination across cell lines, and their individual genotypes were identical to samples from early cell passages or whole blood from the original donor. A genetic profile of microsatellite markers is available and can be used in future monitoring in **Table 4.2**.

4.2.3 Characterization of cell lines

For immunohistochemistry (IHC) analysis of the cell lines BD, OD, PJ, DH82 and normal fibroblasts, cell pellets were first embedded into histogel for stability, then fixed in 10% formalin for up to 17hs and transferred to 70% ethanol until embedding in paraffin. Pellets were embedded into paraffin following routine methods. Sections from the cell pellets were rehydrated and labeled with monoclonal antibodies against CD3, CD18, CD79a and CD204, following standard procedures at the MSU Veterinary Diagnostic Laboratory. Images were acquired using a Nikon H600L Microscope as brightfield images using a 10X dry objective. The images were analyzed using NIS-Elements AR 3.1 software.

In order to evaluate for the presence of mutations in the genes *BRAF/NRAS/KRAS/HRAS*, sequences of the coding regions were determined from RNA-seq data from the HS cell lines. For this purpose, messenger RNA were isolated, assayed for quality and sequenced using the Illumina HiSeq 4000 platform to generate a minimum of 150 million reads at 2X150 BP at MSU Genomics Core. Data acquired

from sequencing was checked for quality using FastQC and low quality bases were trimmed using TrimGalore.

4.2.4 High throughput screening

Cell lines BD (8,500/well) and DH82 (6,500/well), and normal fibroblasts (4,000/well) isolated from skin were plated into 384-well plates. A collection of 1,952 compounds from Prestwick (Prestwick Chemical), Approved Oncology Drugs Set V (NCI Developmental Therapeutics Program) and Published Kinase Inhibitor Set (PKIS, Structural Genomics Center, UNC) libraries were delivered to cells using a Biomek FX Workstation liquid handling system (Beckman Coulter) at a single concentration of 1μmol/L for 48hs. CellTiter-Glo Cell Viability (G7570, Promega) reagent was added and the luminescence signal was read using a Synergy Neo (BioTek) detection platform.

Drugs were selected for further analysis based on the following cutoffs: >20% inhibition in one or both HS cell lines, and <20% inhibition in control normal fibroblasts. Compounds of unknown mechanisms of action were excluded. The OD and PJ cell lines were not yet established at the time of the HTS studies, but were included in further assays, as they became available.

4.2.5 Dose response confirmation assay

Selected compounds from HTS were re-tested in a dose response assay, so their pIC50 values could be used to determine their cytotoxic potency. Cell lines BD (8,500/well), DH82 (6,000/well) and PJ (8,500/well), and normal fibroblasts (8,500/well) were seeded into 384-well plates. The dose response assay was performed prior to the establishment of OD cell line, not included in this assay. Selected compounds were added in 8 escalating concentrations for 48hs. Cell viability was measured as explained above for HTS. pIC50 of each compound was calculated by GRETL software within MScreen, a HTS data storage and analysis system (Center for Chemical Genomics, University of Michigan) [49].

4.2.6 Cell viability assay

HS cell lines BD ($3x10^4$/well), DH82 ($1.5x10^4$/well), PJ ($3x10^4$/well) and OD ($3x10^4$/well), and normal fibroblasts ($2x10^4$/well) seeded on 96-well plates were treated with Trametinib (16292, Cayman) in 1%DMSO for 72hs. Viability of cells was determined using CellTiter 96® Aqueous Proliferation Assay (G3581, Promega). The formazan product was measured using an EnVision plate reader (PerkinElmer). Results were plotted using GraphPad Prism 6 software nonlinear regression curve fitting (GraphPad Software) to calculate the pIC50 of each compound.

4.2.7 Cell cycle assay

HS cell lines BD, OD, PJ and DH82, and normal fibroblasts were treated with 1nM, 10nM, 100nM and 1μM of trametinib for 24hs. Cells were fixed in 70% ethanol for >3hs at 4°C , DNA was stained with 50μg/ml propidium iodine, and RNA cleaned out with 16μg/ml RNase A at 4°C. For analysis of DNA content, the flow cytometer BD LSR II (BD Bioscience) was used, and for data interpretation, ModFit LT V4.1.7 software (VSH) with auto fit and auto linearity settings.

4.2.8 Evaluation of caspase 3/7 activity

HS cell lines BD, OD, PJ and DH82, and normal fibroblasts plated in a white 96-well plate were treated with 1nM, 10nM, 100nM and 1μM of trametinib for 24hs. Caspase-Glo 3/7 Assay (G8090, Promega) reagent was added to the cells for 30minutes, and luminescent signal was detected using an EnVision plate reader (PerkinElmer). Cells treated with 1%DMSO were used as baseline measurement of apoptosis. As an apoptosis inducer, staurosporine (81590, Cayman) was used as a positive control at 10μM [50, 51].

4.2.9 Western blot

HS cell lines BD, OD, PJ, DH82 and normal fibroblasts treated with either vehicle (0.1%DMSO) or trametinib for 2hs were lysed using CellLytic M (C2978, Sigma-Aldrich) supplemented with 1:100 protease inhibitor (P8340, Sigma-Aldrich) and phosphatase inhibitor B (sc-45045, Santa Cruz). Pre-weighed splenic tissues containing xenograft neoplasms were briefly homogenized in CellLytic MT (C3228, Sigma-Aldrich) with 1:100 protease and phosphatase inhibitor using TissueRuptor (Qiagen). Total protein from supernatant was quantified using Qubit (Thermo Fisher). A total of 40-50µg of protein per lane were separated by Novex NuPAGE SDS-PAGE (10%), and transferred to PVDF membrane. Membranes were blocked with 5%BSA in TBS buffer, and probed overnight with primary antibodies at 4˚C **(Table 4.3)**. Secondary antibodies were incubated for 1h at room temperature. Image of bands was detected using Odyssey Imaging System (LI-COR) and analyzed with Image Studio™ Lite software (LI-COR).

4.2.10 Transfection of luciferase vector

Neoplastic cells from the BD cell line were transfected with a luciferase vector to enable cell tracking by In Vivo Imaging System (IVIS). Briefly, BD cells were incubated with vector pGL4.51[*luc2*/CMV/Neo] (E1320, Promega) and Lipofectamine 2000 (11668027, ThermoFisher) for up to 48hs. Transfected cells were selected by Geneticin (G418, ThermoFisher) at 140µg/ml. A bioluminescent signal was detected in as low as 12,500cells/well *in vitro*. BD cells transfected with luciferase will be referred as BD-luc.

4.2.11 Orthotopic xenograft mouse model of HS

Immunodeficient 6-week old, female of NOD scid gamma mice (NOD.Cg-*Prkdc*^{scid} *Il2rg*^{tm1Wjl}/SzJ, JAX) under general anesthesia with 2-3% isoflurane, were injected aseptically with 50µl of 1.5x10^6 BD-luc cells mixed 1:1 with Matrix Matrigel (CB-40234C, Corning) directly into the spleens, through a

laparotomy approach. After 14 days, mice were randomly divided into two groups of five each (treatment group and vehicle control group). Mice were treated daily either with 1mg/kg of trametinib (16292, Cayman) or vehicle β-cyclodextrin 10% (16169, Cayman) intraperitoneally (IP). Animals were euthanized when humane end-points were reached or after 35 days post cells injection. This xenograft study was approved by the MSU IACUC (AUF# 09/15-133-00). Humane endpoints observed were as follows: body condition score <2, weight loss >15%, lack of movement, abnormal posture and haircoat, and/or clinical signs score ≥15 **(Table 3.1)**. Additionally, the animals' health was monitored daily by the veterinary staff of the university's Campus Animal Resources.

4.2.12 In vivo bioluminescence imaging

For monitoring neoplastic growth, mice were imaged using the IVIS Spectrum (CaliperLS) instrument twice a week under anesthesia with isoflurane. Mice were injected with D-luciferin (LUCK-100, GoldBio) 150mg/kg IP and images were acquired 15 minutes later. Bioluminescent radiance (p/sec/cm^2/sr) from each animal was analyzed using Living Image (Caliper) software.

4.2.13 Mass spectrometry analysis

Plasma samples were mixed with acetonitrile in a 1:3 ratio for protein precipitation. A total of 25mg of tissue samples (muscle, heart, brain, kidney, spleen and liver) were briefly homogenized in 100µl PBS buffer using TissueRuptor (Qiagen), and then mixed with 300µl of acetonitrile. Homogenates were centrifuged at 7,500rpm for 10minutes at 4°C, and supernatant collected for analysis. Internal standard (propyl-4-hydrobenzoate) was added to all samples for normalization. Samples were run on the Quattro Premier triple quadrupole LC/MS/MS instrument using an analytical column (53822-U, Ascentis® Express, C18, 5cmx2.1mm, 2.7µm, Supelco, Bellefonte) at 0.4ml/min. Peak integration was done using Quanlynx software (Masslynx).

4.2.14 Histopathology of xenograft mouse tissues

Tissues from each mouse were fixed in 10% formalin for 24hs and transferred to 70% ethanol until embedding in paraffin. Tissues collected included spleen, liver, heart, lung, brain, intestine, pancreas, stomach, kidney, adrenal gland, skeletal muscle, ovary, and uterus. For each mouse, one representative section of each organ was stained with hematoxylin and eosin (H&E) stain. For IHC, sections from the paraffin blocks were deparaffinized in xylene and rehydrated in ethanol at different concentrations. Hydrogen peroxide 3% was used to neutralize endogenous peroxidase. Antigen retrieval was performed on the PT Link (Dako NA), using the EnVision FLEX Target Retrieval Solution, low pH (Dako NA) for 20 minutes. Sections were labeled with a monoclonal antibody against CD204 (KT022, clone SRA-E5, Transgenic), using an Autostainer Link 48 and the EnVision Flex+ detection system (Dako). Immunoreaction was visualized with 3,3′-diaminobenzidine substrate (Dako) and sections were counterstained with haematoxylin. Images were acquired using a Nikon H600L Microscope as brightfield images using a 10X dry objective. The images were analyzed using NIS-Elements AR 3.1 software. Assessment of histopathology of treatment and vehicle groups was performed by a board certified veterinary pathologist (S.C.) who was blinded as to the treatment status of each sample.

4.2.15 Assessment of liver function

Plasma samples collected immediately post-mortem from mice from both treatment and vehicle groups were sent for analysis of albumin, AST and ALT at the *In-vivo* Animal Core (IVAC, University of Michigan). As a control group, plasma samples were obtained from naïve mice of the same strain which had not been transplanted with tumors. All animals had a similar age, had the same diet and were housed under the same conditions.

4.3 Results

4.3.1 Cell lines established from tissues of dogs

Three cell lines were established from HS of dogs. Two cell lines originated from BMD (BD and OD), the breed with highest incidence of HS, and one from a Rottweiler (PJ). A comprehensive characterization of BD cell line was recently published by our group [45]. To confirm the histiocytic phenotype, we used two markers that are routinely used to diagnose canine HS: CD18 (integrin beta chain beta 2) and CD204 (class A macrophage scavenger receptor) [25, 28, 29, 41, 43]. All three cell lines were positive for both markers by IHC, while negative for CD3 and CD79a, ruling out a lymphoid phenotype **(Figure 4.5)**. The BD cell line carries the *PTPN11*^{E76K} mutation.

Coding regions of the genes *BRAF/NRAS/KRAS/HRAS* from the cell lines were evaluated for the presence of mutations. We identified that the *KRAS* Q61H mutation is present in OD cell line. Alignment of regions of *KRAS* and *PTPN11* mutations from HS cell lines and other relevant species can be found in **Figure 4.6**. No additional mutations were identified in any of the cell lines. Gene sequences can be found under Sequence Read Archive (SRA) study identification SRP139948.

4.3.2 Drug screening identifies MEK inhibitor as a drug candidate for HS

Results from HTS indicated trametinib, a MEK inhibitor, as one of the few compounds highly effective against at least one HS cell line (pIC50>7), BD cell line, while safe for normal cells (pIC50<5). To confirm these observations, we performed cell viability assays using four HS cell lines. Three of them were particularly sensitive to trametinib: BD, OD and PJ **(Figure 4.1A)**. In contrast, the DH82 HHS cell line was resistant to trametinib with at least one order of magnitude lower pIC50 (5.8). Two populations of fibroblasts isolated from skin biopsies/necropsy tissue of dogs were used as normal control, one originated from a mixed breed dog, and one from the dog from which the OD cell line had originated.

Both populations of fibroblasts had markedly lower pIC50s, specifically 3.6 and 4.7 vs. 6.7, 7.5 and 7.8 from PJ, BD and OD cell lines, respectively.

4.3.3 Trametinib blocks cell cycle progression in HS cell lines

To verify whether trametinib inhibits HS by disrupting the cell cycle, we performed a propidium iodine based assay. The inhibition of MEK blocked cell cycle progression in all HS cell lines (BD, OD, PJ and DH82) at all ranges of concentrations of trametinib, low and high **(Figure 4.1B)**. Trametinib promoted a significant increase of HS cells in G1 ($p \leq 0.001$), and a subsequent decrease in S and G2 phases of cell cycle, in comparison to untreated cells. In contrast, cell cycle progression of fibroblasts was not affected by trametinib, as the population of cells in each phase of the cell cycle remained unchanged. In general, fibroblasts had a higher percentage of cells in the G1 phase regardless of treatment although they were in an active proliferative state.

4.3.4 Apoptosis is augmented in HS cell lines sensitive to trametinib

To further understand the mechanisms through which trametinib inhibits HS, we assessed the effect on apoptosis based on caspase 3/7 activity after treatment. Interestingly, the level of apoptosis was significantly increased only in the HS cell lines sensitive to trametinib (BD, OD and PJ) vs. DH82 and normal fibroblasts ($p \leq 0.05$) **(Figure 4.1C)**. Apoptosis was enhanced with treatment at low concentrations, with all sensitive cell lines presenting at least two-fold increase in apoptosis at 10nM of trametinib. These results demonstrate that the effect of trametinib on induction of apoptosis is a critical distinction between sensitive and resistant HS cell lines.

4.3.5 PI3K-AKT pathway is upregulated in resistant hemophagocytic HS cell line

Using phosphorylated ERK (p-ERK) as a readout for MAPK pathway activation, we confirmed that the pathway was substantially inhibited with trametinib in a dose dependent manner: p-ERK was decreased at 10^{-8}M, and markedly reduced at 10^{-7}M in all cell lines **(Figure 4.2A)**. We also evaluated key elements upstream of ERK of the MAPK pathway on cells treated with trametinib 10^{-7}M concentration, as this was sufficient to obliterate p-ERK in all cell lines **(Figure 4.2B)**. Expression of BRAF and RAS was similar in intensity across cell lines, and did not change with trametinib.

Since the MAPK pathway crosstalks with the PI3K/AKT pathway in a way that one can counterbalance the inhibition of the other, we evaluated main components of PI3K/AKT signaling. Indeed, the pathway was more activated in the resistant cell lines, DH82 and normal fibroblasts, represented by increase in p-AKT. Interestingly, expression of the tumor suppressor PTEN, an inhibitor of PI3K-AKT pathway, was nearly undetectable in the DH82 cell line. Expression of p-AKT and PTEN remained unchanged after treatment with trametinib in all other cell lines.

In order to evaluate possible off targets events under treatment with trametinib, we also looked at components of p38 and JNK pathways. While p-p38 was not affected by the treatment, expression of p-JNK was undetectable in the neoplastic cell lines, and unchanged in fibroblasts treated with trametinib.

4.3.6 Administration of trametinib inhibited tumor growth and prolonged survival time in a xenograft mouse model

To determine whether the sensitivity to trametinib was re-capitulated *in vivo*, we used an intrasplenic orthotopic xenograft mouse model with BD-luc cells. Tumor growth correlated with an increase in bioluminescent signal over time as shown in **Figure 4.3A**, and graphically represented in **Figure 4.3B**. Mice treated with trametinib had a significantly lower HS growth rate in comparison to untreated mice ($p=0.02$).

Mice were euthanized when the pre-determined humane endpoints were reached. All mice in the control group reached the endpoints prior to 30 days post transplantation, and were humanely euthanized on days 21 (n=2), 23, 25, and 30 post injection of cells, due to their poor health conditions. In contrast, all mice from the treatment group were alive and in fair condition by the end of the study period, at 37 days post injection. Despite the small cohort of mice in each group, mice from the treatment group exhibited a significantly longer survival time (p=0.002), represented in the Kaplan-Meier survival curve **(Figure 4.3C)**.

4.3.7 MAPK signaling was inhibited in HS of mice treated with trametinib

In order to evaluate if the response seen in the mice was associated with inhibition of the target MAPK pathway, we collected HS neoplasms from spleens of mice 24hs post treatment to determine expression of p-ERK. The MAPK pathway was significantly inhibited in tissues from the treatment group ($p \leq 0.01$), represented by a decrease in p-ERK **(Figure 4.4A)**. In HS tissues (spleen), the concentration of trametinib was consistent across animals with an average of 21.4nM (SD=3.2, range:17-25) **(Figure 4.4B)**. The drug was also detected in other tissues and in circulation at variable concentrations. Muscle tissues had the lowest concentrations of trametinib, while liver tissues had the highest concentrations. Trametinib was undetectable from tissues and plasma from mice treated with vehicle only (data not shown).

4.3.8 Trametinib decreased tumor growth in the liver and minimized tumor-associated liver injury

After euthanasia, tissues were immediately harvested from all mice for evaluation of metastases. H&E sections of spleen confirmed that all mice in both treatment and vehicle groups had diffuse infiltration of neoplastic cells. Metastases were present in the liver histologically, confirmed by CD204 IHC to be of tumor origin **(Figure 4.4D)**, and also in the mesentery and pancreas **(Figure 4.7)**. Percentage of cell necrosis within the splenic and hepatic tissues were scored using a semi quantitative system, as

described by Gibson-Corley et al. [52]. When compared to treated mice, the vehicle control group had a significantly higher score of necrosis in the liver ($p \leq 0.05$) and in the spleen ($p \leq 0.01$), using the unpaired t-test **(Figure 4.4E)**. The mitotic count of the splenic neoplasm was similar between both groups ($p=0.916$ - unpaired t-test), with a mean (standard deviation) of 42(9.7) vs. 42.7(10.8), and a median of 42 vs. 42.5 mitoses per 10 high-power (400X) fields, for treatment group and control group, respectively. Furthermore, histologic features of liver injury were more prominent in hepatocytes from vehicle control mice and included hepatocellular coagulative necrosis (5/5 mice), microvesicular vacuolar change (5/5 mice), and cytoplasmic hypertrophy (4/5 mice). In contrast, hepatocytes from treated mice had either minimal microvesicular vacuolar change (1/5 mice) and mild hepatocellular atrophy (1/5 mice), or were histologically normal (3/5 mice).

Liver function tests were conducted from treated and untreated control mice, and untreated naïve non tumor-bearing mice to evaluate the effect of trametinib on hepatic function. Albumin levels of the untreated naïve mice were significantly higher than those mice from control group ($p \leq 0.001$) and trametinib group ($p \leq 0.01$). Liver enzyme ALT was significantly higher in the vehicle control group vs. the untreated naïve group of mice ($p \leq 0.05$) and the trametinib group ($p \leq 0.05$) **(Figure 4.4C)**.

4.4 Discussion and conclusion

Our findings provide further support that the MAPK pathway may represent an important oncogenic driver in canine HS, and provide proof of concept data for initiating clinical trials with trametinib in dogs with HS. While the low incidence of HS in humans constitutes a major challenge both to the study of oncogenesis, as well as the initiation of clinical trials, the dog represents a unique translational model for this orphan disease.

In the present study, we identified trametinib, a MEK inhibitor, as an effective drug against canine HS at concentrations demonstrated to be achievable in plasma [53, 54]. Trametinib is an allosteric, non-ATP-

competitive compound with sub-nanomolar activity against MEK1/2, in the MAPK pathway, a major oncogenic driver in multiple malignancies [48]. It emerged as a promising treatment for melanomas carrying activating mutant *RAF* and *RAS* [46-48], and led to a successful combination therapy, with dabrafenib, a BRAF inhibitor, for a multi-target strategy for melanoma [55] and non-small cell lung cancer [56]. It is currently part of several advanced clinical trials for other solid tumors and leukemia [57].

We validated the inhibition of the target MEK by a decreased expression of downstream molecules p-ERK in the cells treated with trametinib. We also evaluated the presence of off target effects by looking at proteins representing other branches of MAPK network, p38 and JNK, which were unchanged by treatment with trametinib. However, the existence of off targets events cannot be completely ruled out without an investigation at the level of global proteomic activity.

Although the etiology of human HS is unclear, there is evidence suggesting the role of an oncogenic MAPK pathway, based on cases harboring activating mutations in key genes. *BRAF* (V600E, V595L, G464V, G466R) [11, 12, 14, 15, 21], *HRAS* (Q61R) [14], *KRAS* (Q61H) [15], and *MAP2K1* [16, 58] which have been reported; however, because of the small number of cases, their incidence in HS is still unknown. In a few cases, targeted therapy with small inhibitors vemurafenib and trametinib, a BRAF and a MEK inhibitor, respectively, was associated with favorable response [12, 18]. Among those key genes, we detected a mutation in one of the cell lines, $KRAS^{Q61H}$ in the OD cell line. The $KRAS^{Q61H}$ mutation is known to be an activator of MAPK signaling, and previously reported in a human HS by Liu et al. [15]. Mutations in *KRAS* are present in 22% of all cancers [59], in 82.5% of those cancers sensitive to trametinib, as reported by Jing et al. where 33 of 40 (82.5%) *KRAS* mutant cell lines showed IC_{50}<50nM [48, 60]. Genes in this pathway are highly conserved. There is a high degree of identity at the amino acid level between human and dog sequences with *BRAF, KRAS, HRAS*, and *NRAS*, showing 99%, 99% 98% and 100% identities, respectively. Therefore, it is not surprising to see activating mutations be shared

among the two species. No other mutation was found in *BRAF, KRAS, NRAS* and *HRAS* across all HS cell lines.

As recently reported by our group, a gain of function mutation in *PTPN11* was found to be associated with HS in BMDs [37]. Activating mutations in *PTPN11* gene have been also reported in human HS cases [15, 18, 61, 62]. *PTPN11* encodes the SHP2 protein, which is required for the MAPK pathway. Interestingly, among our HS cell lines, BD carries the mutation $PTPN11^{E76K}$, previously reported in two human HS cases [18, 61]. In one of these cases, the patient with multi-organ HS received trametinib after failing several chemotherapy protocols, resulting in a partial remission for two months [18]. Therefore, we hypothesize that the sensitivity to trametinib from BD and OD cell lines is resultant of mutations that activate the oncogenic MAPK pathway. We could not detect mutations in *BRAF/HRAS/KRAS/NRAS* on a third sensitive cell line (PJ), suggesting that looking at only that set of genes is not sufficient to predict sensitivity to trametinib, and other genes that activate MAPK should be investigated through a larger mutation analysis.

Trametinib induces $p15^{INK4b}$ and $p27^{KIP1}$, inhibitors of CDK4/6 [63], leading to the arrest of the cell cycle at the G1 phase [64, 65]. Similarly, trametinib significantly blocked cell cycle progression in G1 phase, however, the effect was similar in magnitude in both sensitive and resistant HS cell lines. In contrast, the level of apoptosis was significantly augmented in sensitive cell lines (BD, OD and PJ) at concentrations close to their IC_{50}s, while minimal in resistant cells (DH82 and FB), indicating that apoptosis is a key event of growth suppression in HS cells by trametinib, and that it may represent a marker for sensitivity to this drug. Likewise, induction of apoptosis has been reported as a major mechanism of inhibition in other cancer cells treated with MEK inhibitor [66-68], and indicative of *in vivo* efficacy [64]. These findings suggest that trametinib sensitive HS cell lines are more dependent on activated MAPK signaling, whereas HHS DH82 cells are able to evade apoptosis under MEK inhibition, likely by an alternative mechanism of survival.

Rescue from apoptosis induced by trametinib has been previously linked to a hyperactivated PI3K-AKT pathway, counterbalancing the inhibition of MAPK pathway [64, 69, 70]. Indeed, our results suggest that the PI3K/AKT pathway was upregulated in DH82 cells, as indicated by the lack of PTEN expression and overexpression of p-AKT. We hypothesize that in DH82 cells, PI3K/AKT is a major driver. This mechanism of resistance was demonstrated when the MEK inhibitor-sensitive status of *KRAS* mutant cells was reversed through *PTEN* depletion [70]. Although the role of the PI3K/AKT pathway in HS is unknown, formation of HS was observed in PTEN mutant mice, suggesting its role as contributor for tumorigenesis [71]. Comparison of such pathways in HS may help delineate sensitivity to MEK inhibitor-based treatment, and indicate targets for alternative drugs, i.e. AKT inhibitors.

In order to evaluate our *in vitro* findings *in vivo*, we used a mouse model that initially presents an intrasplenic tumor that later spread to multiple intra-abdominal organs, and thus, can be considered an orthotopic model of a metastatic/disseminated form of HS, the most clinically challenging one due to the lack of specific systemic treatments. In this model, trametinib significantly suppressed tumor growth ($p=0.02$ - Student t-test) and increased survival time ($p=0.002$ - Mantel Cox test). Untreated mice reached humane endpoints and were euthanized between days 21 and 30 post-cells injection, while treated mice survived beyond 37 days and were alive by the end of the study. Similar findings were observed in *BRAF* and *KRAS* mutant cancer xenograft models with inhibition of tumor growth at doses ranging from 0.1mg/kg to 1mg/kg once daily orally [48, 64, 72, 73]. A marked drop in bioluminescent signal in some mice at the final reading is likely associated with poor vascularization and central necrosis within the tumor, limiting the substrate and oxygen that generate the bioluminescent signal [74]. Although trametinib is an oral drug, the IP route for treatment was chosen as a reasonably easy method to administer the drug, minimizing the stress to the animals. Moreover, we anticipated that when given IP, trametinib should be mostly absorbed through the surface of membranes into the portal vein [75]. Due to the drug's long half-life, steady state was certainly achieved at day 23 of treatment when average

plasma concentration was 21.4nM (17-25nM), and tissue concentration was 30.2nM (5-53nM), which are higher than the IC_{50} of most of cell lines. Pharmacokinetic studies for drug approval showed that mice treated orally with 1mg/kg daily, had significantly higher plasma concentrations (459nM) [76]. Although the route chosen diverged from the actual route of administration in patients, our results are within an achievable concentration seen in human patients treated with trametinib at the regular dose scheme (2mg/day), reported as steady state concentrations of 19.3-19.6nM [77, 78], and 34nM [54]. Moreover, we demonstrated that treatment with trametinib resulted in a sustained target engagement, with significant downregulation of p-ERK in tumor tissues after 24hs of dosing. Similarly, other studies have reported that trametinib caused inhibition of p-ERK in xenograft tumors of colorectal cancer for more than 8hs after a single dose [64], and over 24hs when administered PO for 7 days in a model for melanoma [48]. Higher plasma levels of trametinib (>300nM) were reported in mice at doses of 3mg/kg/day PO [48], and thus additional studies with even higher doses of trametinib can be undertaken. However, our findings do indicate that trametinib can be an effective treatment for HS.

As we used humane endpoints for decisions for euthanasia, control mice were euthanized at different time points, as the disease advanced. Due to the variable time points of euthanasia, the metastatic rate could not be compared across groups. When metastatic foci were further studied, we observed smaller metastatic foci and a less compromised hepatic architecture in the liver of mice in the treatment group as compared to the control group **(Figure 4.7)**, suggesting that trametinib may have inhibited growth at metastatic sites. Untreated control mice had a diffuse metastatic pattern and abnormal architecture of the liver with higher level of cell necrosis, which may be associated with an impaired hepatic function, as reflected in the higher plasma liver enzyme concentrations. However, the difference in liver function could also be related to the fact that euthanasia was performed at the end stage of all untreated mice, whereas it was done to treated mice at a predetermined time when study ended. Therefore, an impaired liver function could be related to the moribund state of untreated mice rather than tumor

burden. Treatment alone did not seem to have an effect on liver function as no difference was observed between untreated naïve mice and treated mice. Untreated naïve mice had significantly higher levels of albumin when compared to either vehicle control or trametinib treatment groups, indicating that the lower levels of albumin in the vehicle control and the treatment group are likely caused by the presence of the xenograft tumor, decreasing liver tissue and affecting the liver function as well as a poor body condition and malnutrition due to their moribund state.

Our results suggest that a dysfunctional MAPK pathway plays a role in canine HS, and that targeting MEK is a promising therapeutic strategy. Two of the four canine cell lines carry previously described mutations in genes associated with the activation of MAPK pathway, *PTPN11* and *KRAS*. These mutations can be potentially used as indicators of sensitivity to trametinib, however, a larger number of cases are needed before this can be confirmed. We hypothesize that additional activating mutations are present in the oncogenic MAPK cascade in canine HS and can be targeted by trametinib. Thus genomic sequencing studies are needed to unravel potential driver mutations, in these and other genes, which are currently underway in our laboratory. Understanding other activated signaling pathways such as PI3K/AKT, may help predict sensitivity or resistance to MEK inhibition, and identify other targeted therapies.

In conclusion, trametinib represents a novel targeted therapy for HS in dogs. Clinical trials in human patients with HS are challenging as case accrual would take an extended time due to the low incidence of HS. Dogs, on the other hand, present with an appreciable frequency of HS, and therefore represent an important translational model and can contribute with valuable information regarding mechanisms of tumorigenesis, novel targets for therapy, and provide proof of concept studies that can translate to humans. Clinical trials to test the safety and efficacy of trametinib in canine patients with HS are warranted to further generate relevant information in this large model of spontaneously occurring cancer.

APPENDIX

Figure 4.1. Trametinib causes cell cycle blockage and promotes apoptosis in sensitive HS cell lines**. (A)** Cell viability was measured using CellTiter Glo assay on three HS cell lines (BD, OD, PJ), a hemophagocytic HS cell line (DH82) and two normal dog fibroblast cell lines (FB BMD, FB) treated with trametinib for 72hs. **(B)** Cells were treated with either vehicle, 1nM, 10nM, 100nM or 1μM trametinib for 24hs, and analyzed for DNA content based on propidium iodine uptake. Trametinib blocked cell cycle progression and triggered G1 phase arrest in all cancer cell lines BD, OD, PJ and DH82, but not in normal fibroblasts. Statistical analysis was done using Tukey's multiple comparison two-way ANOVA test. **(C)** Level of apoptosis was measured using Caspase-Glo 3/7 on cells treated with either vehicle, 1nM, 10nM, 100nM or 1μM trametinib, or staurosporine (positive control) for 24hs. Apoptosis was significantly increased in the cell lines that are sensitive to trametinib (BD, OD and PJ), while the effect was not observed in the resistant cell lines (DH82 and FB). Data were statistically analyzed using a multiple comparison two-way ANOVA test. For all assays (A, B and C), values correspond to averages and error bars to standard deviations generated from three experimental repeats.

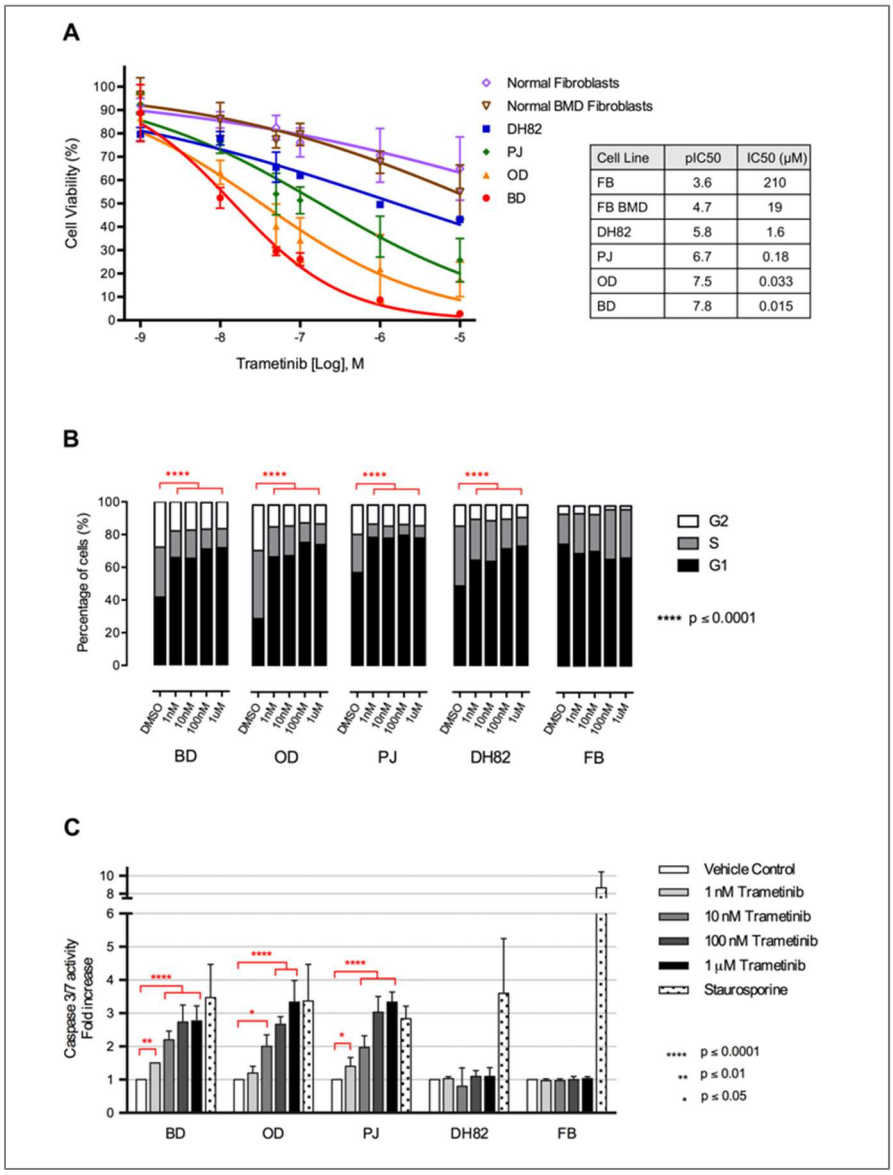

Figure 4.2. MEK inhibitor trametinib downregulates downstream p-ERK in a dose dependent manner. Levels of proteins of cells treated with trametinib for 2hs were analyzed using Western-Blots. **(A)** In all cell lines, the level of p-ERK decreased as the concentration of trametinib increases. Expression of pERK was significantly reduced at trametinib concentrations of 10^{-8} M, and undetectable at 10^{-7} M. **(B)** Increased expression of p-Akt and decreased expression of PTEN were observed in the resistant hemophagocytic HS cell line DH82. There was no difference in expression of other components of the MAPK pathway.

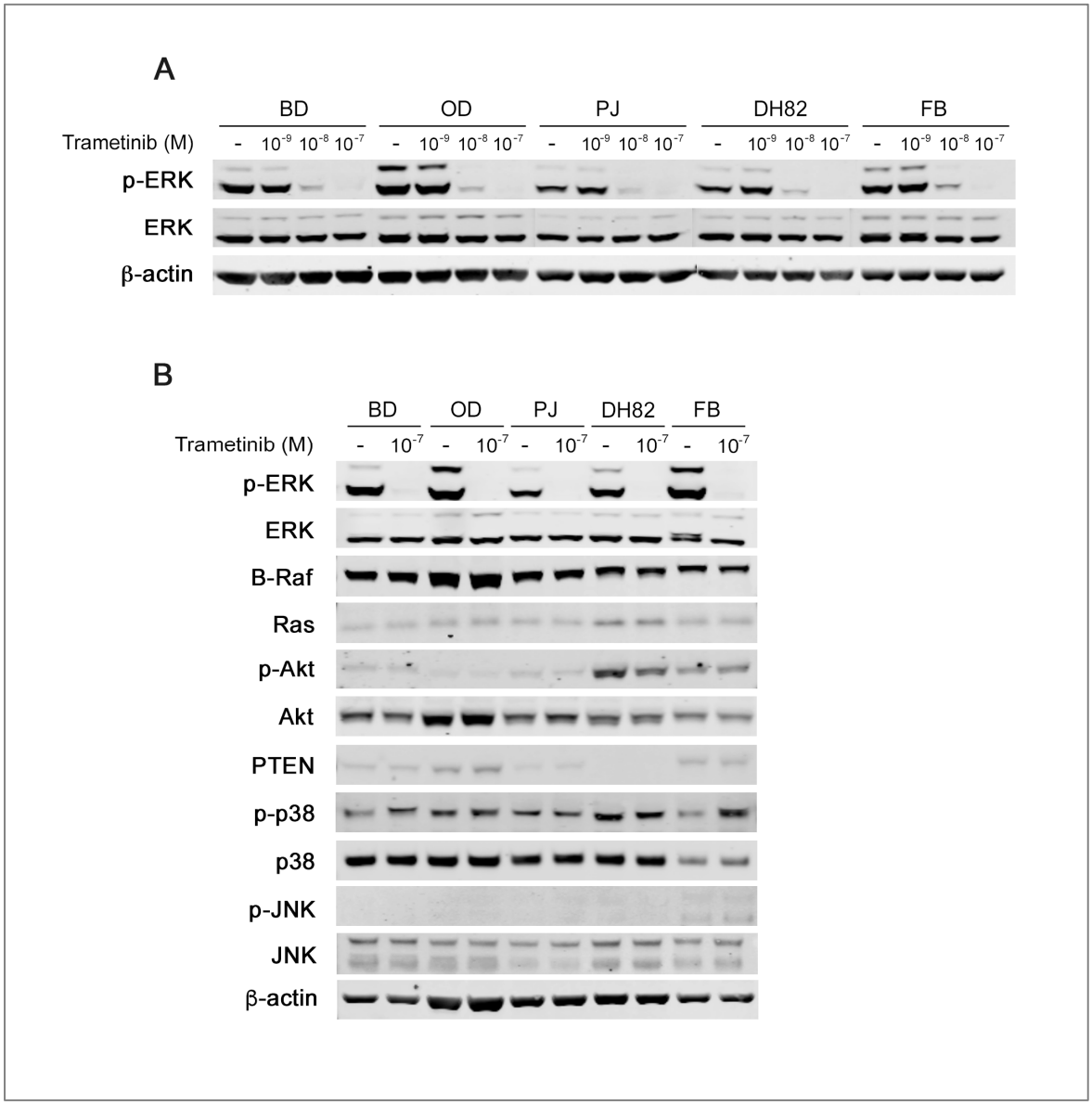

Figure 4.3. Trametinib decreases the rate of tumor growth and increases survival time of xenograft mice injected intrasplenically with BD-luc cells. Immunocompromised mice were injected into the spleen with $1.5x10^6$ BD-luc cells. After 14 days, mice were randomized in two groups to receive daily treatment with either 1mg/kg trametinib or vehicle IP. Animals were euthanized as humane endpoints were reached, or after 20 days of treatment. The intensity of the bioluminescence signal of mice from the vehicle group increased more rapidly than the intensity of the signal in the treatment group. Images were taken biweekly using IVIS as shown in few representative pictures of different stages of treatment **(A)**, and graphically **(B)**. The values of each group of mice were statistically different based on Student t-test analysis (thicker lines represent mean values of each group). The Kaplan-Meier survival curve shows that trametinib increased survival time of mice **(C)**, and the difference was statistically significant based on Mantel-Cox test.

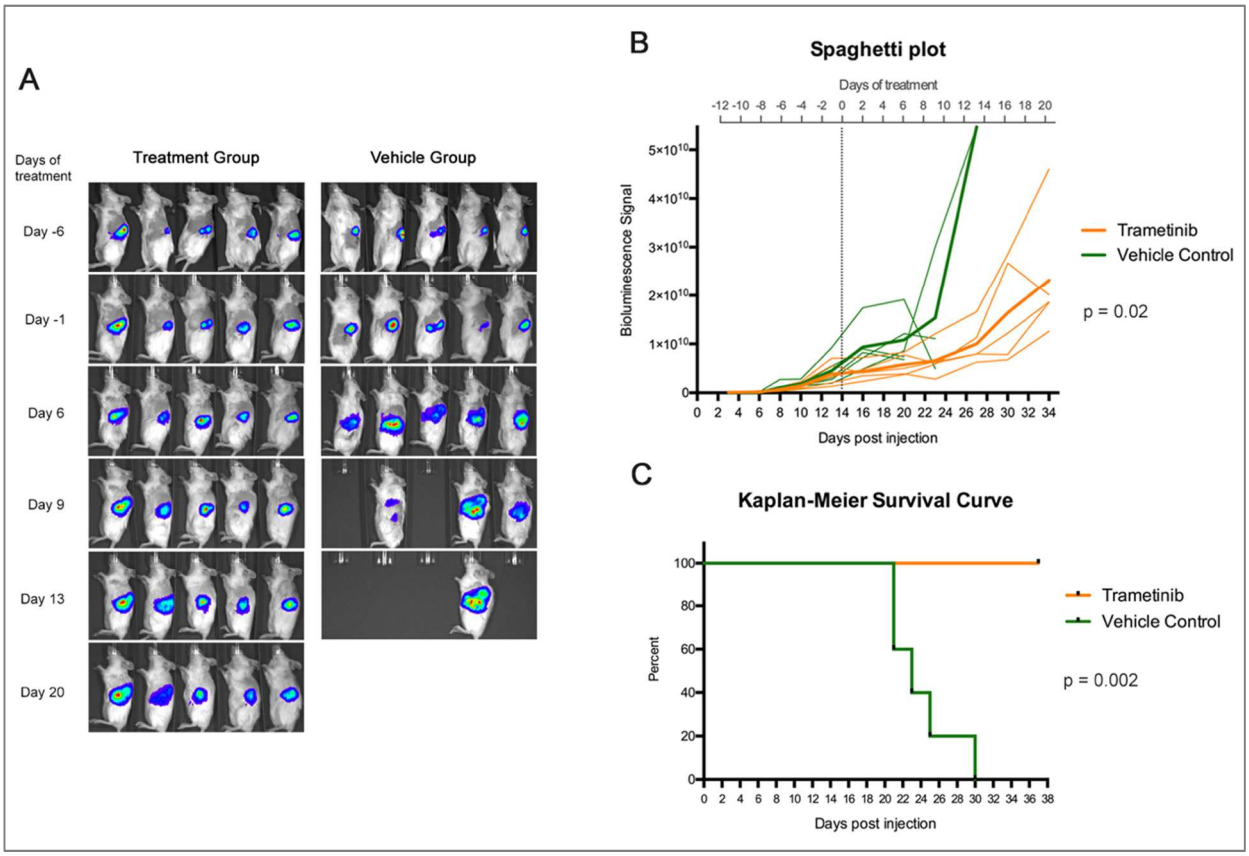

Figure 4.4. Trametinib decreases activity of MAPK signaling in tissues, where the drug was present at concentrations consistent with therapeutic levels and mitigates liver injury associated with tumor burden**. (A)** Trametinib significantly decreased p-ERK of splenic tissues of treated mice (each column represents one mouse). Statistical analysis used was Mann-Whitney one-tail t test (p-ERK was normalized with values of tERK). **(B)** Samples of different organs and plasma were collected post-mortem 24hs after last dosing and analyzed for the concentration of trametinib. Data points represent individual mouse, identified by a specific number (1-5). Trametinib was found in splenic tissues and in other tissues, and plasma at variable concentrations. Bars represent mean values and standard deviations.

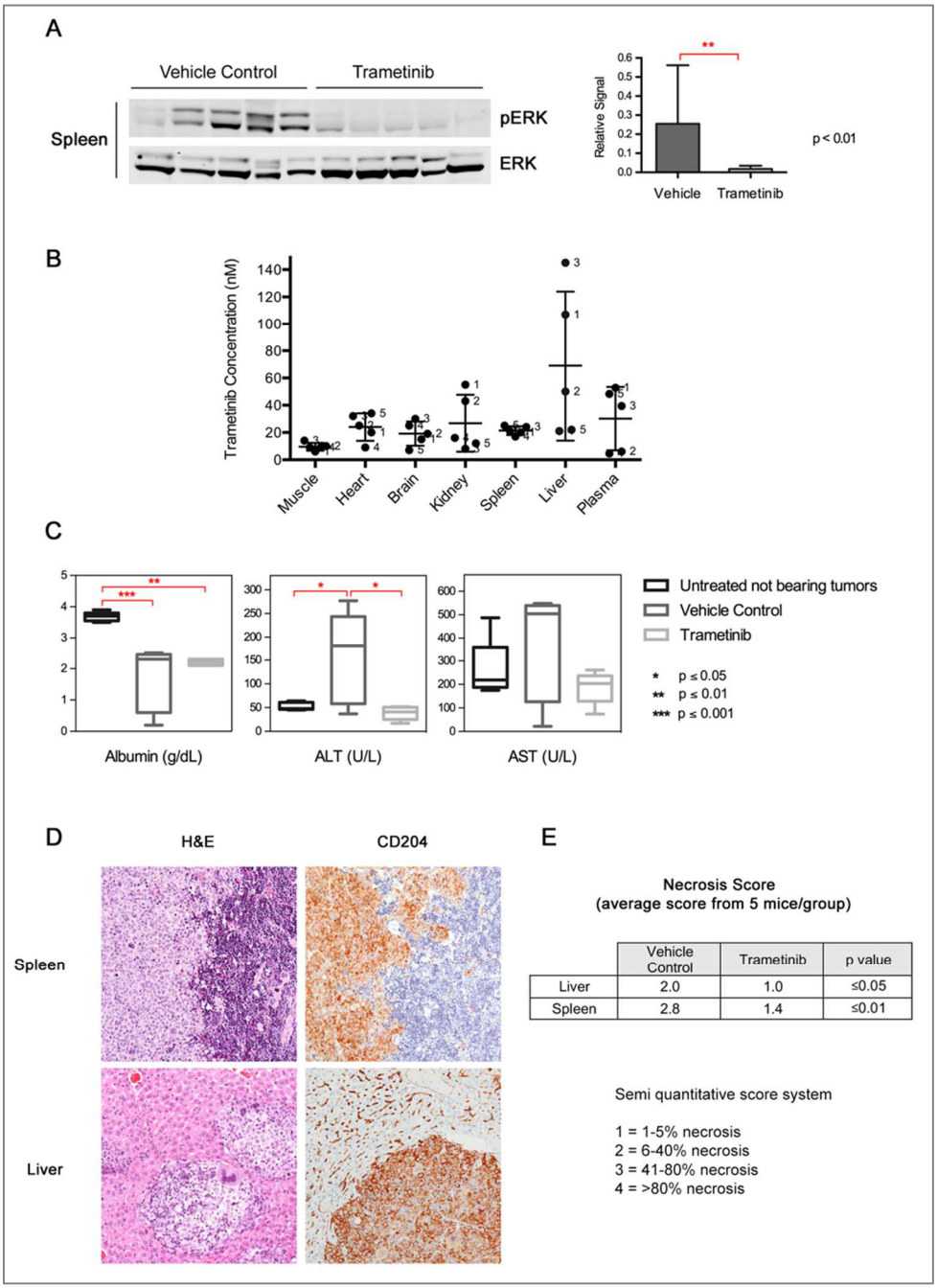

	Vehicle Control	Trametinib	p value
Liver	2.0	1.0	≤0.05
Spleen	2.8	1.4	≤0.01

Figure 4.4. (cont'd)
(C) Mice bearing tumors presented significant lower levels of albumin than naïve non-bearing tumors mice. Mice from vehicle control group had significant higher levels of ALT, when compared to non-bearing tumor mice and trametinib treated mice. AST levels were not different across the groups. **(D)** Histologically, splenic tumors consisted of diffuse infiltration by highly pleomorphic, neoplastic round cells, with marked anisocytosis, anisokaryosis, and numerous multinucleated cells. Variably sized, nodular accumulations of neoplastic cells were also present within the liver. Neoplastic cells within the spleen and hepatic metastatic foci had strong positive cytoplasmic immunoreactivity for CD204. **(E)** Untreated mice had a significantly higher level of cell necrosis within their splenic and hepatic tissues, based on a semi quantitative score system.

Figure 4.5. Immunohistochemical characterization of HS cell lines. CD204 and CD18 are standard cell surface markers expressed by HS in dogs. Newly established HS cell lines were positive with both CD204 and CD18 by IHC of sections of cell pellets. CD3 and CD79a were used to rule out a lymphoid phenotype, for which all cell lines were negative. Calibration bar: 100 μm.

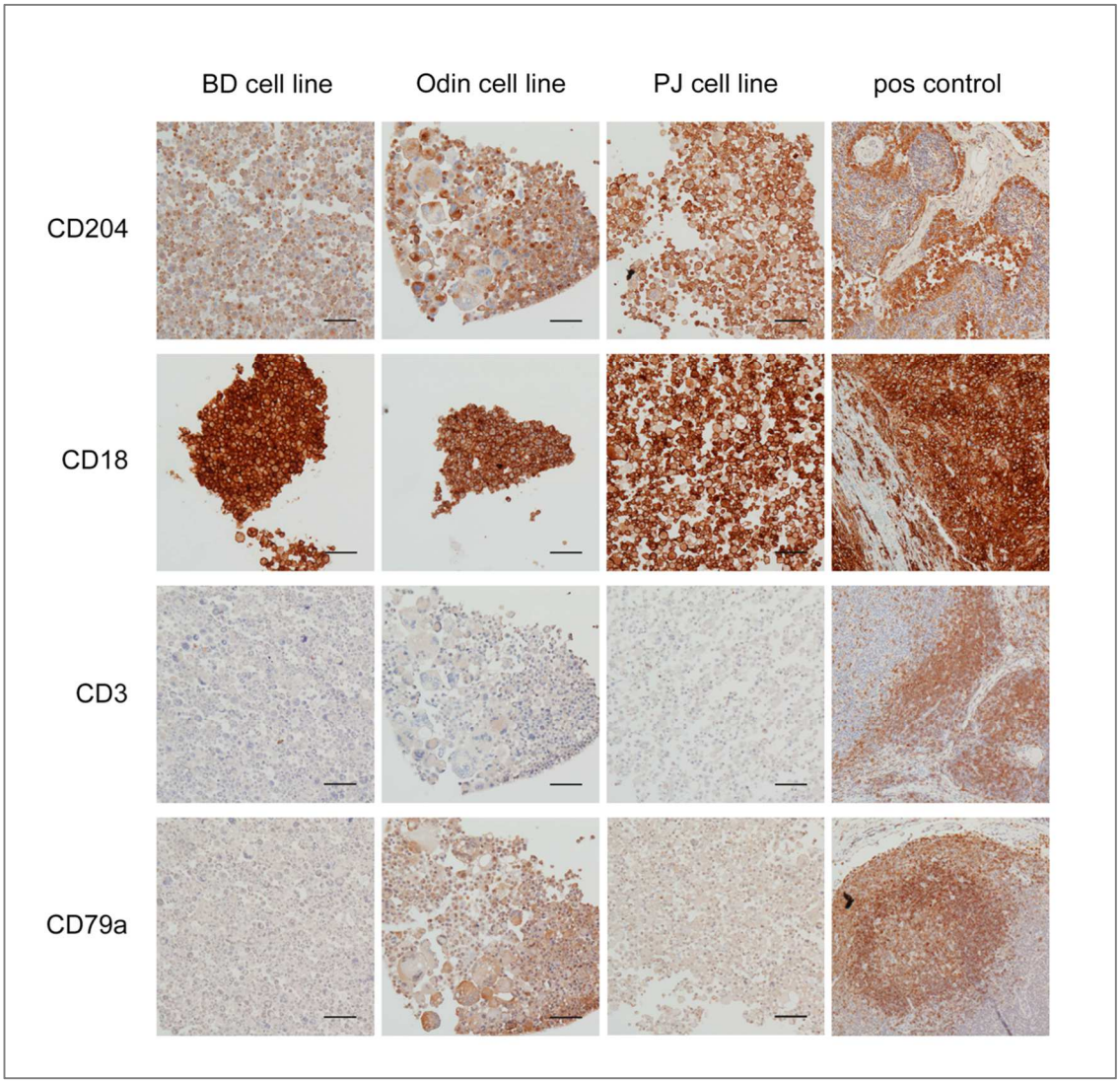

Figure 4.6. Alignment of regions of genes *KRAS* and *PTPN11* from HS cell lines and relevant species.

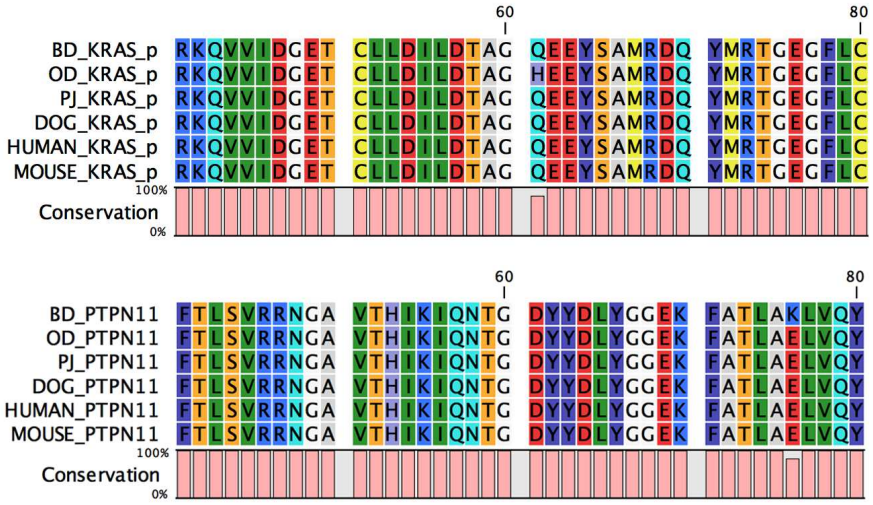

Figure 4.7. Images of metastatic sites of the HS xenograft mice. **(A)** Small, well-demarcated metastatic foci in the liver in the treated mice compared to more diffuse hepatic metastasis in the vehicle control group **(B). (C)** Metastatic foci obscure the intestinal mesenteric adipose tissue. **(D)** Metastatic nodules obscure the exocrine pancreas.

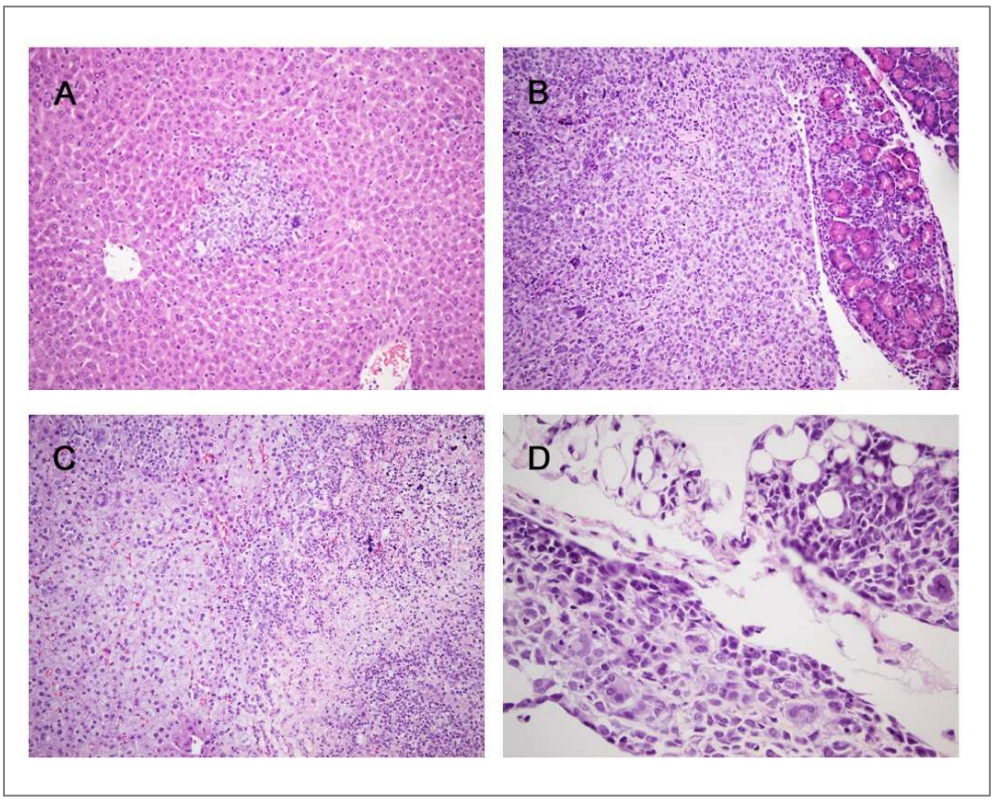

Table 4.1. General characteristics of cell lines

Cell line	Breed	Source	Gender	Age (years)	Tissue of origin	Diagnosis	Cell Markers
BD	BMD	Current study	SF	8	Abdominal mass	HS	CD204+, CD18+, CD11c+
OD	BMD	Current study	M	10	Lung	HS	CD204+, CD18+, CD11c+
PJ	Rottweiler	Current study	M	8	Lung	HS	CD204+, CD18+, CD11c+
DH82	Golden Retriever	ATCC	M	10	Bone marrow	HHS	CD204+, CD18+, CD11c-
FB BMD*	BMD	Current study	M	10	Skin	Normal tissue	
FB	Mixed breed dog	Current study	F	5	Skin	Normal tissue	

(F: female intact, SF: spayed female, M: male intact)

*OD and FB BMD were established from tissues of the same dog.

Table 4.2. Genetic profile of a panel of microsatellite markers for genotyping of BD, OD and PJ cell lines

Genetic profile of a panel of microsatellite markers for genotyping of BD, OD and PJ cell lines (CellCheck STR profile - IDEXX BioResearch)					
Marker	Locus	Chromosome	BD cell line	OD cell line	PJ cell line
Canine 1	FH3210	2	285, 293	269	281, 305
Canine 17	PEZ12	3	301	267, 297	267
Canine 2	FH3241	8	260, 264	256	260
Canine 3	FH2004	11	170, 174	170, 174	174, 178
Canine 16	FH2054	12	156, 160	152	156, 176
Canine 4	FH2658	14	116	116, 124	113, 116
Canine 5	FH4012	15	119, 127	127	131, 135
Canine 6	REN214L11	16	150	154	150, 154
Canine 13	WILMS-TF	18	279	283, 299	283, 291
Canine 7	FH2010	24	155	155	159
Canine 14	PEZ6	27	183, 188	196	184
Canine 19	VWF.X	27	155	161	179
Canine 8	FH2361	33	248	240	248
Canine 15	FH2611	36	193, 197	204	196
Sex	AR (X), Sry1.1 (Y)	X, Y	X, X	X, Y	X, Y

Table 4.3. Description of antibodies used for protein detection

Primary antibodies						
Protein	*Catalog#*	*Clone*	*Lot#*	*Host*	*Manufacturer*	*Conc.*
p-ERK	4370	D13.14.4E	15	Rabbit	Cell Signaling	1:500
ERK1/2	4695	137F5	14	Rabbit	Cell Signaling	1:1,000
BRAF	sc-5284	F-7	F2216	Mouse	Santa Cruz	1:500
RAS	610001	18/Ras	6056961	Mouse	BD	1:500
ß-actin	3700	8H10D10	13, 14	Mouse	Cell Signaling	1:2,000
ß-actin	4970	13E5	12	Rabbit	Cell Signaling	1:2,000
p-AKT (Ser473)	9271	D9E	12	Rabbit	Cell Signaling	1:500
AKT	9272		9	Rabbit	Cell Signaling	1:500
p28	8690	D13E1	8	Rabbit	Cell Signaling	1:1,000
p-p28	4511	D3F9	13	Rabbit	Cell Signaling	1:1,000
JNK	9252		17	Rabbit	Cell Signaling	1:500
p-JNK	9251		26	Rabbit	Cell Signaling	1:1,000
Secondary Antibodies						
Protein	*Catalog#*	*Lot#*	*Host*	*Target*	*Manufacturer*	*Conc.*
IRDye 800CW	926-32210	C50113-06	Goat	Mouse	LI-COR	1:15,000
IRDye 680RD	926068071	C41217-03	Goat	Rabbit	LI-COR	1:15,000

BIBLIOGRAPHY

BIBLIOGRAPHY

1. Swerdlow SH, Campo E, et al., *The 2016 revision of the World Health Organization classification of lymphoid neoplasms.* Blood, 2016. 127(20): p. 2375.

2. Shimono J, Miyoshi H, et al., *Prognostic factors for histiocytic and dendritic cell neoplasms.* Oncotarget, 2017. 8(58): p. 98723.

3. Jaffe ES and World Health Organization., *Pathology and genetics of tumours of haematopoietic and lymphoid tissues*. World Health Organization classification of tumors. 2001, Lyon: IARC Press. 351 p.

4. Jaffe ES, *Histiocytoses of lymph nodes: biology and differential diagnosis.* Semin Diagn Pathol, 1988. 5(4): p. 376.

5. Takahashi E and Nakamura S, *Histiocytic sarcoma : an updated literature review based on the 2008 WHO classification.* Journal of clinical and experimental hematopathology : JCEH, 2013. 53(1): p. 1.

6. Hornick JL, Jaffe ES, et al., *Extranodal histiocytic sarcoma: clinicopathologic analysis of 14 cases of a rare epithelioid malignancy.* Am J Surg Pathol, 2004. 28(9): p. 1133.

7. Dalia S, Jaglal M, et al., *Clinicopathologic characteristics and outcomes of histiocytic and dendritic cell neoplasms: the moffitt cancer center experience over the last twenty five years.* Cancers (Basel), 2014. 6(4): p. 2275.

8. Gounder M, Desai V, et al., *Impact of surgery, radiation and systemic therapy on the outcomes of patients with dendritic cell and histiocytic sarcomas.* Eur J Cancer, 2015. 51(16): p. 2413.

9. Vos JA, Abbondanzo SL, et al., *Histiocytic sarcoma: a study of five cases including the histiocyte marker CD163.* Mod Pathol, 2005. 18(5): p. 693.

10. Kommalapati A, Tella SH, et al., *Histiocytic sarcoma: a population-based analysis of incidence, demographic disparities, and long-term outcomes.* Blood, 2018. 131(2): p. 265.

11. Michonneau D, Kaltenbach S, et al., *BRAFV600E Mutation in a Histiocytic Sarcoma Arising From Hairy Cell Leukemia.* J Clin Oncol, 2014. 32(35): p. e117.

12. Idbaih A, Mokhtari K, et al., *Dramatic response of a BRAF V600E-mutated primary CNS histiocytic sarcoma to vemurafenib.* Neurology, 2014. 83(16): p. 1478.

13. Curry RC, Faivre G, et al., *High-dose methotrexate-based chemotherapy as treatment for histiocytic sarcoma of the central nervous system.* Leuk Lymphoma, 2016: p. 1.

14. Kordes M, Roring M, et al., *Cooperation of BRAF(F595L) and mutant HRAS in histiocytic sarcoma provides new insights into oncogenic BRAF signaling.* Leukemia, 2016. 30(4): p. 937.

15. Liu Q, Tomaszewicz K, et al., *Somatic mutations in histiocytic sarcoma identified by next generation sequencing.* Virchows Arch, 2016. 469(2): p. 233.

16. Facchetti F, Pileri SA, et al., *Histiocytic and dendritic cell neoplasms: what have we learnt by studying 67 cases.* Virchows Arch, 2017. 471(4): p. 467.

17. Go H, Jeon YK, et al., *Frequent detection of BRAF(V600E) mutations in histiocytic and dendritic cell neoplasms.* Histopathology, 2014. 65(2): p. 261.

18. Voruz S, Cairoli A, et al., *Response to MEK inhibition with trametinib and tyrosine kinase inhibition with imatinib in multifocal histiocytic sarcoma.* Haematologica, 2018. 103(1): p. e39.

19. Lee LH, Gasilina A, et al., *Real-time genomic profiling of histiocytoses identifies early-kinase domain BRAF alterations while improving treatment outcomes.* JCI Insight, 2017. 2(3): p. e89473.

20. Badalian-Very G, Vergilio JA, et al., *Recurrent BRAF mutations in Langerhans cell histiocytosis.* Blood, 2010. 116(11): p. 1919.

21. Haroche J, Charlotte F, et al., *High prevalence of BRAF V600E mutations in Erdheim-Chester disease but not in other non-Langerhans cell histiocytoses.* Blood, 2012. 120(13): p. 2700.

22. Brown NA, Furtado LV, et al., *High prevalence of somatic MAP2K1 mutations in BRAF V600E-negative Langerhans cell histiocytosis.* Blood, 2014. 124(10): p. 1655.

23. Chakraborty R, Hampton OA, et al., *Mutually exclusive recurrent somatic mutations in MAP2K1 and BRAF support a central role for ERK activation in LCH pathogenesis.* Blood, 2014. 124(19): p. 3007.

24. Bruner SR, *Updates in therapeutics for veterinary dermatology.* The Veterinary clinics of North America. Small animal practice, 2006. 36(1): p. 39.

25. Abadie J, Hedan B, et al., *Epidemiology, pathology, and genetics of histiocytic sarcoma in the Bernese mountain dog breed.* J Hered, 2009. 100 Suppl 1: p. S19.

26. Ruple A and Morley PS, *Risk Factors Associated with Development of Histiocytic Sarcoma in Bernese Mountain Dogs.* J Vet Intern Med, 2016. 30(4): p. 1197.

27. Dervisis NG, Kiupel M, et al., *Clinical prognostic factors in canine histiocytic sarcoma.* Vet Comp Oncol, 2016.

28. Klahn SL, Kitchell BE, et al., *Evaluation and comparison of outcomes in dogs with periarticular and nonperiarticular histiocytic sarcoma.* J Am Vet Med Assoc, 2011. 239(1): p. 90.

29. Affolter VK and Moore PF, *Localized and disseminated histiocytic sarcoma of dendritic cell origin in dogs.* Vet Pathol, 2002. 39(1): p. 74.

30. Craig LE, Julian ME, et al., *The diagnosis and prognosis of synovial tumors in dogs: 35 cases.* Vet Pathol, 2002. 39(1): p. 66.

31. Skorupski KA, Clifford CA, et al., *CCNU for the treatment of dogs with histiocytic sarcoma.* J Vet Intern Med, 2007. 21(1): p. 121.

32. Fidel J, Schiller I, et al., *Histiocytic sarcomas in flat-coated retrievers: a summary of 37 cases (November 1998-March 2005).* Vet Comp Oncol, 2006. 4(2): p. 63.

33. Cannon C, Borgatti A, et al., *Evaluation of a combination chemotherapy protocol including lomustine and doxorubicin in canine histiocytic sarcoma.* J Small Anim Pract, 2015. 56(7): p. 425.

34. Rassnick KM, Moore AS, et al., *Phase II, open-label trial of single-agent CCNU in dogs with previously untreated histiocytic sarcoma.* J Vet Intern Med, 2010. 24(6): p. 1528.

35. Hedan B, Thomas R, et al., *Molecular cytogenetic characterization of canine histiocytic sarcoma: A spontaneous model for human histiocytic cancer identifies deletion of tumor suppressor genes and highlights influence of genetic background on tumor behavior.* BMC Cancer, 2011. 11: p. 201.

36. Shearin AL, Hedan B, et al., *The MTAP-CDKN2A locus confers susceptibility to a naturally occurring canine cancer.* Cancer Epidemiol, 2012. 21(7): p. 1019.

37. Thaiwong T, Sirivisoot S, et al., *Gain-of-function mutation in PTPN11 in histiocytic sarcomas of Bernese Mountain Dogs.* Vet Comp Oncol, 2017.

38. Vos JA, Abbondanzo SL, et al., *Histiocytic sarcoma: a study of five cases including the histiocyte marker CD163.* Mod Pathol, 2005. 18(5): p. 693.

39. Lau SK, Chu PG, et al., *CD163: a specific marker of macrophages in paraffin-embedded tissue samples.* Am J Clin Pathol, 2004. 122(5): p. 794.

40. Nguyen TT, Schwartz EJ, et al., *Expression of CD163 (hemoglobin scavenger receptor) in normal tissues, lymphomas, carcinomas, and sarcomas is largely restricted to the monocyte/macrophage lineage.* Am J Surg Pathol, 2005. 29(5): p. 617.

41. van Kuijk L, van Ginkel K, et al., *Peri-articular histiocytic sarcoma and previous joint disease in Bernese Mountain Dogs.* J Vet Intern Med, 2013. 27(2): p. 293.

42. Kato Y, Funato R, et al., *Immunocytochemical detection of the class A macrophage scavenger receptor CD204 using air-dried cytologic smears of canine histiocytic sarcoma.* Vet Clin Pathol, 2014. 43(4): p. 589.

43. Kato Y, Murakami M, et al., *The class A macrophage scavenger receptor CD204 is a useful immunohistochemical marker of canine histiocytic sarcoma.* J Comp Pathol, 2013. 148(2-3): p. 188.

44. Thongtharb A, Uchida K, et al., *Histological and immunohistochemical studies on primary intracranial canine histiocytic sarcomas.* J Vet Med Sci, 2016. 78(4): p. 593.

45. Takada M, Parys M, et al., *A novel canine histiocytic sarcoma cell line: initial characterization and utilization for drug screening studies.* BMC Cancer, 2018. 18(1): p. 237.

46. Flaherty KT, Infante JR, et al., *Combined BRAF and MEK inhibition in melanoma with BRAF V600 mutations.* N Engl J Med, 2012. 367(18): p. 1694.

47. Johnson DB and Puzanov I, *Treatment of NRAS-mutant melanoma.* Curr Treat Options Oncol, 2015. 16(4): p. 15.

48. Gilmartin AG, Bleam MR, et al., *GSK1120212 (JTP-74057) is an inhibitor of MEK activity and activation with favorable pharmacokinetic properties for sustained in vivo pathway inhibition.* Clin Cancer Res, 2011. 17(5): p. 989.

49. Distaso GBaW, *GRETL: Econometric software for the GNU generation.* Journal of Applied Econometrics, 2003. 18: p. 105.

50. Kabir J, Lobo M, et al., *Staurosporine induces endothelial cell apoptosis via focal adhesion kinase dephosphorylation and focal adhesion disassembly independent of focal adhesion kinase proteolysis.* Biochem J, 2002. 367(Pt 1): p. 145.

51. Belmokhtar CA, Hillion J, et al., *Staurosporine induces apoptosis through both caspase-dependent and caspase-independent mechanisms.* Oncogene, 2001. 20(26): p. 3354.

52. Gibson-Corley KN, Olivier AK, et al., *Principles for valid histopathologic scoring in research.* Vet Pathol, 2013. 50(6): p. 1007.

53. Kim KB, Kefford R, et al., *Phase II study of the MEK1/MEK2 inhibitor Trametinib in patients with metastatic BRAF-mutant cutaneous melanoma previously treated with or without a BRAF inhibitor.* J Clin Oncol, 2013. 31(4): p. 482.

54. Ouellet D, Kassir N, et al., *Population pharmacokinetics and exposure-response of trametinib, a MEK inhibitor, in patients with BRAF V600 mutation-positive melanoma.* Cancer Chemother Pharmacol, 2016. 77(4): p. 807.

55. Long GV, Stroyakovskiy D, et al., *Dabrafenib and trametinib versus dabrafenib and placebo for Val600 BRAF-mutant melanoma: a multicentre, double-blind, phase 3 randomised controlled trial.* Lancet, 2015. 386(9992): p. 444.

56. Planchard D, Besse B, et al., *Dabrafenib plus trametinib in patients with previously treated BRAF(V600E)-mutant metastatic non-small cell lung cancer: an open-label, multicentre phase 2 trial.* Lancet Oncol, 2016. 17(7): p. 984.

57. Institute NC. *Clinical trials using trametinib*. 2018 [cited 2018 February 24]; Available from: https://www.cancer.gov/about-cancer/treatment/clinical-trials/intervention/trametinib?pn=1.

58. Hung YP, Lovitch SB, et al., *Histiocytic sarcoma: New insights into FNA cytomorphology and molecular characteristics.* Cancer Cytopathol, 2017. 125(8): p. 604.

59. Prior IA, Lewis PD, et al., *A comprehensive survey of Ras mutations in cancer.* Cancer Res, 2012. 72(10): p. 2457.

60. Jing J, Greshock J, et al., *Comprehensive predictive biomarker analysis for MEK inhibitor GSK1120212.* Mol Cancer Ther, 2012. 11(3): p. 720.

61. Zhang Q, Shibani A, et al., *an aggressive multifocal primary CNS histiocytosis with PTPN11 (Shp2) mutation.* Neuropathol Appl Neurobiol, 2017.

62. Batra S, Martin SC, et al., *Histiocytic Sarcoma Associated with Coombs Negative Acute Hemolytic Anemia: A Rare Presentation.* Case Rep Oncol Med, 2016. 2016: p. 3179147.

63. Yamaguchi T, Yoshida T, et al., *Identification of JTP-70902, a p15(INK4b)-inductive compound, as a novel MEK1/2 inhibitor.* Cancer Sci, 2007. 98(11): p. 1809.

64. Yamaguchi T, Kakefuda R, et al., *Antitumor activities of JTP-74057 (GSK1120212), a novel MEK1/2 inhibitor, on colorectal cancer cell lines in vitro and in vivo.* Int J Oncol, 2011. 39(1): p. 23.

65. Solit DB, Garraway LA, et al., *BRAF mutation predicts sensitivity to MEK inhibition.* Nature, 2006. 439(7074): p. 358.

66. Meng J, Fang B, et al., *Apoptosis induction by MEK inhibition in human lung cancer cells is mediated by Bim.* PLoS One, 2010. 5(9): p. e13026.

67. Baranski Z, Booij TH, et al., *MEK inhibition induces apoptosis in osteosarcoma cells with constitutive ERK1/2 phosphorylation.* Genes Cancer, 2015. 6(11-12): p. 503.

68. Lassen A, Atefi M, et al., *Effects of AKT inhibitor therapy in response and resistance to BRAF inhibition in melanoma.* Mol Cancer, 2014. 13: p. 83.

69. Mirzoeva OK, Das D, et al., *Basal subtype and MAPK/ERK kinase (MEK)-phosphoinositide 3-kinase feedback signaling determine susceptibility of breast cancer cells to MEK inhibition.* Cancer Res, 2009. 69(2): p. 565.

70. Wee S, Jagani Z, et al., *PI3K pathway activation mediates resistance to MEK inhibitors in KRAS mutant cancers.* Cancer Res, 2009. 69(10): p. 4286.

71. Carrasco DR, Fenton T, et al., *The PTEN and INK4A/ARF tumor suppressors maintain myelolymphoid homeostasis and cooperate to constrain histiocytic sarcoma development in humans.* Cancer Cell, 2006. 9(5): p. 379.

72. Abe H, Kikuchi S, et al., *Discovery of a Highly Potent and Selective MEK Inhibitor: GSK1120212 (JTP-74057 DMSO Solvate).* ACS Med Chem Lett, 2011. 2(4): p. 320.

73. Mazur PK, Reynoird N, et al., *SMYD3 links lysine methylation of MAP3K2 to Ras-driven cancer.* Nature, 2014. 510(7504): p. 283.

74. Khalil AA, Jameson MJ, et al., *The Influence of Hypoxia and pH on Bioluminescence Imaging of Luciferase-Transfected Tumor Cells and Xenografts.* Int J Mol Imaging, 2013. 2013: p. 287697.

75. Lukas G, Brindle SD, et al., *The route of absorption of intraperitoneally administered compounds.* J Pharmacol Exp Ther, 1971. 178(3): p. 562.

76. Administration UFaD, *Center for drug evaluation and research. Application #204114Orig1s000. PHARMACOLOGY REVIEW(S).* 2013.

77. Rousset M, Dutriaux C, et al., *Trough dabrafenib plasma concentrations can predict occurrence of adverse events requiring dose reduction in metastatic melanoma.* Clin Chim Acta, 2017. 472: p. 26.

78. Infante JR, Fecher LA, et al., *Safety, pharmacokinetic, pharmacodynamic, and efficacy data for the oral MEK inhibitor trametinib: a phase 1 dose-escalation trial.* Lancet Oncol, 2012. 13(8): p. 773.

CHAPTER 5

POPULATION STUDY OF MUTATIONS IN *PTPN11* IN BERNESE MOUNTAIN DOGS WITH HISTIOCYTIC SARCOMA

5.1 Introduction

Histiocytic sarcoma (HS) in dogs is a highly aggressive neoplasm originating from malignant cells of dendritic cell lineage. It is a rare disease, accounting for less than 1% of all cancers in dogs [1], however it is frequently seen in certain breeds, including more than 25% of BMDs [2, 3], flat-coated retrievers [4, 5], golden retrievers and Rottweilers [6-8]. There is no sex predilection for HS, and dogs in adult age (8-10 years) are most commonly affected [3, 9]. HS develops most often in the skin, bone/joint, spleen, lymph node, lungs, and liver [3, 6, 10], where it rapidly disseminates to other organs in 70-91% of the cases [3, 5, 7, 8, 10]. Patients respond poorly to current treatment protocols, such as with lomustine and/or doxorubicin, which results in a median survival time of 3-6 months [3, 8, 11, 12]. Although the deregulation of the tumor suppressor genes *MTAP/CDKN2A*/*B* located within the region homologous to human chr9p21 [13, 14] has been implicated with HS predisposition in genome wide association studies, the disease pathogenesis remains unclear.

The *PTPN11* gene encodes SHP-2, a non-receptor protein tyrosine phosphatase engaged in enhancement of signaling downstream of growth factor, cytokines and extracellular receptors. SHP-2 contains two SRC homology 2 domains (N- and C-SH2), a catalytic PTP, protein tyrosine phosphatase domain, and a C-terminal domain containing tyrosyl phosphorylation sites [15]. The N-SH2 domain interacts with the PTP domain, blocking its active site. Phosphotyrosyl peptide binding to the N-SH2 domain induces a conformational change that reverses the auto-inhibitory state [15].

In humans, *PTPN11*^{E76K} is the most common gain-of-function mutation seen in juvenile myelomonocytic leukemia (JMML) [16], and was reported in acute myeloid leukemia (AML) [17], while the *PTPN11*^{G503V} mutation was reported in AML [18] and childhood leukemia [19]. Functional analyses demonstrated that these two variants led to an increase in the phosphatase activity level of SHP-2 and/or hyperactivation of downstream ERK and PI3K pathways [16, 19-21], indicating their role as activating oncogenic mutations.

Interestingly, *PTPN11* mutations were also reported in four cases of human HS [22-25], a counterpart to the same disease in dogs. HS in humans is an extremely rare malignancy (<1% of all hematopoietic neoplasms) [26, 27] that is equally aggressive. There is a lack of effective treatment options and survival times rarely reach beyond one year [28, 29]. Among the four individuals with mutated *PTPN11*, two carried the E76K mutation [22, 25], one carried the G503V variant [23], and one carried Y63S and Q506R variants [24].

In canine HS, our group has recently reported the somatic mutation *PTPN11*^{E76K} on chr26 in a cohort of HS from 30 BMDs and from 23 dogs of other breeds [30]. *PTPN11*^{E76K}, a substitution mutation (c.226G>A, p.Glu76Lys) located in exon 3 of the N-SH2 domain **(Figure 5.1A and B)**, was present in 36.67% of HS from BMDs and 9% of HS from other breeds, indicating its potential as a driver mutation in canine HS, particularly in BMDs.

Our goal in this study was to evaluate the prevalence of *PTPN11*^{E76K} mutation in a larger cohort of BMDs with HS, as well as in a cohort of BMDs with lymphoma, the second most common malignancy in this breed. Additionally, we investigated the prevalence of a second missense mutation, *PTPN11*^{G503V} (c.1,508G>T, p.Gly503Val), located in exon 13 of the PTP domain of SHP-2 **(Figure 5.1A and B)**, which has recently been identified by our group in two HS cell lines that have been established in our laboratory (one originating from a BMD and one from a Rottweiler), and DH82, a commercially available cell line originated from a hemophagocytic HS from a golden retriever. In addition, we wanted to examine if there were any correlations with age, sex or clinical characteristics.

5.2 Materials and Methods

5.2.1 Subjects

Samples of HS from 32 dogs (19 BMDs and 13 golden retrievers) were obtained from archival formalin-fixed paraffin embedded tissues from the Veterinary Diagnostic Laboratory at Michigan State University

(VDL-MSU). Samples from the 13 golden retrievers were previously reported [30]. Frozen tissues of 92 HS and 23 lymphoma cases from BMDs were selected from the BMD DNA and Tissue Repository initiative at MSU. Selection criteria included a confirmed diagnosis of the disease (HS or lymphoma) verified by a board certified pathologist. Most samples were submitted by veterinary practitioners/dog owners for diagnostic purposes or to contribute to the BMD repository at our institution. HS cell lines derived by our laboratory from BMDs (BD and OD), a Rottweiler (PJ) and a golden retriever (DH82, obtained from ATCC (CRL-10389)) were also included in the study. A comprehensive characterization of the BD cell line was recently reported by our group [31]. DH82 is a commercially available cell line reportedly derived from a hemophagocytic HS from a golden retriever. Normal tissue adjacent to the neoplasm in the paraffin block, or blood was used as to obtain constitutive (normal) DNA for each case. All neoplastic tissues were obtained from client owned dogs and were left over tissues during treatment with surgical resection of the tumor, or post-mortem during necropsy. The use of left over specimens was approved by MSU IACUC, through an IACUC exemption process. Blood samples were obtained from client owned dogs and shipped with cold packs to MSU, where they were kept in aliquots at -80°C. This procedure was approved by the MSU IACUC (AUF# 08/15-127-00). All dog owners provided a written consent allowing the use of this material for research.

5.2.2 DNA sample acquisition

For genomic DNA extraction of the formalin-fixed paraffin embedded tissues, H&E slides were first marked around the areas containing neoplastic tissue. Samples of the marked areas were collected from the paraffin block with a scalpel blade. DNA extraction was performed using the RecoverAll Kit (AM1975, ThermoFisher) following the manufacturer's instructions.

In the case of frozen tissue samples, HS cell lines and blood samples, genomic DNA was extracted from up to 25mg of tissue, about $1x10^6$ cells or 100µl of blood per sample using the DNeasy Blood & Tissue kit

(69504, Qiagen). Quantification of DNA was carried out using the Qubit dsDNA HS kit (Q33230, ThermoFisher) and a Qubit 2.0 fluorometer (ThermoFisher).

5.2.3 Methods for PTPN11 mutation identification and analysis

PTPN11^{E76K} was recently reported by our group [30], and *PTPN11*^{G503V} was identified in sequences of the coding regions from RNA-seq data of the HS cell lines. For this purpose, messenger RNA was isolated, assayed for quality and sequenced using the Illumina HiSeq 4000 platform to generate a minimum of 150 million reads at 2X150 BP at the MSU Genomics Core. Data acquired from sequencing were checked for quality using FastQC and low quality bases were trimmed using TrimGalore. *PTPN11* gene sequences of HS cell lines can be found under Sequence Read Archive (SRA) study accession SRP139948.

HS samples were genotyped using custom made TaqMan SNP Genotyping Assays specific for the missense mutations c.226G>A (p.Glu76Lys) (Assay ID ANT2AD7), and c.1,508G>T (p.Gly503Val) (Assay ID ANDJ2M3) for the dog *PTPN11* gene (4332077, ThermoFisher). This assay enables the genotyping of individuals for a single nucleotide polymorphism (SNP) through two sequence-specific probes, one labeled with VIC dye that detects Allele 1 sequence (wild type), and the second labeled with FAM dye that detects Allele 2 sequence (mutant). Using a 96-well plate, each reaction contained 0.5µl of 20X TaqMan Custom SNP Assay, 5µl of TaqMan Genotyping Master Mix (4371355, ThermoFisher), and 5µl of genomic DNA 2ng/µl. For each assay, a no-template negative control containing DNA-se free water, and positive controls with known genotypes (mutant and wild type) were included. Genotyping was conducted in real-time PCR mode using a StepOnePlus PCR System (4376600, ThermoFisher) following the cycling conditions instructed by the manufacturer. All assays were performed in duplicate experiments. Samples with ambiguous results were submitted for Sanger sequencing for confirmation using the primers 5'-TTTGTTTCCCCCTAATGGAC-3' (forward) and 5'-GAACACCTATGGCATGGAAGA-3' [30]

for E76K, and 5’-CGACATTGATGTTCCCAAAA-3’ (forward) and 5’-GGACAGCCATATAAATGAATCG-3’ (reverse) for G503V mutation.

5.2.4 Statistical Methods

Categorical parameters including age (<5.5y vs. 5.5-10y vs. >10y), sex (female vs. male), breed (BMD vs. golden retriever), and disease (HS vs. lymphoma) were statistically analyzed by Fisher Exact Probability test or Chi-square test. P values were always given as two-tail analysis and were considered statistically significant below 0.05. All statistical analyses were performed using the VassarStats website [32].

5.3 Results

5.3.1 Cases characteristics

One hundred eleven cases of HS from BMDs were initially selected for the study, 15 cases were excluded due to the lack of available paired normal tissue, which resulted in the remaining 96 cases. These cases had histological confirmation of the diagnosis by a board certified pathologist, and for a few, IHC for CD18 was included in the diagnostic panel. Only for one case, the diagnosis was based on cytology report (assessed by a veterinary pathologist), and supportive clinical signs and diagnostics. From 92 cases of known age, the median was 8.3 years (range: 1.9 - 12.5) **(Figure 5.1C)**. Forty-three female dogs, 50 male dogs and three dogs with unidentified sex were included in the study. At least two organs were affected with HS in 44% of the cases in BMDs, with the most commonly organs affected being the lung (50%), liver (34%), spleen (34%) and lymph node (20%). Other locations affected at low frequency included mediastinum (7%), stifle (6%), peritoneum (4%), urinary tract (4%), intestine (4%), skin/subcutis (4%), cervical area (4%), heart base (3%), prostate (1%) and pancreas (1%).

All HS samples from breeds other than BMDs had histologically confirmed diagnoses. Among 13 golden retrievers with HS, the median age was 8 years (range: 4 - 13) **(Figure 5.1C)**, and 6 were female and 7

were male dogs. The PJ cell line was derived from a HS of an 8-year old male Rottweiler, whereas DH82 was derived from a HHS in a 10-year old male golden retriever. At least two anatomical locations were affected by HS in 3 of 13 golden retrievers and affected organs included the spleen (5/13), liver (4/13), skin/subcutis (4/13), lung (3/13), lymph node (3/13), peritoneum (3/13), pancreas (2/13) and stifle (1/13).

The BMD lymphoma cohort contained 23 lymphomas, from which 22 samples originated from lymph nodes, and one sample originated from the spleen. The diagnosis of malignant lymphomas was based on examination of the surgical biopsy by a board certified pathologist for fifteen cases and 8 cases were diagnosed based on cytology by a board certified clinical pathologist. Median age of this group was 8.4 years (range: <1 - 12.1), and among them 13 were female and 10 were male dogs.

5.3.2 PTPN11 mutation status

PTPN11 mutations were present in 41 of 96 (42.7%) HS from BMDs, 31 (32.3%) HS were positive for the E76K variant, and 10 (10.4%) for the G503V variant **(Table 5.1)**. Interestingly, 12 of 41 (29.2%) HS with mutant *PTPN11* alleles were homozygous/or hemizygous for the particular mutation, i.e. they did not have any wild type allele. Additionally, there were no neoplasms that were compound heterozygous with regard to the mutant alleles.

Across 15 HS cases of dogs from breeds other than BMD, *PTPN11* mutations were identified in 4 cases (26.7%). Although frequency of the mutation was notably higher in BMDs, no significant association was seen between the presence of the mutation and breed of dogs (p=0.39) based on two-tail Fisher Exact Probability test. Mutation status across all HS was stratified within groups of different ages and sex, and two-tail Fisher Exact Probability test was used to evaluate for any association between groups **(Table 5.1)**. When the prevalence of the *PTPN11* mutation was compared across different ages, the its

presence was significantly associated with BMDs older than 10 years (p=0.03). There was no statistical significant difference of *PTPN11* mutation status between sexes (p=1.0).

As previously mentioned, among the HS samples, we included four HS cell lines. We identified *PTPN11* mutations in all four cell lines, where the BD cell line was positive for *PTPN11*^{E76K}, and OD, PJ and DH82 were all positive for the *PTPN11*^{G503V} mutation.

Interestingly, none of the 23 lymphomas from BMDs carried any *PTPN11* mutation. Therefore, when comparing HS and lymphoma from BMDs, the mutation was significantly associated with HS (p=0.0001) based on two-tail Fisher Exact Probability Test.

We only included cases that we had a normal paired tissue for comparison. Paired normal tissues from all cases were wild type for *PTPN11*.

5.4 Discussion and conclusion

Our results demonstrated that somatic mutations in *PTPN11* are common in canine HS, suggesting the role of *PTPN11*^{E76K} and ^{G503V} as oncogenic drivers for this malignancy. *PTPN11* encodes SHP-2, the first reported mutant protein tyrosine phosphatase acting as an oncoprotein [16]. SHP-2 has a key role in signal enhancement in several signal transduction pathways associated with cell proliferation, differentiation and migration [33]. Qu and colleagues demonstrated that *PTPN11* function is required for the development of the hematopoietic system, and that the deficiency of SHP-2 in mice was lethal at mid-gestation with defects in mesodermal patterning [34].

Gain of function mutations in *PTPN11* are associated with 35% of human JMML [16, 17], a disorder with excessive proliferation of myelomonocytic cells, and have been reported in a low percentage of myelodysplastic syndrome (MDS) and AML cases [16], and a few cases of solid tumors [18].

Similar to that seen in patients with JMML, MDS and AML, the *PTPN11* mutations in canine HS affected residues located at the N-SH2 (E76K) and PTP (G503V) interacting surfaces. Mutations in N-SH2 such as

E76K, have been shown to cause a decrease in the binding affinity between the N-SH2 and PTP domains, that shape the auto-inhibitory SHP-2 conformation, allowing access to the phosphatase catalytic site, which results in 5-fold increase of phosphatase activity when compared to wild type SHP-2 [16, 18, 35]. In addition, a *PTPN11*^{E76K} mutation was shown to induce activation of the ERK and PI3K pathways through the increase and sustained interaction to Grb2, and Gab2/p85 subunit, respectively [20]. In the case of PTPN11^{G503V}, functional analysis reported by Niihori et al. demonstrated that the phosphatase activity was 2.7 higher than wild type SHP-2 [19].

We have recently identified and reported the frequency of the *PTPN11*^{E76K} mutation as 36.7% of HS in 30 BMDs [30]. In the present study, we have evaluated both the *PTPN11*^{E76K} mutation and a second missense mutation, *PTPN11*^{G503V}, in an expanded population of 95 cases of HS in BMDs. Our results showed that the prevalence of the *PTPN11*^{E76K} mutation in this larger cohort of HS from BMDs was 32.2%, and therefore did not differ significantly from our previous findings (p=0.66 – Chi-Square Test with Pearson correction). While the *PTPN11*^{G503V} mutation was present in only 10.4% of HS from BMDs, this increases the overall prevalence of *PTPN11* mutations to 42.7% in HS in BMDs and emphasizes the prevalent oncogenic role of this particular gene in canine HS, specifically in BMDs. Constitutive DNA from cases from all cohorts were wild type for both mutational spots in the *PTPN11* gene, demonstrating their somatic nature. Interestingly, the identical mutations have also been reported in human HS [22-25]. Among the four human HS cases with mutated *PTPN11*, two carried the E76K variant [22, 25], while one carried the G503V variant [23], and another carried Y63S and Q506R variants [24].

In our cohort of BMDs with HS, female and male dogs were equally represented, and most dogs were of adult age (median = 8.3 years). The prevalence of mutations was not statistically different between sexes. On the other hand, mutation status was significantly associated with dogs older than 10 years compared to dogs of younger age (p=0.03). This is not surprising, as there is a higher chance of acquiring mutations with aging. Interestingly, in 44% of the cases, multiple organs were affected with HS, and 16

of 41 (39%) HS with *PTPN11* mutations affected multiple organs. Our information was based on histopathology reports which were available for all cases, and any clinical comments included.

The prevalence of *PTPN11* mutations was higher in HS of BMDs (42.7%) vs. other breeds (26.7%). However, studies with larger cohorts of HS from other breeds are needed for confirmation.

None of the lymphomas from BMDs had *PTPN11* mutations, indicating that within this breed of dogs, this mutation appears to be specifically associated with HS (p=0.0001 - Fisher Exact Probability Test). However, we cannot exclude the possibility that similar mutations occur in other hematopoietic diseases, including other histiocytic diseases in BMDs, i.e. reactive histiocytosis, or other round cell neoplasm, i.e. mast cell tumors.

The clinical implications of caring for canine patients with HS with mutations in *PTPN11* are not known. Clinical studies are warranted to understand whether neoplasms with or without *PTPN11* mutation behave differently in terms of rate of progression of the disease, rate of metastasis, or prognosis. It would also be important to understand whether neoplasms that are heterozygous, i.e. which contain one wild type allele, are clinically distinct from those that appear homozygous for the mutant allele. In the current study, our assays did not allow us to differentiate hemizygosity from homozygosity for the mutant allele. It is possible that those neoplasms carrying two copies of the mutant allele, or zero copies of the wild type allele would behave more aggressively. Interestingly, in our study, 12.5% of the mutations were homo- or hemizygous and 30.2% were heterozygous for the mutations. The percentage of homozygosity/hemizygosity might not be accurate in that it may be underestimated due to possible presence of normal tissue in the tissue sections utilized, despite efforts to minimize this. Understanding the molecular mechanisms involved will certainly help in management of affected patients, with application of precision medicine to those canine patients.

Most importantly, our results indicated that *PTPN11* mutations play an important role in canine HS oncogenesis, and open the venue to novel potential molecular targets for this currently untreatable

disease in dogs and humans. The development of SHP-2 inhibitors represents an active area of research. Compounds such as 11a-1, that binds to the SHP-2 activation pocket, and SHP099, that allosterically inhibits SHP-2, have demonstrated promising results both in experiments *in vitro* and in mouse xenograft models of cancer [21]. Downstream to SHP-2, MAPK and PI3K/AKT pathways are also potential targets for neoplasms with mutated *PTPN11*, and for which several FDA-approved inhibitors are current available. For instance, one human HS carrying the mutation *PTPN11*^{E76K}, was treated with trametinib, a MEK inhibitor, which resulted in a significant partial response [22]. Similarly, we have observed that treatment with trametinib of *PTPN11* mutated canine HS cell lines BD, OD and PJ *in vitro* resulted in effective inhibition of cell proliferation. In addition, immunodeficient mice harboring xenograft HS originated from BD cells presented suppression of tumor growth and survived longer when treated with trametinib (Takada et al. under review).

In conclusion, we demonstrated that mutations in the *PTPN11* gene are commonly present in canine HS, especially in BMDs, indicating their important role as oncogenic drivers. Furthermore, these findings unravel a novel targetable molecule and therapeutic pathways for HS in dogs, and similar diseases in humans.

APPENDIX

Figure 5.1. Sites of *PTPN11* mutation and distribution of HS cases by age. **(A)** Schematic representation of *PTPN11* gene product with corresponding functional domains of SHP-2, indicating the locations of E76K and G503V mutations. Top bar is a schematic representation of the intron structure, and the lower bar depicts the functional domains. **(B)** Alignment of SHP-2 protein sequences from HS cell lines (BD, OD and PJ), normal canine dendritic cells (DCs), and reference sequences from relevant species (Dog, Human and Mouse). Missense mutations identified in canine HS are highlighted in pink (E76K) and green (G503V), are located within highly conserved genetic regions. Protein sequences were aligned using Clustal Omega software. **(C)** Age distribution in years of cases of HS from BMDs and golden retrievers. Blue horizontal lines represent the median age value.

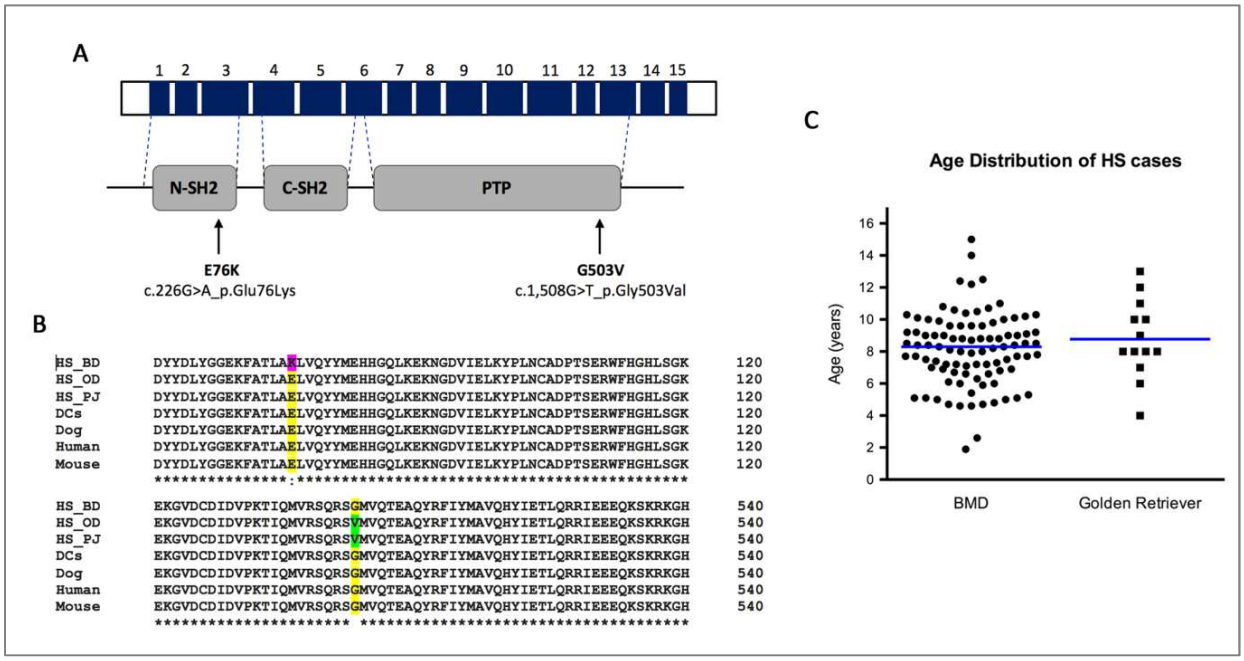

Table 5.1. Frequency of *PTPN11* mutation status based on breed, age, sex, and disease type.

Characteristics	**N**	***PTPN11* mutant**	***PTPN11* wild type**	***P***	**E76K**	***P***	**G503V**	***P***
HS BMD	**96**	41(43%)	55(57%)		31(32%)		10(10%)	
Age								
<5.5 years	**14**	6(43%)	8(57%)	*>0.4*	3(21%)		3(21%)	
5.5 – 10 years	**60**	19(32%)	41(68%)		16(27%)	*>0.2*	3(5%)	*>0.07*
>10 years	**18**	11(61%)	7(39%)	*0.03*	8(44%)		3(17%)	
Sex								
Female	**43**	17(39%)	26(60%)	*1.0*	*13(30%)*	*1.0*	*4(9%)*	*0.74*
Male	**50**	21(42%)	29(58%)		15(30%)		6(12%)	
HS other breeds	**15**	4(27%)	11(73%)	*0.39*	*1(7%)*	*0.06*	*3(20%)*	*0.38*
Lymphoma BMD	**23**	0	23(100%)	*0.0001*	-	*0.003*	-	*0.2*

BIBLIOGRAPHY

BIBLIOGRAPHY

1. Bruner SR, *Updates in therapeutics for veterinary dermatology.* The Veterinary clinics of North America. Small animal practice, 2006. 36(1): p. 39.

2. Abadie J, Hedan B, et al., *Epidemiology, pathology, and genetics of histiocytic sarcoma in the Bernese mountain dog breed.* J Hered, 2009. 100 Suppl 1: p. S19.

3. Dervisis NG, Kiupel M, et al., *Clinical prognostic factors in canine histiocytic sarcoma.* Vet Comp Oncol, 2016.

4. Dobson J, Hoather T, et al., *Mortality in a cohort of flat-coated retrievers in the UK.* Vet Comp Oncol, 2009. 7(2): p. 115.

5. Fidel J, Schiller I, et al., *Histiocytic sarcomas in flat-coated retrievers: a summary of 37 cases (November 1998-March 2005).* Vet Comp Oncol, 2006. 4(2): p. 63.

6. Affolter VK and Moore PF, *Localized and disseminated histiocytic sarcoma of dendritic cell origin in dogs.* Vet Pathol, 2002. 39(1): p. 74.

7. Craig LE, Julian ME, et al., *The diagnosis and prognosis of synovial tumors in dogs: 35 cases.* Vet Pathol, 2002. 39(1): p. 66.

8. Skorupski KA, Clifford CA, et al., *CCNU for the treatment of dogs with histiocytic sarcoma.* J Vet Intern Med, 2007. 21(1): p. 121.

9. Ruple A and Morley PS, *Risk Factors Associated with Development of Histiocytic Sarcoma in Bernese Mountain Dogs.* J Vet Intern Med, 2016. 30(4): p. 1197.

10. Klahn SL, Kitchell BE, et al., *Evaluation and comparison of outcomes in dogs with periarticular and nonperiarticular histiocytic sarcoma.* J Am Vet Med Assoc, 2011. 239(1): p. 90.

11. Cannon C, Borgatti A, et al., *Evaluation of a combination chemotherapy protocol including lomustine and doxorubicin in canine histiocytic sarcoma.* J Small Anim Pract, 2015. 56(7): p. 425.

12. Rassnick KM, Moore AS, et al., *Phase II, open-label trial of single-agent CCNU in dogs with previously untreated histiocytic sarcoma.* J Vet Intern Med, 2010. 24(6): p. 1528.

13. Hedan B, Thomas R, et al., *Molecular cytogenetic characterization of canine histiocytic sarcoma: A spontaneous model for human histiocytic cancer identifies deletion of tumor suppressor genes and highlights influence of genetic background on tumor behavior.* BMC Cancer, 2011. 11: p. 201.

14. Shearin AL, Hedan B, et al., *The MTAP-CDKN2A locus confers susceptibility to a naturally occurring canine cancer.* Cancer Epidemiol, 2012. 21(7): p. 1019.

15. Hof P, Pluskey S, et al., *Crystal structure of the tyrosine phosphatase SHP-2.* Cell, 1998. 92(4): p. 441.

16. Tartaglia M, Niemeyer CM, et al., *Somatic mutations in PTPN11 in juvenile myelomonocytic leukemia, myelodysplastic syndromes and acute myeloid leukemia.* Nat Genet, 2003. 34(2): p. 148.

17. Loh ML, Vattikuti S, et al., *Mutations in PTPN11 implicate the SHP-2 phosphatase in leukemogenesis.* Blood, 2004. 103(6): p. 2325.

18. Bentires-Alj M, Paez JG, et al., *Activating mutations of the noonan syndrome-associated SHP2/PTPN11 gene in human solid tumors and adult acute myelogenous leukemia.* Cancer Res, 2004. 64(24): p. 8816.

19. Niihori T, Aoki Y, et al., *Functional analysis of PTPN11/SHP-2 mutants identified in Noonan syndrome and childhood leukemia.* J Hum Genet, 2005. 50(4): p. 192.

20. Yu WM, Daino H, et al., *Effects of a leukemia-associated gain-of-function mutation of SHP-2 phosphatase on interleukin-3 signaling.* J Biol Chem, 2006. 281(9): p. 5426.

21. Frankson R, Yu ZH, et al., *Therapeutic Targeting of Oncogenic Tyrosine Phosphatases.* Cancer Res, 2017. 77(21): p. 5701.

22. Voruz S, Cairoli A, et al., *Response to MEK inhibition with trametinib and tyrosine kinase inhibition with imatinib in multifocal histiocytic sarcoma.* Haematologica, 2018. 103(1): p. e39.

23. Liu Q, Tomaszewicz K, et al., *Somatic mutations in histiocytic sarcoma identified by next generation sequencing.* Virchows Arch, 2016. 469(2): p. 233.

24. Batra S, Martin SC, et al., *Histiocytic Sarcoma Associated with Coombs Negative Acute Hemolytic Anemia: A Rare Presentation.* Case Rep Oncol Med, 2016. 2016: p. 3179147.

25. Zhang Q, Shibani A, et al., *an aggressive multifocal primary CNS histiocytosis with PTPN11 (Shp2) mutation.* Neuropathol Appl Neurobiol, 2017.

26. Jaffe ES and World Health Organization., *Pathology and genetics of tumours of haematopoietic and lymphoid tissues*. World Health Organization classification of tumors. 2001, Lyon: IARC Press. 351 p.

27. Jaffe ES, *Histiocytoses of lymph nodes: biology and differential diagnosis.* Semin Diagn Pathol, 1988. 5(4): p. 376.

28. Vos JA, Abbondanzo SL, et al., *Histiocytic sarcoma: a study of five cases including the histiocyte marker CD163.* Mod Pathol, 2005. 18(5): p. 693.

29. Kommalapati A, Tella SH, et al., *Histiocytic sarcoma: a population-based analysis of incidence, demographic disparities, and long-term outcomes.* Blood, 2018. 131(2): p. 265.

30. Thaiwong T, Sirivisoot S, et al., *Gain-of-function mutation in PTPN11 in histiocytic sarcomas of Bernese Mountain Dogs.* Vet Comp Oncol, 2017.

31. Takada M, Parys M, et al., *A novel canine histiocytic sarcoma cell line: initial characterization and utilization for drug screening studies.* BMC Cancer, 2018. 18(1): p. 237.

32. Lowry R. *VassarStats: Website for Statistical Computation*. 1998-2018; Available from: http://vassarstats.net/index.html.

33. Neel BG, Gu H, et al., *The 'Shp'ing news: SH2 domain-containing tyrosine phosphatases in cell signaling.* Trends Biochem Sci, 2003. 28(6): p. 284.

34. Qu CK, Nguyen S, et al., *Requirement of Shp-2 tyrosine phosphatase in lymphoid and hematopoietic cell development.* Blood, 2001. 97(4): p. 911.

35. Tartaglia M, Mehler EL, et al., *Mutations in PTPN11, encoding the protein tyrosine phosphatase SHP-2, cause Noonan syndrome.* Nat Genet, 2001. 29(4): p. 465.

CHAPTER 6

FUTURE DIRECTIONS

In the present manuscript, our findings provide support that the MAPK signaling pathway is a key oncogenic pathway in canine HS. We demonstrated that HS cell lines derived from relevant breeds of dogs were highly sensitive to MEK inhibition by trametinib. We showed that trametinib also inhibited tumor growth in a xenograft orthotopic mouse model of HS, and prolonged their survival time. Similar findings were observed with the multi-kinase inhibitor dasatinib. Our findings provide proof of concept data for initiating clinical trials with these two drugs in dogs with HS.

Studies using dasatinib [1-3] and trametinib [4] in dogs have been reported in small cohorts mostly for verification of safety and tolerability purposes. Data from these studies provide a reference dosage and schedule to be considered in a clinical trial undertaken by us. We envision an efficacy study with canine HS patients from the Veterinary Medical Center at MSU using a dose escalation scheme.

In addition, we found that HS cell lines sensitive to trametinib carry activating somatic mutations in *PTPN11* and *KRAS*, known to be associated with the activation of MAPK pathway. Among four HS cell lines used in our studies, BMD BD cell line carries *PTPN11*^{E76K} mutation, BMD OD cell line carries *PTPN11*^{G503V} and *KRAS*^{Q61H} mutations, while both Rottweiler PJ and golden retriever DH82 cell lines present *PTPN11*^{G503V} mutation. The variability of mutation status across the HS cell lines was expected and represents the intertumoral heterogeneity, a well-established concept in cancer. Within a larger population of BMDs, the *PTPN11* mutations was present in 43% (41 of 96), indicating an important role as driver mutations in canine HS, particularly in BMDs. *KRAS* mutation was much less frequent, with a prevalence of 3% (3 of 96).

We found that DH82, the most resistant HS cell line to trametinib (pIC50 of 5.8) had a substantially lower expression of PTEN and an increased expression of phospho-AKT by western blotting assay, which suggests that PI3K/AKT pathway seems to play a role in DH82 cells. We hypothesize that the resistance to trametinib is because DH82 cells are driven by PI3K/AKT signaling pathway, and thus less dependent on MAPK signaling.

MAPK pathway is certainly not the only driver of canine HS as we understand that cancer is a multifactorial disease and deregulation of other pathways is likely present. Our selection of candidate drugs from the HTS assay resulted in a group of eight compounds with diverse targets and mechanisms of action **(Table 6.1)**. Romidepsin, a histone deacetylase inhibitor, was a highly effective drug, suggesting that epigenetic modifications may play a role in HS. Proteasome is also a potential target for HS. We have previously observed promising *in vitro* responses of HS cells under treatment with bortezomib, a first generation proteasome inhibitor. When we tested efficacy of bortezomib in intrasplenic HS xenograft mice, bortezomib was highly toxic, and significant dose reduction had to be made within the first week of treatment (data not shown). At adjusted dosages, bortezomib was not effective in inhibiting tumor growth or increasing survival time of mice. In this aspect, treatment with carfilzomib may have different results as it seems to induce less toxicity to normal cells when compared to bortezomib. Pyrvinium pamoate is an anti-helmintic drug with increasing potential as anti-cancer functions [5]. There are evidences suggesting the inhibition of WNT pathway as an anti-tumor mechanism of pyrvinium pamoate [6]. A few conventional cytotoxic drugs have shown to be effective against HS in our HTS (mithramycin, mitoxantrone, methotrexate and pralatrexate), none of them is part of the standard protocol for canine HS. These selected group of drugs need further investigation to evaluate efficacy and safety in an *in vivo* mouse model.

More recently, we sequenced the three HS cell lines derived from two Bernese mountain dogs and a Rottweiler using RNA-Seq approach, along with dendritic cells derived from PBMCs of a healthy dog as a normal control sample. Further studying the sequence of these cell lines and sequences from additional HS samples will be important to unravel additional mechanisms of tumorigenesis in HS through the identification of oncogenic drivers, gene fusions, and alterations of gene expression associated with the disease. Loss of heterozygosity studies will be critical to address tumor suppressor genes involved in canine HS.

We were able to take advantage of relevant cancer models of HS, cell lines and xenograft mouse model, to better understand drivers of oncogenesis and to identify novel candidate drugs for treatment. Moving from bench to bedside, our research provided data that can be further integrated into clinical trials in dogs with HS. The dog represents a unique translational model for human HS, and current and future understandings on canine HS can potentially be translated to similar diseases in humans.

APPENDIX

Table 6.1: Selected drugs from HTS with pIC50>6.7 (HS) AND pIC50<6 (FB)

	BD	PJ	DH82	FB	Mechanism of action
Romidepsin	**9.0**	**7.0**	**6.7**	6.0	HDAC inhibitor
Carfilzomib	**7.0**	5.8	5.8	5.8	Proteasome inhibitor
Trametinib	**7.8**	6.5	5.8	5.0	MEK1/2 inhibitor
Mithramycin	**6.8**	6.1	5.7	6.0	Antibiotic
Mitoxantrone	**6.7**	5.7	6.2	6.0	Topoisomerase inhibitor
Methotrexate	5.0	5.0	**7.5**	5.0	Antimetabolite
Pralatrexate	5.1	5.0	**7.0**	5.5	Antimetabolite
Pyrvinium pamoate	5.8	5.7	**6.7**	5.6	Anti-helmintic/AKT and WNT inhibitor

BIBLIOGRAPHY

BIBLIOGRAPHY

1. Davis LE, Hofmann NE, et al., *A case study of personalized therapy for osteosarcoma.* Pediatr Blood Cancer, 2013. 60(8): p. 1313.

2. Dickerson EB, Marley K, et al., *Imatinib and Dasatinib Inhibit Hemangiosarcoma and Implicate PDGFR-beta and Src in Tumor Growth.* Transl Oncol, 2013. 6(2): p. 158.

3. Marley K, Gullaba J, et al., *Dasatinib Modulates Invasive and Migratory Properties of Canine Osteosarcoma and has Therapeutic Potential in Affected Dogs.* Transl Oncol, 2015. 8(4): p. 231.

4. Institute NC, *FDA Approval for Trametinib*.

5. Momtazi-Borojeni AA, Abdollahi E, et al., *The novel role of pyrvinium in cancer therapy.* J Cell Physiol, 2018. 233(4): p. 2871.

6. Thorne CA, Hanson AJ, et al., *Small-molecule inhibition of Wnt signaling through activation of casein kinase 1alpha.* Nat Chem Biol, 2010. 6(11): p. 829.